GULF STATES UTILITIES COMPANY

RIVER BEND STATION POST OFFICE BOX 220 ST. FRANCISVILLE, LOUISIANA 70775

AREA CODE 504 635-6094 346-8651

July 8, 1985
RBG- 21487
File Nos. G9.5,G9.8.6.2

Mr. Harold R. Denton, Director
Office of Nuclear Reactor Regulation
U.S. Nuclear Regulatory Commission
Washington, D.C. 20555

Dear Mr. Denton:

River Bend Station - Unit 1
Docket No. 50-458

Enclosed is Gulf States Utilities' (GSU) final response to the NRC Staff's Request for Additional Information 210.110 delineated in Mr. A. Schwencer's letter of April 30, 1985 (RBC-31,879). Pursuant to our discussions with your Mechanical Engineering Branch, a confirmatory analysis has been completed and is provided as Enclosure 2 to supplement our initial response of May 20, 1985 (RBG-21,042). Enclosure 1 will be incorporated into a future Final Safety Analysis Report amendment.

Sincerely,

J. E. Booker

J. E. Booker
Manager-Engineering,
Nuclear Fuels & Licensing
River Bend Nuclear Group

JEB/ERG/je

Enclosures

B001
1/12

RESPONSE

The original calculation demonstrating that the feedwater check valves can perform their intended function following a feedwater line break outside the containment (See Question 210.82) was based on an inelastic analysis assuming no strain hardening.

The conclusions from this approach have been confirmed by an inelastic analysis done in accordance with Appendix F of the ASME III Code (1977) for Class 1 service, using the ANSYS computer program (Appendix 3A of the FSAR). The non-linear stress/strain relationship will be conservatively approximated by a bilinear curve with the strain at ultimate stress equal to 2/3 the elongation at temperature as provided in ASME II, adjusted for strain rate and temperature effects. This analysis has verified that structural integrity of the feedwater check valves is maintained. Any long term leakage through the check valves is controlled by redundant motor-operated valves which are closed and sealed by the penetration valve leakage control system at approximately 25 min. after the accident. Note that, as discussed in FSAR Section 15.6.6, a feedwater line break outside containment is less limiting than other postulated LOCA's.

ENCLOSURE 2

Calculation for River Bend Station Feedwater Check Valve
Integrity Following Pipe Rupture Outside Containment

Appendix F has been added to the calculation which confirms that both feedwater isolation valves will withstand rapid closure and that the pressure boundary will be maintained.

QUESTION 210.82 (3.6.2)

Provide the basis for assuring that the feedwater isolation check valves can perform their function following a postulated pipe break of the feedwater line outside containment.

RESPONSE

The response to this request is provided in revised
11 Appendix 3C, Section 3C.2.2. See also Question and Response 210.110.

QUESTION 210.110

Your response to Q 210.82 regarding the basis for assuring that the feedwater check valves can perform their intended function following a feedwater line break outside containment is not totally acceptable. In your letter from J. E. Booker to H. Denton dated December 17, 1984, you provided a table which summarized the results of your feedwater check valve analysis. The staff finds that additional information is needed to justify the allowable values used for the disk shear load and strain limits.

In Note (1) to Enclosure 2 of your letter you state:

> "Strain due to absorption of energy must be less than 0.7 times the ultimate elongation (based on Table CB-3700-1 of the ASME Code, Section III, Division II, 1983 Edition)."

The staff does not find the use of Table CB-3700-1 to be acceptable for Division 1 components including valves. Table CB-3700-1 is applicable to Division 2 components (i.e, concrete reactor vessels and containment).

Furthermore, in Note (1) you state:

> "It is assured that strain rates are sufficiently high to warrant doubling the material allowables (Ref. Juvinal, R. C., Stress, Strain, and Strength - McGraw-Hill, 1967, pg-168)."

The staff finds that the figure provided in the referenced text book shows the effect of strain rate on tensile properties of typical mild steel at room temperature. However, the text book figure provides only general information not suitable for specific design application without more details. The use of the figure in the text book is not appropriate for the specific valve design because it does not represent the yield strength of the disk material (i.e., SA-216 WCC) at temperature. Furthermore, the text book states that because it is difficult to predict the conditions of impact strain rate, it is common to design parts for impact based on empirically determined stress impact factors together with the static strength of the materials. It appears that the shear load on the disk for check valve 1B21*AOVF032A, B is near the allowable value. (Factor of Safety equal to 1.05). Thus, the staff is concerned that the acceptability of doubling the material allowables at temperature is not well-justified, and because of the small design margin and the uncertainties involved, the shear load on the disk might be unacceptable. Additionally, it appears the calculated values were established assuming strain hardening effects. Provide the basis for this assumption if used. Furthermore, it has been shown for mild steel at elevated temperatures that a negative slope occurs in the stress-strain rate curve at the higher strains which is generally associated with strain aging.

The staff requests that you provide a detailed discussion of the valve parts which do not satisfy linear stress limits per the ASME Code and the basis for concluding that the leakage of the reactor coolant pressure boundary through the feedwater check valves following the postulated break in the feedwater line outside containment is acceptable using your calculated strain values.

Stone and Webster Engineering Corporation
CALCULATION SHEET

Calculation Identification Number				
J.O. OR W.O. NO. 12210	DIVISION & GROUP NM(C)	CALCULATION NO. 2043	OPTIONAL CODE SQE	PAGE 2 REV 1

REVIEW STATEMENT

This calculation has been reviewed in accordance with EMDM 82-12 and was found to be adequate. The method of review utilized was (circle one):

a. Comparison with a similar previous Calculation No.______

b. Review of calculation.

c. Alternate Calculation No.______

Signature of Reviewer — REV. 1 C.T.Y, REV. 2 C.T.Y

Signature of Independent Reviewer (where different from Reviewer) — REV 1 S.M.F.

Stone and Webster Engineering Corporation
CALCULATION SHEET

Calculation Identification Number				PAGE 3
J.O./W.O. NO. 12210	DIVISION & GROUP NM(C)	CALCULATION NO. 2043	OPTIONAL CODE SQE	

TABLE OF CONTENTS

	Page
Title Page	1
Review Page	2
Contents	3
Revision Page	6
SUMMARY	7
1. Objective/Introduction	8
2. Method	13
3. Assumptions	14
4. Design Input	15
. Mass Properties	
. Materials	
. Dimensions	
. Material Properties	
. Section Properties	
. Impact Speed and Hammer Pressure	
. Allowables	
5. Summary of Results	19
6. Conclusions	20
7. References	21
8. Loads Analysis	22
. Pre-Impact	
. Kickback	
9. Integrity of Check Valve 1B21*F010A,B	9-1
10. Integrity of Testable Check Valve 1B21*AOVF32A,B	10-1

APPENDIX

REV.2

A-Plastic Strain Energy for Beams of Various Cross-section

B-Plastic Strain Energy for a Circular Plate in Bending

C-Miscellaneous Reference Material

D-Computer Log and Microfiche

E-Voided Pages from Revisions (1)

F-Confirmation of Conclusions (2)

LIST OF TABLES

		Page
4.1	Mass Properties	15
4.2	Materials	15
4.3	Dimensions	16
4.4	Material Properties at 500F	17
4.5	Section Properties	17
4.6	Impact Speed and Hammer Pressure	17
5.1	Summary of Results	19
8.1	Pre-impact Loads	22
8.2	Point Impact - Kickback Loads on AOVF32	26
8.3	Point Impact - Kickback Loads on F010	27
8.4	Uniform Impact - Kickback Loads on AOVF32	28
8.5	Uniform Impact - Kickback Loads on F010	28
8.6	Disk Rim Nodal Loads for AOVF32	29

List of Figures(Cont.)

8.1 Computer Model - F010 Tail-Link/Disk Kickback Loads 24

8.2 Computer Model - AOVF32 Tail-Link/Disk Kickback Loads 25

8.3 Disk Impact Load vs Time for AOVF32 31 REV. 1

Stone and Webster Engineering Corporation
CALCULATION SHEET

Calculation Identification Number				
J.O./W.O. NO. 12210	DIVISION & GROUP NM(C)	CALCULATION NO. 2043	OPTIONAL CODE SQE	PAGE 6 REV. 2

REVISION STATUS TABLE

REV NO.	PAGES REVISED		DESCRIPTION & REASON	ORIGINATOR & DATE	REVIEWER & DATE
	CHANGED	ADDED			
0	-	-	Original Issue	J. Gwinn 10/26/84	Cam Ly 10/27/84
(1)	Title Page 2,4,5 7,9,13 15 17-19 21-30 D-8,-9 Sect'ns 9.&10.		Revisions to clarify the results of analysis and data input sources.	J. Gwinn 12-7-84	Cam Ly 12-7-84
(2)			Appendix F added to confirm the conclusions of Revision 1.	J. Gwinn	Cam Ly

SUMMARY

The reactor vessel water is protected from blowdown following a postulated rupture of the feedwater piping outside the containment, by the Velan check valve 1B21*F010A,B inside the containment and by the Atwood/Morrill testable check valve 1B21*AOVF32A,B outside the containment. Breaks are not postulated in the piping between the valves because that region is classified as break exclusion.

The reverse flow caused by the sudden pressure reduction at the break rapidly closes both valves. This calculation examines the ability of these valves to withstand the impact of the disk on the seat without excessive leakage thereafter.

Loads on the critical elements,i.e., the disk, tail link, rockshaft and seat, were computed by simulation of the impact dynamics using the STARDYNE and GTSTRUDL computer programs. Both uniform and point impact were considered in search of the worst case kickback loads generated by the point of impact not being at the center of percussion. Seismic, hydrodynamic and dead loads were not considered because of their insignificant magnitude compared to impact loads.

In those cases where linear stresses were not below their allowables, a strain energy analysis or a non-linear time history strain analysis was conducted to demonstrate integrity. (1)

It is concluded that both valves will remain intact and that the leakage will be within the make-up capability of the High Pressure Core Spray(HPCS) or the Reactor Core Injection Cooling(RCIC) system, following rupture of the feedwater piping outside the containment.

Revision 2 adds Appendix F, an inelastic systems and component analysis using the non-linear option of the ANSYS computer program to confirm the conclusions. (2)

Stone and Webster Engineering Corporation
CALCULATION SHEET

Calculation Identification Number				
J.O./W.O. NO. 12210	DIVISION & GROUP NM(C)	CALCULATION NO. 2043	OPTIONAL CODE SQE	PAGE 8

1. OBJECTIVE/INTRODUCTION

The purpose of this calculation is to evaluate the ability of River Bend ASME III class 1 feedwater check valves 1B21*AOVF32(specification 228.218) and 1B21*F010(specification 228.211) to withstand rapid closure following the postulated pipe break outside the containment shown in Figure 1.1. The acceptance criterion is that gross leak rates do not occur because of disk rupture, serious fracture of the seat/disk interface or misalignment of the disk with respect to the seat from this faulted event.

There are no consequences defined for a High Energy Line Break(HELB) outside the containment. The other feedwater system is not available for make-up because loss-of-off-site power is postulated and this system is not on the emergency diesel generators. Single active failure of the HPCS(465 GPM) or the RCIC(600 GPM) systems is assumed, leaving at least one of these systems available as a source of water to the vessel required to make-up for any leakage.

Feedwater pump trip from high water level in the vessel, a normal operating condition, was found by the analysis of Reference 8 not to cause high energy impact of the disk on the seat. The inertia of the motor was sufficiently high that the pump took approximately 1000 seconds to completely stop. From the stand point of the valve, two(2) seconds were required to generate a reverse flow rate equal to the normal flow rate, resulting in a very gentle closing of these check valves. Pump trip is not considered a critical loading condition and is, therefore, not treated in this analysis.

Added to pipe rupture loads on a square-root-sum- of-squares basis are the seismic and hydrodynamic loads. However, they are not considered in this analysis because of insignificant magnitudes as compared to the impact forces generated by reverse flow following rupture of the feedwater line. For the same reason, dead load and opening loads are not considered in this analysis.

Figures 1.2 and 1.3 show a cross-section of these valves from the vendor drawing. Figure 1.4 is a sketch labelling the dimensions and elements of importance to the integrity of swing check valves. The coordinate system used to identify the loading directions is also shown therein.

Calculation Identification Number				
J.O. OR W.O. NO. 12210	DIVISION & GROUP NM(C)	CALCULATION NO. 2043	OPTIONAL CODE SQE	PAGE 9 REV 1

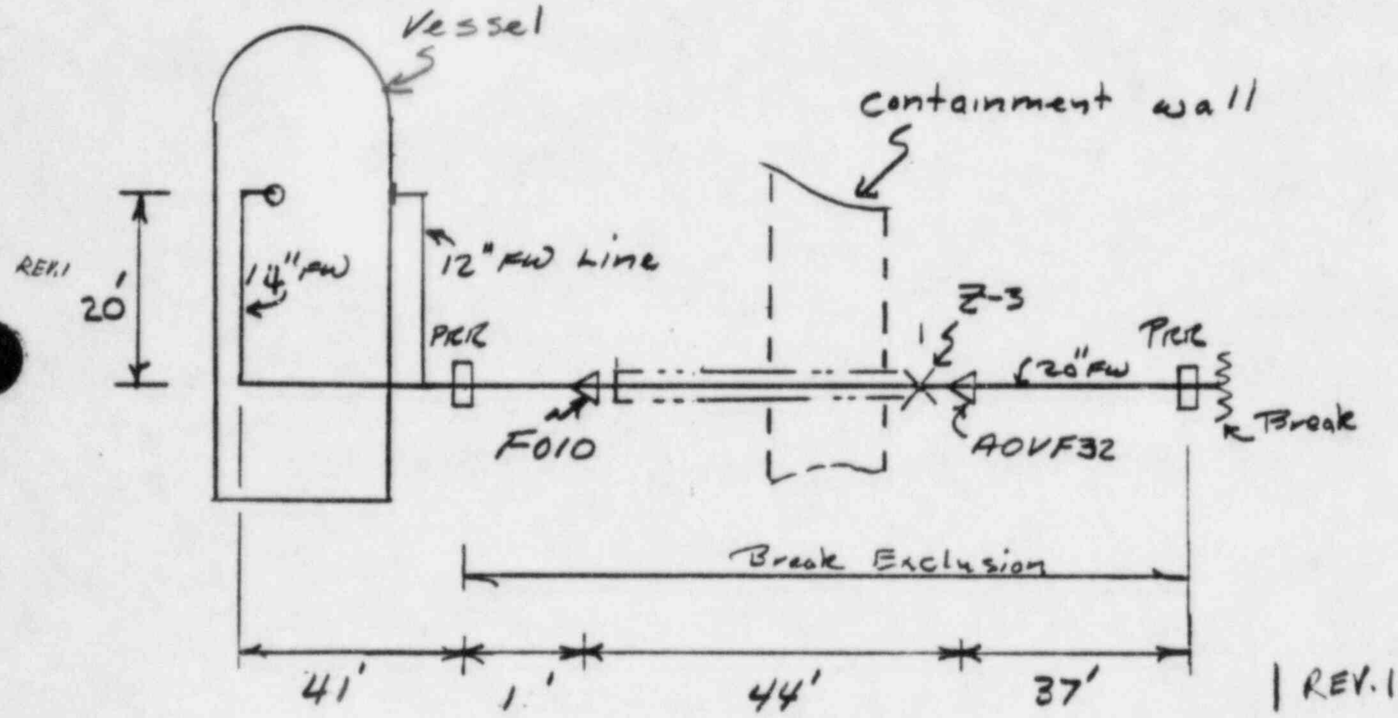

Figure 1.1 Sketch of Piping Model(Ref.17)

Stone and Webster Engineering Corporation
CALCULATION SHEET

Calculation Identification Number				
J.O. OR W.O. NO. 12210	DIVISION & GROUP NM(C)	CALCULATION NO. 2043	OPTIONAL CODE SQE	PAGE 10

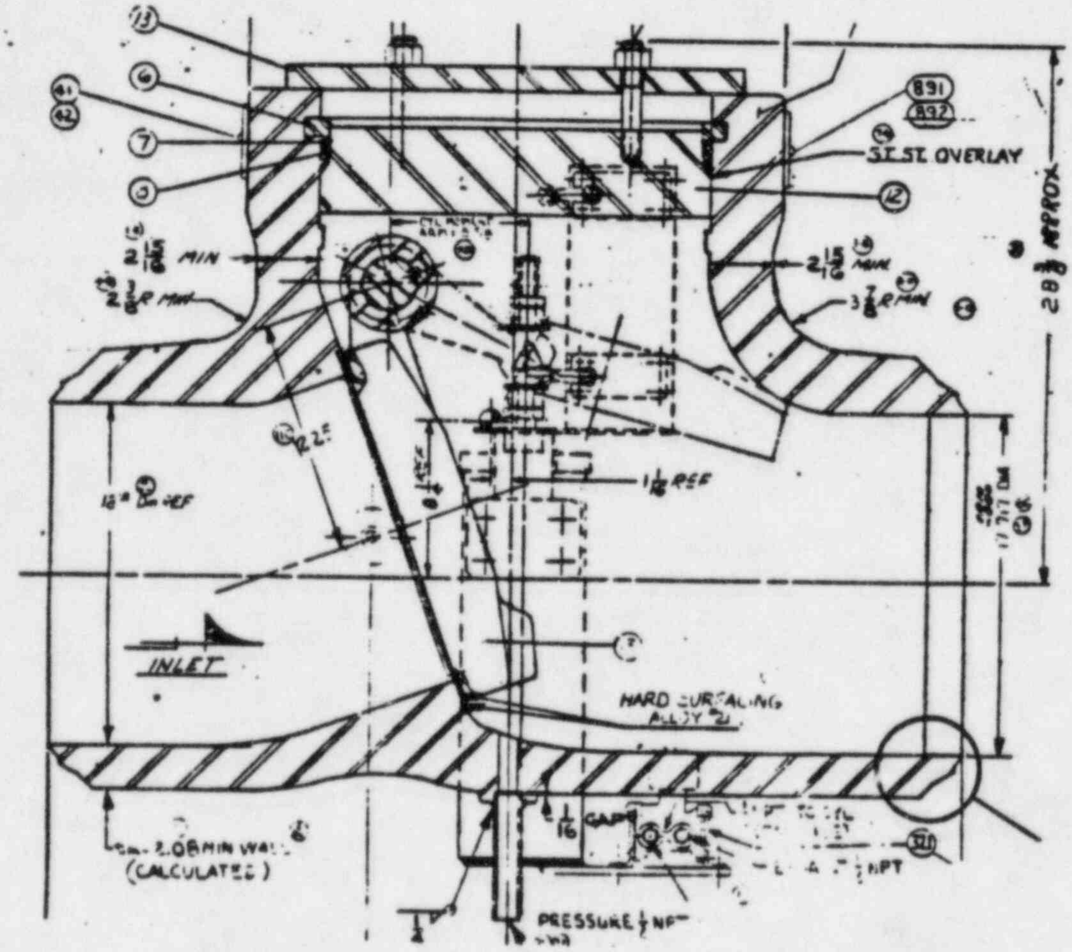

Figure 1.2 Cross-section of the AOVF32 Check Valve(Ref.2)

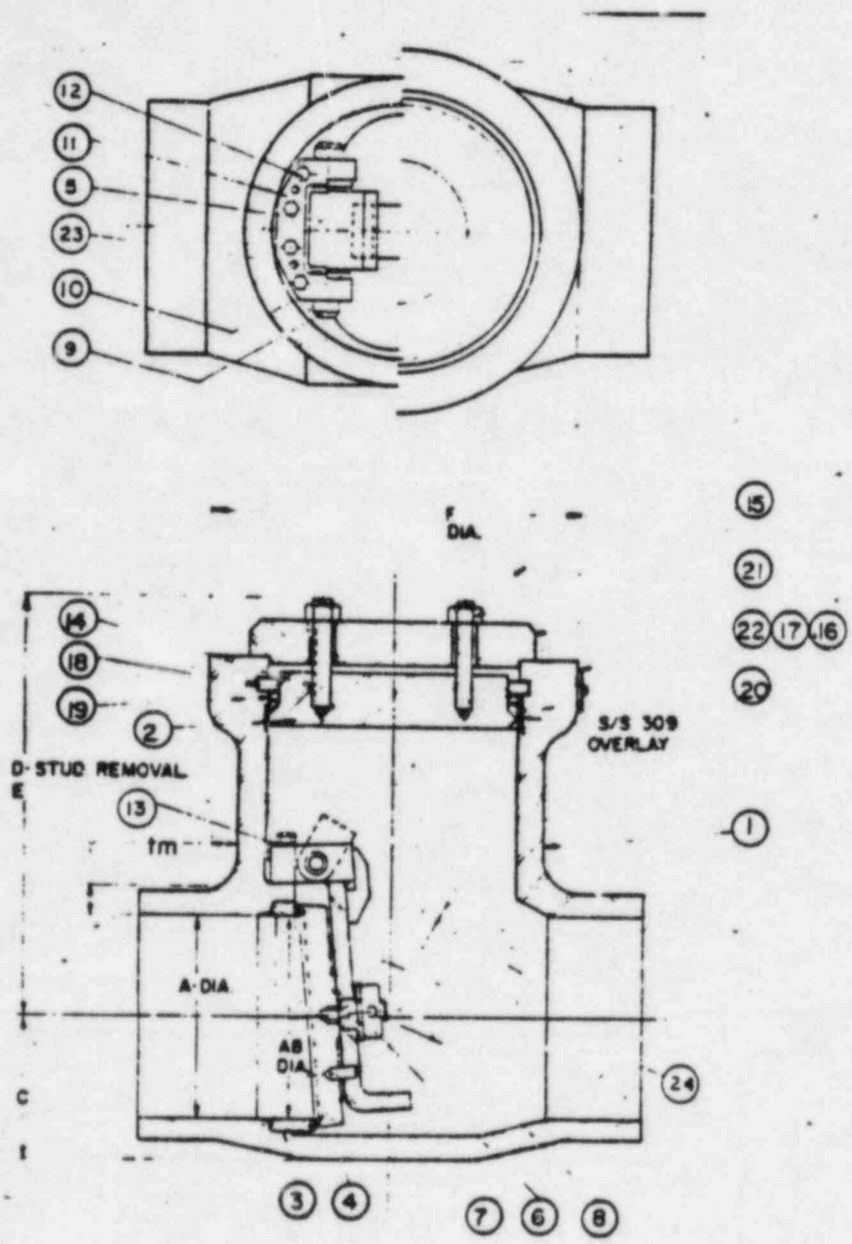

Figure 1.3 Cross-section of the F010 Check Valve(Ref.3)

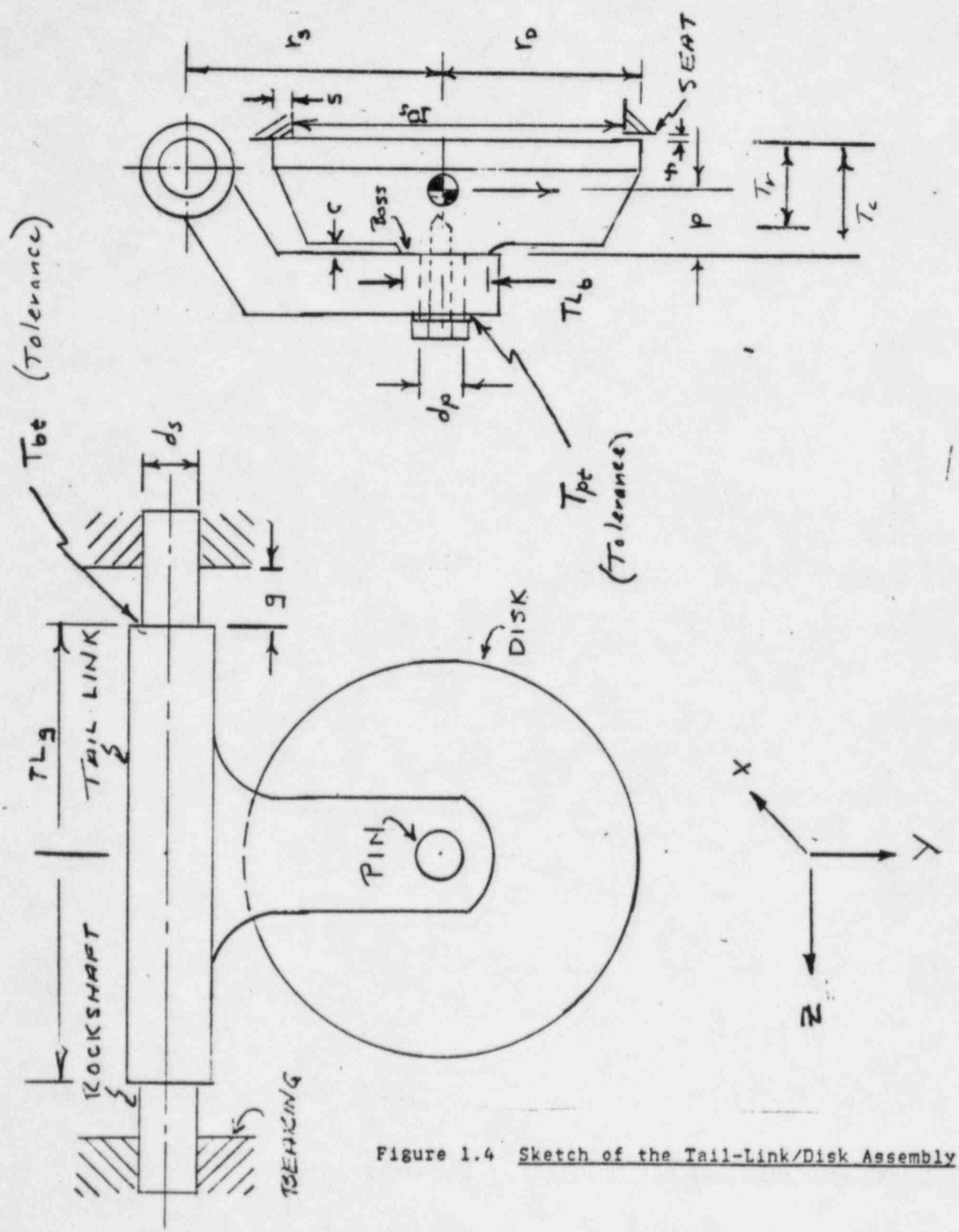

Figure 1.4 Sketch of the Tail-Link/Disk Assembly

2. METHOD

Elements critical to the integrity of a check valve identified in Figure 1.4, are the disk, tail link, the pin which connects the tail link to the disk(F010 only - AOVF32 tail link and disk are integral), the rockshaft and the seat/disk interface.

The dynamic loading just before impact is purely centrifigal, reacted by the rockshaft, pin and tail link. Acting simultaneously with this load are kickback forces arising from the disk impacting the seat at a single arbitrary point(non-uniform impact) not at the center of percussion. These loads may be worst case for the tail link, pin and rockshaft. For the seat and disk, worst case loads are generated by a uniform impact of the disk on the seat combined with the pressure surge from water hammer.

Kickback loads are neither obvious nor easily calculated manually and were therefore modelled on GTSTRUDL and STARDYNE , using the integration option for specified initial conditions. Typical initial conditions were the impact speed at all nodes except a node suffering impact, its speed being set equal to zero. Note that all dynamic loads are conservatively calculated based on a linear stress-strain relationship.

The details associated with calculating these loads are presented in Section 8. The integrity analyses of Sections 9 & 10 are linear elastic for faulted service, supplemented as necessary by a plastic strain energy analysis to treat limited energy loading. Although not an ASME III code analysis, certain methods and allowables from Appendix F(Ref.9) were used in this analysis for convenience. REV 1

3. ASSUMPTIONS

1) The strain rates are sufficiently high to warrant doubling the material allowables, as provided in reference 6, page 168. (confirmation not required)

Stone and Webster Engineering Corporation
CALCULATION SHEET

Calculation Identification Number				
J.O./W.O. NO. 12210	DIVISION & GROUP NM(C)	CALCULATION NO. 2043	OPTIONAL CODE SQE	PAGE 15 REV 1

4. DESIGN INPUT

Mass Properties

TABLE 4.1	Atwood/Morrill Check Valve 1B21*AOVF32A,B	REF.	Velan Check Valve 1B21*F010A,B	REF.
Disk - wt.	260	12	185#	13
Tail Link - wt.	71 (Integral/Disk)	12	20	13
Mass Moment of Inertia/Rockshaft	13.9 slug-ft**2	2	6.8	13

REV. 1

Materials

TABLE 4.2	Atwood/Morrill Check Valve 1B21*AOVF32A,B	REF.	Velan Check Valve 1B21*F010A,B	REF.
Disk	cs SA216 WCC	2	cs SA105 Stellite #6 facing	3
Rock Shaft	ss A182 F6a	2	ss SA564 630 Hardened(1100 degF)	3
Seat	cs SA216 WCC Stellite #21 facing	2	cs SA105 Stellite #6 facing	3
Tail Link	cs SA216 WCC	2	cs SA105	3
Pin & Stud	N/A	N/A	cs SA 105	3
Nut	N/A	N/A	ss SA564 630	3

Dimensions

TABLE 4.3	Atwood/Morrill 1B21*AOVF32A,B			Velan alve 1B21*F010A,B	
		SYMBL	REF.		REF.
Diam of Disk	19. in.	2*Rd	16	17.5	11
Dist - Rkshft/Dsk Ctr	14.	Rs	16	11.25	3
Diam of Pin	N/A	Dp	N/A	2.5 (welded to disk)	3
Diam - Stud for Tlk	N/A	Dsd	N/A	1.0 (Threaded)	3
Diam - TailLink Nut	N/A		N/A	3.5	3
Diam of Rockshaft	1.88	Ds	16	1.0	3
Gap - Tlk/Bearing	.56	g	16	.1 or less	3
Dist - Dsk CG/Pin Seat	N/A	p	N/A	1.375	11
Clearance - Disk/Tlk	N/A	c	N/A	.125	3
Thickness of Disk	3.75ctr,2.5rim	Tc/Tr	16	2.75	11
Seat Annulus	.5+	s	2	.56	3
Tail Link Section	2.9 x 15.0	hxw	16	1.0 x 4.5	3
Tail Link Grip	16.4	TLg	16	5.25	3
Seat Inside Diam	16.75	IDs	13	15.75	3
Diam of Tlk Boss	N/A	TLb	N/A	3.5	3
Fit - Seat/Disk Face	*	f		.015 (at rim)	3
Tolerance - Brg/Rkshft	*	Tbr		+.004,-0.0	3
Tolerance - Pin/Tlk	N/A	Tpt	N/A	.010 (nut prevents rot'n)	3
Tolerance - Rkshft/Tlk	*	Trt		+0.0,-.005	3

* Assumed same as Velan

Stone and Webster Engineering Corporation
CALCULATION SHEET

Calculation Identification Number				
J.O./W.O. NO. 12210	DIVISION & GROUP NM(C)	CALCULATION NO. 2043	OPTIONAL CODE SQE	PAGE 17 REV 1

Material Properties at 500F (Ref. 9, Appendix I)

TABLE 4.4	Sy (ksi)	Su (ksi)	Elong.* (%)	E (psi*e-6)	Remarks
cs SA 216 WCC	40	70	22	27	
cs SA 105	29.1	70	22	27	
ss SA 564 630	95.2	133	16	27	
ss A 182 F6a	34.7	66.3	18	27	

* Ref.10(ambient temperatures) REV.1

Section Properties(calculated from Table 4.3)

TABLE 4.5		AOVF32	F010
Tail Link	- Area	43.0 in**2	4.5(2.@pin)
	- Mom of Inert/z	30.0 in**4	.375(.167@pin)
	- Torsion Const/y	119.0 in**4	1.5
Rockshaft	- Area	2.8	.79
	- Mom of Inert/z	.61	.049
Pin	- Area	N/A	4.9
	- Mom of Inert/z	N/A	1.9
Stud	- Area	N/A	.60(root)

Impact Speed and Hammer Pressure(Ref. 1, page 31)

TABLE 4.6	AOVF32	F010
Impact Speed(rad/sec)	42	58
Max Pressure(psi) - six(6) milliseconds after impact	3100	3200

Allowables for Faulted Service

The primary stress from a steady-state load must be less than .7 times the ultimate strength(Su) of the material(Ref.9, App.F). Stresses acting for a very short time(less than .5 milliseconds) must be less than the ultimate strength of the material. If not, then it is necessary to recognize that the real question is the ability of the configuration to absorb the energy of impact at acceptable values of strain, taken here to be .7 times the ultimate elongation, based on Table CB-3700-1 of Ref.9A. Strains acting for a very short time(.5 ms) must be less than the ultimate elongation. Because the specific reduction of elongation with temperature was not available, the ambient values of elongation in Table 4.4 were used without benefit of the increase from high strain rate loading. REV. 1 REV 1

5. SUMMARY OF RESULTS

TABLE 5.1		AOVF32				F010			
		Calc'd	Allow.	FS	PG10-	Calc'd	Allow.	FS	PG9-
Disk	-shear #	7.9E6	8.3E6	1.05	2	2.7E6	7.7E6	2.9	2
	-strain %	2.1	15.4	7.3	3	3.6	15.4	4.3	4
Rockshaft	-stress ksi	N/A	N/A	-	-	13.6	53.8	4.0	12
	-ratio(1)	.65	1.0	1.5	11	N/A	N/A	-	-
Tail Link	-stress ksi	46.4	98.	2.1	16	68.1	70.0	1.03	8
	-ratio(1)	.48	1.0	2.1	17	N/A	N/A	-	-
Pin	-stress ksi	N/A	N/A	-	-	23.	49.	2.1	7
Stud	-stress ksi	N/A	N/A	-	-	41.	49.	1.2	6
Seat/Disk Interface	-stress ksi	74.	98.	1.3	18	98.8	140.	1.4	15

(1) Appendix A9231, Ref. 9

Calculation Identification Number				
J.O./W.O. NO. 12210	DIVISION & GROUP NM(C)	CALCULATION NO. 2043	OPTIONAL CODE SQE	PAGE 20

6. CONCLUSIONS

It is concluded that both 1B21*AOVF32A(specification 228.218) and 1B21*F010A(specification 228.211) valves will withstand rapid closure and remain intact. In addition, any leakage will be within the make-up capability of the HPCS or RCIC system, following rupture of the feedwater piping outside the containment.

7. REFERENCES

1) SWEC Calculation 12210-NP(B)-1007-PX, Feedwater Check Valve Closure Following a Pipe Rupture Event, April 1984

2) Atwood/Morrill Drawing 13464-04-H11 (SWEC File No. 228.218-020-4I)

3) Velan Drawing 7890-015 (SWEC File No. 228.211-049-26D)

4) SWEC Specification 228.211 for Check Valves, July 1983

5) SWEC Specification 228.218 for Reactor Feed and Testable Check Valves, Oct 1983

6) Juvinal,R.C., Stress, Strain and Strength, McGraw-Hill, 1967

7) Wambold,J.C. & Ju,F., Safe Impact Speeds for Hollow Circular Cylinders, Journal of Applied Mechanics, June 1970

8) SWEC Calculation 12210-NP(C)1000-PX, Water Hammer Analysis of Feedwater Piping for Pump Trip, May 1984.

9) ASME B & PV code, 1974 through winter 1976, Section III

9A) ASME B & PV code, 1983, Section III, Division II

10) Manual of ASTM Standards, 1977

11) Velan Design Report for Class 1 20" Forged Carbon Steel Check Valve, ASME class 900#, DR-1204, February 1981

12) Atwood/Morrill Design Report for Class 1 Feedwater Check Valve, Procedure No. 205-13464-04, December 1976

13) Telex No. 05-826599 from Velan dated 2-14-84 (App. C herein)

14) Atwood/Morrill Report No. 300-15202-00 dated 4-17-84, Valve Data for Performing Closure Analysis (App. C herein)

15) Rourke,R.J., Formulas for Stress and Strain, McGraw-Hill, 4th Edition

16) SWEC Internal Correspondence(EM# 2697) dated 17 October 1984 from J. MacIntosh, FW Check Valve AOVF32B Measurements (App. C herein).

17) Feedwater piping drawings 12210 EP 17C-7 and EP 17F-5 | REV 1.

8. LOADS ANALYSIS

8.1 Pre-Impact Loads

The centrifigal force(Fc) arising from the angular speed(Omega) of the disk just prior to impact is given by

$$Fc = W*Omega**2*R/g$$

where R is the distance from the rockshaft to the disk/tail link center of gravity and W is its weight. Table 8.1 below contains the pre-impact loads on the rockshaft calculated from the above expression:

TABLE 8.1	AOVF32	F010	REF REV.1
Omega - rad/sec	45	60	1
W - #	331	205	Table 4.1
R - in	14.0	11.25	Table 4.3
Fc - #	24400	21500	calculated

8.2 Kickback Loads

Kickback loads arise when a body rotating about one point is impacted at any other point not at the center of percussion. Although the anticipated angle between the plane of the seat and the disk is very small, nonetheless, extremely high loads are possible by such a point contact(non-uniform) of the disk rim on the seat. They disappear in less than one(1) millisecond because after that time, the disk rim is in uniform contact with the seat. They are much reduced if sufficient articulation is provided by the tolerances in the shaft bearing and/or a pinned attachment of the disk to the tail link, because this limits the kickback forces to those arising only from uniform impact of the disk rim on the seat. Under this condition, the forces from rotation of the large mass of the disk about center-line tail link after impact do not occur.

Computer Model

The Velan valve 1B21*F010A has a separate tail link(Figure 1.2) attached to the disk by a pin whereas the tail link and disk are integral(Figure 1.3) in the design of the Atwood/Morrill valve 1B21*AOVF32A.

Both tail-link/disk assemblies were modelled as shown in Figures 8.1 and 8.2, for computation of the kickback loads under conditions of uniform and point impact of the disk rim on the seat. The postulated impact points(IP) are identified as a, b, c, d, e, f, & g therein.

Results

Tables 8.2 and 8.3 give the kickback loads at the attachment of the tail link to the rockshaft and to the pin at the disk center for non-uniform impact at several points(IP) on the seat, as shown in Figure 8.1. These loads for the F010 valves are much smaller than those for the AOVF32 valves because its tail link(see sketch in Ref. 14, App. C herein) is extremely rigid compared to the F010 tail link(see sketch in section 9.2 herein). Tables 8.4 and 8.5 provide kickback loads at these points plus the load on the seat for the case of uniform impact. REV 1

The kickback loads from point impact are small compared to uniform impact loads because the fit of the disk to the seat in the closed position is tight for both valves, the specified tolerance(Table 4.3) being .015 inches. The loads in Tables 8.2 and 8.3 are based on a tolerance of twice that amount, .030 inches.

The 7200 kip load on the disk rim in Table 8.4 is the sum of the loads appearing at each node on the rim. Table 8.6 presents the loads taken from the computer run which is plotted in Figure 8.3. /REV. 1

Stone and Webster Engineering Corporation
CALCULATION SHEET

Calculation Identification Number				
J.O./W.O. NO. 12210	DIVISION & GROUP NM(C)	CALCULATION NO. 2043	OPTIONAL CODE SQE	PAGE 24 REV 1

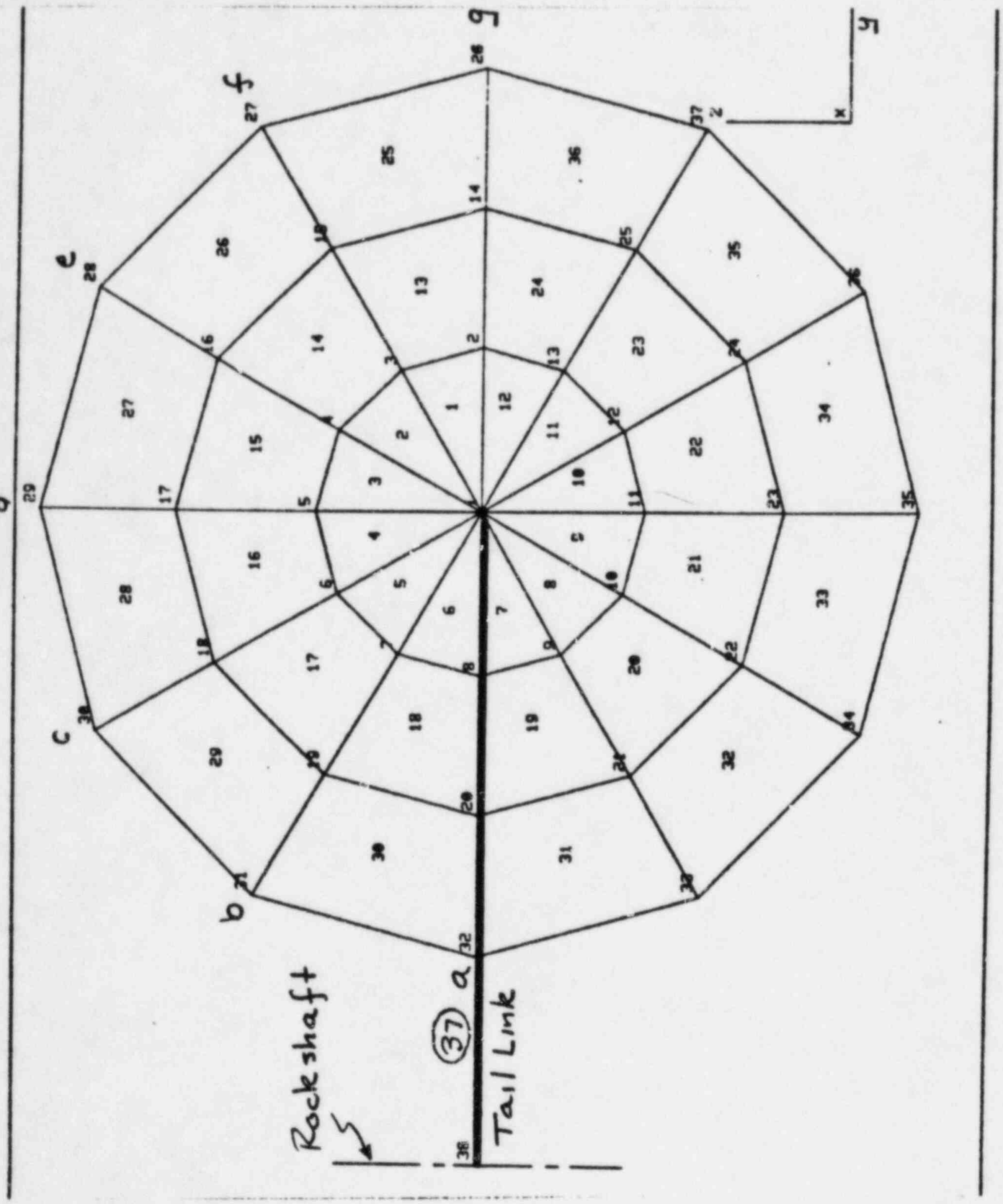

Figure 8.1 Computer Model - F010 Tail-Link/Disk Kickback Loads

Stone and Webster Engineering Corporation
CALCULATION SHEET

Calculation Identification Number				
J.O./W.O. NO. 12210	DIVISION & GROUP NM(C)	CALCULATION NO. 2043	OPTIONAL CODE SQE	PAGE 25 REV 1

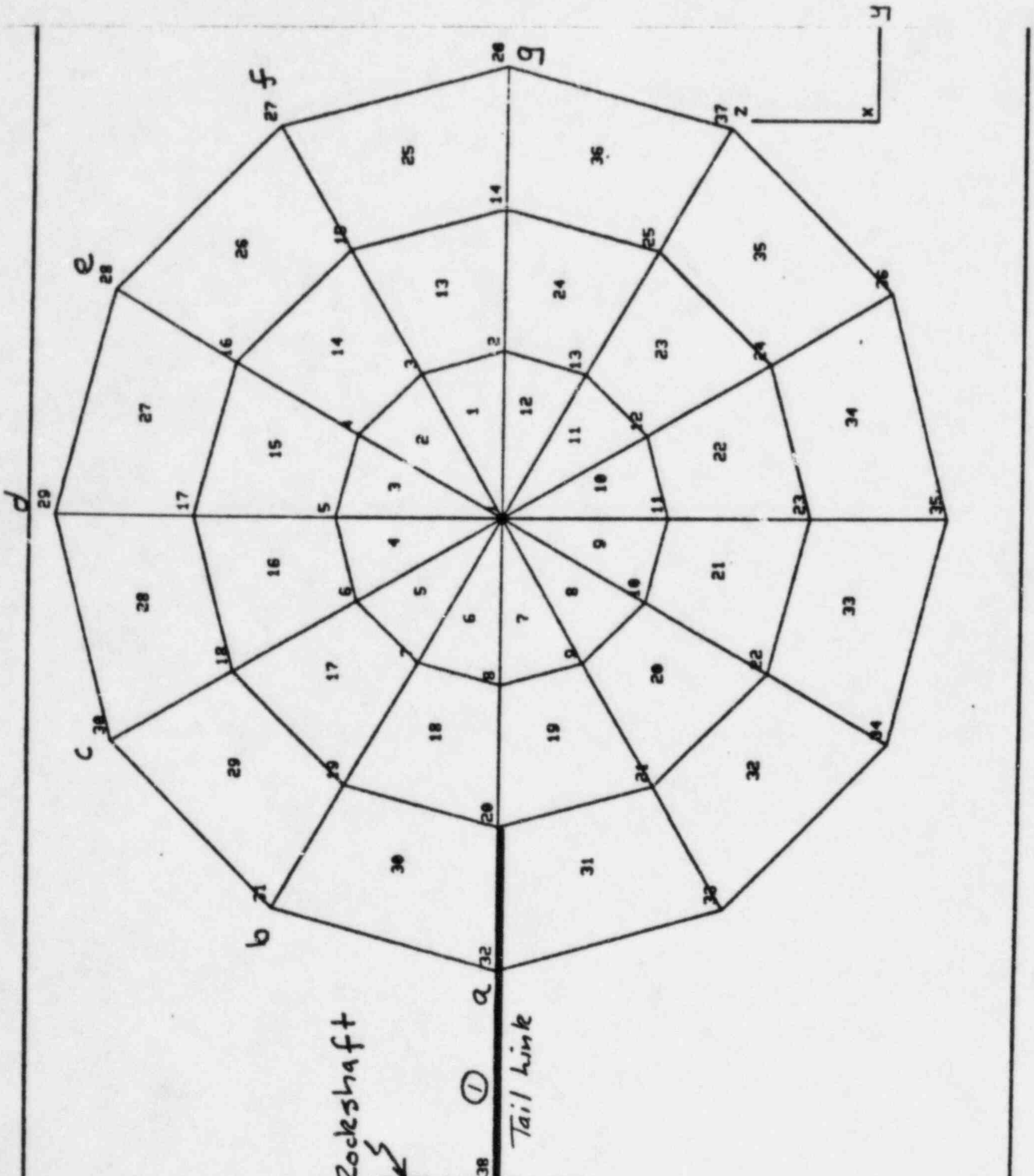

Figure 8.2 Computer Model - AOVF32 Tail-Link/Disk Kickback Loads

Stone and Webster Engineering Corporation
CALCULATION SHEET

Calculation Identification Number				
J.O./W.O. NO. 12210	DIVISION & GROUP NM(C)	CALCULATION NO. 2043	OPTIONAL CODE SQE	PAGE 26 REV 1

TABLE 8.2		POINT IMPACT - KICKBACK LOADING TABLE						Equipment AOVF32
IP	LOAD POINT	FXK (kips)	FYK (kips)	FZK (kips)	MXK (in-k)	MYK (in-k)	MZK (in-k)	REMARKS
a	ROCK SHAFT	60	-	-	-	0.0	-	
b		20	-	-	-	160	-	
c		1	-	-	-	30	-	
d		1	-	-	-	60	-	
e		5	-	-	-	10	-	
f		10	-	-	-	15	-	
g		10	-	-	-	0.0	-	
	Worst Case	60	-	-	-	160	-	
a	Tail Link Fairing to Disk	70	-	-	-	0.0	450	
b		20	-	-	-	160	130	
c		1	-	-	-	30	10	
d		1	-	-	-	60	60	
e		5	-	-	-	10	30	
f		10	-	-	-	15	50	
g		10	-	-	-	0.0	60	
	Worst Case	70	-	-	-	160	450	

These loads are based on an impact speed of 60 rad/sec.

Stone and Webster Engineering Corporation
CALCULATION SHEET

Calculation Identification Number				
J.O./W.O. NO. 12210	DIVISION & GROUP NM(C)	CALCULATION NO. 2043	OPTIONAL CODE SQE	PAGE 27 REV 1

TABLE 8.3	POINT IMPACT - KICKBACK LOADING TABLE	Equipment F010

IP*	LOAD POINT	FXK (kips)	FYK (kips)	FZK (kips)	MXK (in-k)	MYK (in-k)	MZK (in-k)	REMARKS
a	ROCK SHAFT	.01	-	-	-	0.0	-	
b		.01	-	-	-	.04	-	
c		.01	-	-	-	.13	-	
d		.01	-	-	-	.23	-	
e		.03	-	-	-	.28	-	
f		.06	-	-	-	.20	-	
g		.07	-	-	-	0.0	-	
	Worst Case	.07	-	-	-	.28	-	
a	DISK CENTER	.01	-	-	-	0.0	.10	
b		.01	-	-	-	.04	.12	
c		.01	-	-	-	.13	.13	
d		.01	-	-	-	.23	.01	
e		.03	-	-	-	.28	.28	
f		.06	-	-	-	.20	.67	
g	(Pin)	.07	-	-	-	0.0	0.0	
	Worst Case	.07	-	-	-	.28	.67	

Calculation Identification Number				
J.O./W.O. NO. 12210	DIVISION & GROUP NM(C)	CALCULATION NO. 2043	OPTIONAL CODE SQE	PAGE 28 REV 1

TABLE 8.4	UNIFORM IMPACT - KICKBACK LOADING TABLE						Equipment AOVF32
LOAD POINT	FXK (kips)	FYK (kips)	FZK (kips)	MXK (in-k)	MYK (in-k)	MZK (in-k)	REMARKS
Rockshaft -Unif. Impact	240	-	-	-	-	-	
Tail Link/Disk -Unif. Impact	240	-	-	-	-	960*	
Disk Rim -Unif. Impact	7200	-	-	-	-	-	

* Weakest section of the tail link(intersection with disk)

These loads are based on an impact speed of 60 rad/sec.

TABLE 8.5	UNIFORM IMPACT - KICKBACK LOADING TABLE						Equipment F010
LOAD POINT	FXK (kips)	FYK (kips)	FZK (kips)	MXK (in-k)	MYK (in-k)	MZK (in-k)	REMARKS
Rockshaft -Unif. Impact	5	-	-	-	-	-	
Tail Link/Disk -Unif. Impact	5	-	-	-	-	35	
Disk Rim -Unif. Impact	2070	-	-	-	-	-	

STONE & WEBSTER ENGINEERING CORPORATION

CALCULATION SHEET

5010.65

CALCULATION IDENTIFICATION NUMBER				
J.O. OR W.O. NO.	DIVISION & GROUP	CALCULATION NO.	OPTIONAL TASK CODE	PAGE 29
12210	NM(C)	2043	SQE	REV 1

TABLE 8.6 DISK RIM NODAL IMPACT LOADS OF 182/4AOV7022A

NODE \ Seconds-(x10^4)	.34	0.2	3.8	1.0	1.0	16.	15.	.4	2.	4	6	6.8	8.
26 (Kips)	576	553	505	400	400	481	481	354	100.	505	180	216	158
27	365	525	490	410	410	242	242	335	45	489	194	409	186
28	420	285	625	610	610	2	2	283	347	521	258	532	205
29	290	210	605	756	756	180	180	206	484	604	247	500	116
30	215	105	325	693	693	448	448	102	349	521	277	362	349
31	410	100	370	515	515	741	741	98	401	368	578	311	77
32	875	325	685	810	810	1380	1385	320	900	384	932	554	8
SUM.	4251	3328	6320	7178	7178	5087	5095	2722	4252	6095	4620	5098	2032

REF RUN # 35N, TDB 10/24/84

DISK IMPACT LOADS ARE CALCULATED BY ABSOLUTE SUM OF ALL THE NODAL LOADS WITH THE CONSIDERATION OF THE SYMMETRICAL OF THE NODES :

SUM = 1 * (LOAD OF NODE 26) + 2 * (SUMMATION OF LOADS FROM NODE 26 TO NODE 31) + 1 * (LOAD OF NODE 32)

STONE & WEBSTER ENGINEERING CORPORATION

CALCULATION SHEET

5010.65

CALCULATION IDENTIFICATION NUMBER				
J.O. OR W.O. NO.	DIVISION & GROUP	CALCULATION NO.	OPTIONAL TASK CODE	PAGE 30
12210	NM(C)	2043	3QE	REV 1

TABLE 8.6 DISK RIM NODAL IMPACT LOADS OF 1B31 # ADV7032A (CONT.)

Seconds x10⁴ / NODE	.8	1.6	2.4	4.4	5.6	6.4	7.6	8.4	9.2	
26 (KIPS)	449	481	323	306	55	296	76	287	257	
27	415	242	258	267	38	250	116	218	195	
28	333	2	56	177	1.	172	200	138	271	
29	320	180	89	97	30	179	218	169	341	
30	413	448	29	94	74	280	119	197	253	
31	278	741	47	366	167	486	145	116	442	
32	128	1280	149	940	330	932	409	107	821	
SUM	4095	5087	2148	3248	1055	3962	2081	2070	4282	

REF RUN # 35N, TDB 10/24/84

SUM = 1* (LOADS OF NODE 26) + 2* (SUMMATION OF LOADS FROM NODE 26 TO NODE 31) + 1* (LOADS OF NODE 32)

Stone and Webster Engineering Corporation
CALCULATION SHEET

Calculation Identification Number				
J.O./W.O. NO. 12210	DIVISION & GROUP NM(C)	CALCULATION NO. 2043	OPTIONAL CODE SQE	PAGE 31 REV 1

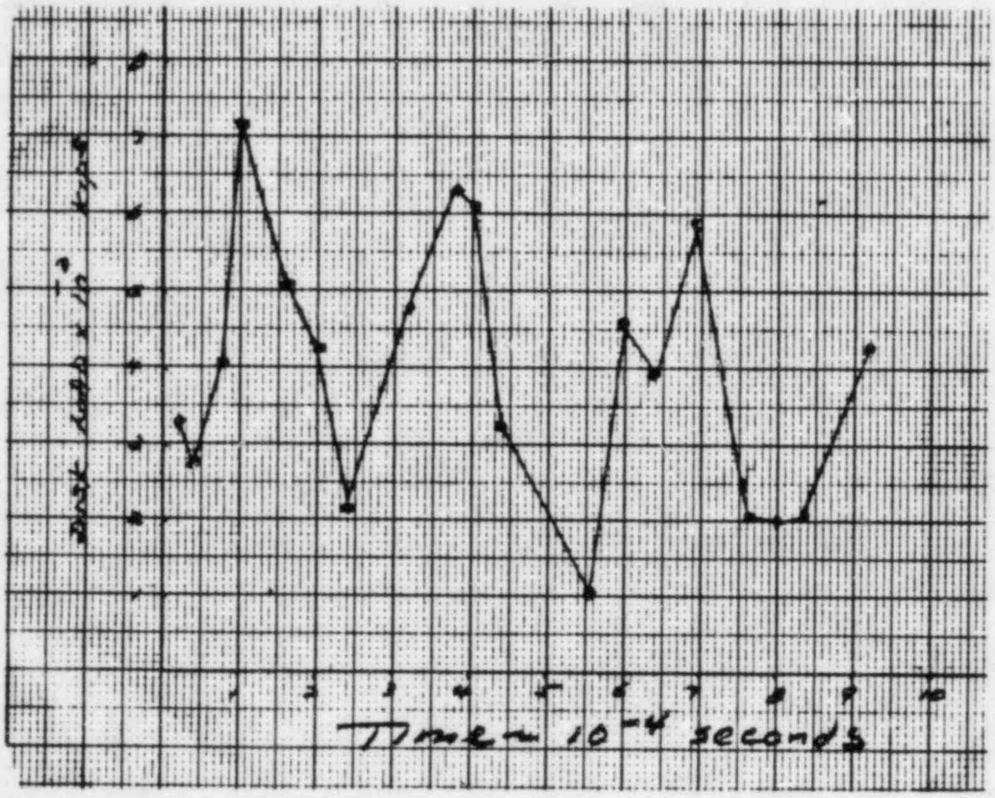

Figure 8.2 Disk Impact Load vs Time for AOVF32

9. INTEGRITY OF VELAN CHECK VALVE 1821*F010

9.1 DISK (SA105)

Uniform impact of the disk on the seat generates a reaction of 2.07×10^6 #, as given by FXK in Table 8.5. Acting simultaneously with impact is the pressure surge from rapidly closing the valve. The maximum pressure is used although it occurs several milli seconds after impact.

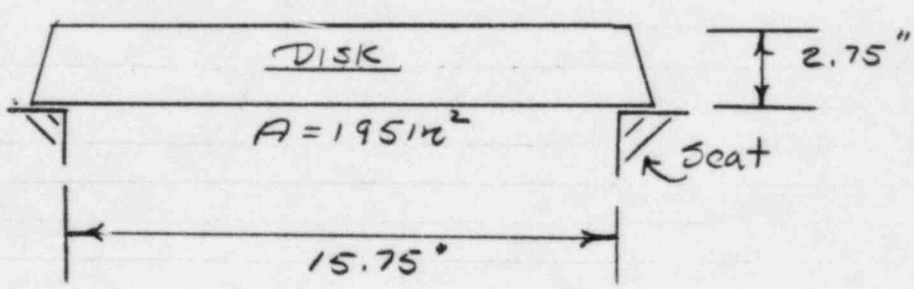

$.62 \times 10^6$ # (3200 psi)

2.07×10^6 # (impact)

2.69×10^6 #

STONE & WEBSTER ENGINEERING CORPORATION

CALCULATION SHEET

5010.65

CALCULATION IDENTIFICATION NUMBER				REV. 1
J.O. OR W.O. NO.	DIVISION & GROUP	CALCULATION NO.	OPTIONAL TASK CODE	PAGE 9-2
12210	NM(C)	2043	SQE	

Shear Out

The allowable shear load in the disk at the inside diameter of the seat where the bending stress in the disk is zero, is given by

$$P_u = .7 \frac{\sigma_u}{\sqrt{3}} \cdot \text{shear area} \cdot \text{strain rate factor}$$

$$= .7 \left(\frac{70000}{1.73}\right) (15.75\,\pi\, 2.75)(2)$$

$$= 7.7 \times 10^6 \ \#$$

since $7.7 \times 10^6 \# > 2.7 \times 10^6$, FS = 2.9 OK

the integrity of the disk in shear out is demonstrated.

Rupture

The disk must absorb the impact energy at strains below the rupture level. The impact energy

$$= \frac{192}{32} (60)^2 \frac{12}{2} = 129,000 \text{ in}\#$$

where effective disk weight $= 185 + \frac{20}{3} = 192^{\#}$ = 190

CALCULATION IDENTIFICATION NUMBER				REV. 1
J.O. OR W.O. NO. 12210	DIVISION & GROUP NA(C)	CALCULATION NO. 2043	OPTIONAL TASK CODE SQE	PAGE 9-3

The plastic strain energy of a circular disk from Appendix B

$$= \frac{\pi}{2}\left(\frac{\pi}{2}-1\right) \sigma_y t^2 y_0$$

$$= .89\ (29100)\ (2.75)^2\ y_0 \quad = \quad 196,000\ y_0$$

Equating to the impact energy and solving for the deflection at the center of the disk

$$y_0 = \frac{129,000}{196000} = .66''$$

From Appendix B, the maximum strain associated with this deflection is

$$\epsilon = \frac{t}{2}\left(\frac{\pi}{D}\right)^2 y_0 \quad = \frac{2.75}{2}\left(\frac{\pi}{15.75}\right)^2 (.66)$$

$$= .036 \text{ in/in}$$

which neglects the deflection of the disk from the pressure, it being in the elastic range and therefore negligible.

CALCULATION IDENTIFICATION NUMBER				
J.O. OR W.O. NO.	DIVISION & GROUP	CALCULATION NO.	OPTIONAL TASK CODE	PAGE 9-4
12210	NM(C)	2043	SQE	REV. 1

The allowable strain

FS= 4.3

$= .7 \times \text{Elongation} = .7(.22) = .154 > .036$ OK

which shows that the disk will not rupture under impact and pressure surge loading combined.

9.2 Pin (SA105)

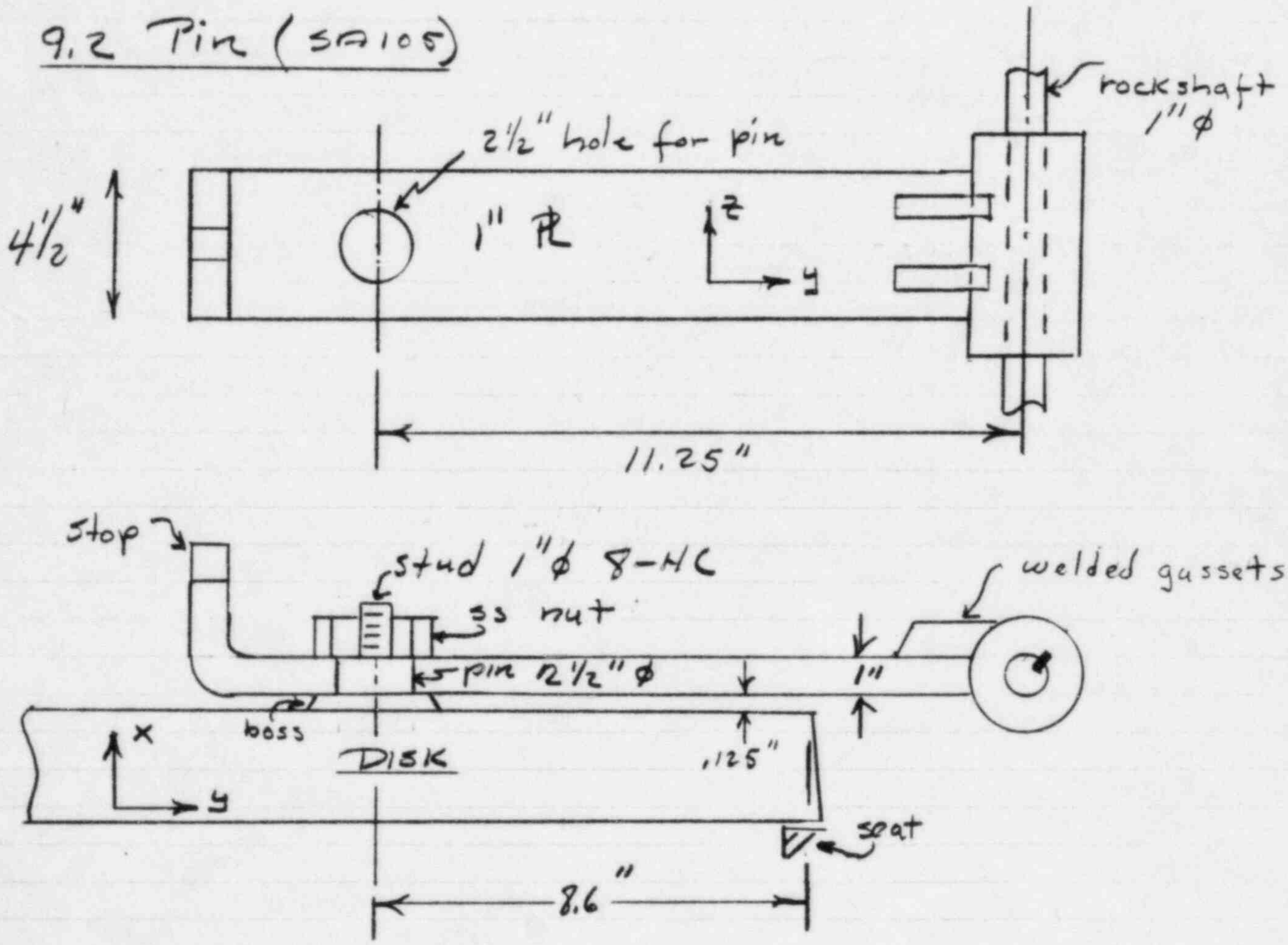

STONE & WEBSTER ENGINEERING CORPORATION

CALCULATION SHEET

5010.65

CALCULATION IDENTIFICATION NUMBER				
J.O. OR W.O. NO. 12210	DIVISION & GROUP NM(C)	CALCULATION NO. 2043	OPTIONAL TASK CODE SQE	PAGE 9-5 REV. 1

The pin and stud are integral and welded to the disk. A ss nut locked to the stud keeps the tail link tight to the boss.

Pre-impact

The centrifigal force, Fc, is reacted by shear on the pin. The shear stress on the pin

$$= F_c / \text{Area of pin}$$

$$= 21500/4.9 = 4400 \text{ psi}$$

the allowable shear stress

$$= .7 S_u/\sqrt{3} = .7(70000)/1.73$$

$$= 28300 \text{ psi} > 4400 \qquad \underline{FS = 6.4} \quad \text{OK}$$

the centrifigal force is eccentric to the tail link, generating a moment which is reacted by the stud in tension and the boss in compression.

$$= F_c\left(\frac{2.75}{2} + .125 + \frac{1}{2}\right)$$

CALCULATION IDENTIFICATION NUMBER				
J.O. OR W.O. NO.	DIVISION & GROUP	CALCULATION NO.	OPTIONAL TASK CODE	PAGE 9-6
12210	NM(C)	2043	SQE	REV. 1

$= 21,500 (2.0) = 43,000$ in#

The distance between the edge of the boss and the ℄ stud = 3.5/2 = 1.75 in. Dividing into the moment yields the force on the stud

$= 43,000 / 1.75 = 24,600$#

which corresponds to a tensile stress

$= 24,600 / .60$

$= 41,000$ psi

The allowable stress in tension on the stud

$= .7 S_u = .7 (70000)$

$= 49,000$ psi $> 41,000$ FS=1.2 OK

Hence, the integrity of the stud is demonstrated for pre-impact loads.

CALCULATION IDENTIFICATION NUMBER				
J.O. OR W.O. NO.	DIVISION & GROUP	CALCULATION NO.	OPTIONAL TASK CODE	PAGE 9-7
12210	NM(C)	2043	SQIE	REV. 1

Uniform Impact

From Table 8.5, a force FXK = 5 Kips acts in compression at the disk center which is in no way carried by the pin or stud. Also acting is a moment MZK = 35 ink, resulting in a bending stress on the pin

$$= \frac{Mc}{I} = 35000\left(\frac{2.5}{2}\right)/1.9$$

$$= 23{,}000 \text{ psi} < 49000, \quad \underline{FS = 2.1} \quad OK$$

which demonstrates the integrity of the pin under uniform impact loads.

Point Impact

These forces and moments from Table 8.3 are much lower than those resulting from pre-impact and uniform impact, because of the flexibility of the tail link in bending and

torsion. Hence, integrity of the pin is demonstrated for point impact loading.

9.3 Tail Link (SA105)

Pre-Impact

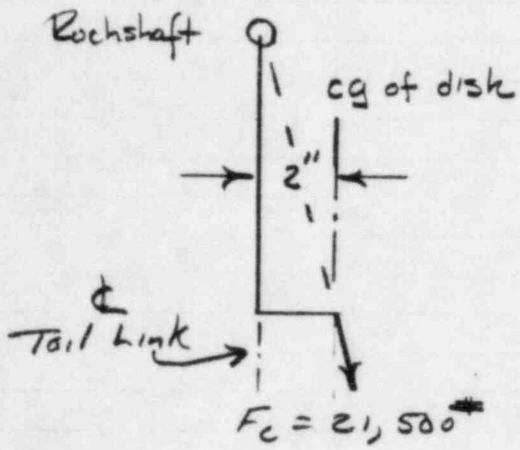

The centrifugal force, F_c, loads the tail link in direct tension and bending, Assuming that the nut makes the full tail link section effective in bending, the total tensile stress

$$= \frac{F_c}{Area} + F_c(2''\text{arm})\,c/I$$

$$= \frac{21,500}{2} + 21500(2)(.5)/.375$$

$$= 10,800 + 57,300 = 68,100 \text{ psi}$$

which is greater than the tensile allowable, but less than the ultimate stress of 70,000 psi. 015

FS = 1.03

STONE & WEBSTER ENGINEERING CORPORATION

CALCULATION SHEET

5010.65

CALCULATION IDENTIFICATION NUMBER				
J.O. OR W.O. NO.	DIVISION & GROUP	CALCULATION NO.	OPTIONAL TASK CODE	PAGE 9-9
12210	NM(C)	2043	SQE	REV. 1

Referring to pg A4 of Ref. 1, it is observed that the duration of this stress is less than 1 ms which is not of sufficient duration to develop the strain necessary for serious failure.

The deflection of the disk off the seat just prior to impact

$$= PL/AE = 21500(11.25)/4.5 \times 27E6$$

$$= .002 \text{ inches}$$

which is insignificant compared to the allowable deflection of .25". Hence, the integrity and operability of the tail link under pre-impact loading is demonstrated.

Uniform Impact

The worst case bending for the tail link is caused by deflection of the disk center following impact with the seat, calculated in section 9.1 to be .66 inches including the contribution from the pressure surge. From Appendix A, the

plastic strain corresponding to a deflection, y_o, of a simply supported beam of length = 2 × 11.25

$$\epsilon = \frac{\pi^2}{2} \frac{D y_o}{L^2} = \frac{\pi}{2}^2 \frac{(1)(.66)}{(2 \times 11.25)^2}$$

FS = 26

$$= .006 < .7(22) = .154$$ OK

Since this occurs after the initial kickback loads, the contribution from shear is negligible.

CALCULATION IDENTIFICATION NUMBER				
J.O. OR W.O. NO.	DIVISION & GROUP	CALCULATION NO.	OPTIONAL TASK CODE	PAGE 9-11
12210	NM(C)	2043	SQE	REV. 1

The worst case shear loads, from Table 8.5, are 5 Kips at the rock shaft end and 5 Kips at the pin end. Maximum shear stress

$= 5000/\text{area} = 5000/4.5$

$= 1100$ psi

The allowable shear stress

$= .7\,S_u/\sqrt{3} = .7(70000)/1.7$

$= 28,300 > 1100$ psi   FS = 26   OK

Hence, integrity of the tail link is demonstrated for uniform impact loading.

Point Impact

Point impact loads, as seen from Table 8.5, are much smaller than pre- or uniform impact. Hence, integrity for point impact loads is demonstrated.

9.4 Rock shaft (SS SA564 630, 1100°F draw)

Pre-impact

the rock shaft reacts the centrifigal force in double shear, the stress

$= 21{,}500 / 2\,(\text{Area})$

$= 21{,}500 / 2\,(.79) = 13{,}600$ psi

which is below the allowable

$= .7(133000)/\sqrt{3}$

$= 53{,}800 > 13600$ psi FS=4.0 OK

Uniform Impact

From Table 8.5, the kickback load is 5 kips in double shear, resulting in a stress

$= 5000/(2)(\text{area}) = 2500/.79$

$= 3200$ psi

STONE & WEBSTER ENGINEERING CORPORATION

CALCULATION SHEET

5010.65

CALCULATION IDENTIFICATION NUMBER				PAGE 9-13
J.O. OR W.O. NO.	DIVISION & GROUP	CALCULATION NO.	OPTIONAL TASK CODE	
12210	NM(C)	2043	SQE	REV. 1

the allowable shear stress

$$= .7 S_u/\sqrt{3} = .7(133{,}000)/1.73$$

$$= 53{,}800 \text{ psi} > 3200, \quad \underline{F_S = 17} \quad \text{OK}$$

Point Impact

Referring to Table 8.3 shows that the point impact loads on the rockshaft are much smaller than the loads from pre-impact and uniform impact.

~

Hence, the rockshaft integrity is demonstrated for all critical loads.

9.5 Seat/Disk Interface

The stress caused by impact in the seat and disk material at the interface is calculated from the hammer equation

$$\Delta\sigma = \frac{\Delta u}{c} E$$

where c is the speed of sound in steel. Thus

$$\Delta\sigma = \frac{60}{16{,}400}\, 27E6 = 98{,}800 \text{ psi}$$

The allowable stress for

$$= .7\, S_u\, (\text{strain rate factor})$$

$$= .7\,(70000)(2) = 98000 \text{ psi}$$

Although slightly above the allowable, it is below ultimate and since this stress acts for a time less than 1/2 millisecond (Fig. 8.2), very little damage to the

STONE & WEBSTER ENGINEERING CORPORATION

CALCULATION SHEET

5010.65

CALCULATION IDENTIFICATION NUMBER				
J.O. OR W.O. NO.	DIVISION & GROUP	CALCULATION NO.	OPTIONAL TASK CODE	PAGE 9-15
12210	NM(B)	2043	SQIE	REV. 1

seat/disk interface is indicated. Hence, the leakage will remain within the limits of the RCIC or HPCS systems.

Thus, the allowable becomes

FS=1.4

$$2\,S_u = 2(70{,}000) = 140{,}000 > 98{,}800 \text{ psi}$$ OK

10. INTEGRITY OF ATWOOD/MORRILL CHECK VALVE 1321* AOVF32

10.1 Disk (SA 216 WCC)

Uniform impact of the disk on the seat generates a reaction of 7.2×10^6 #, as given by F×K in Table 8.4. Acting simultaneously with impact is the pressure surge from rapidly closing the check valve.

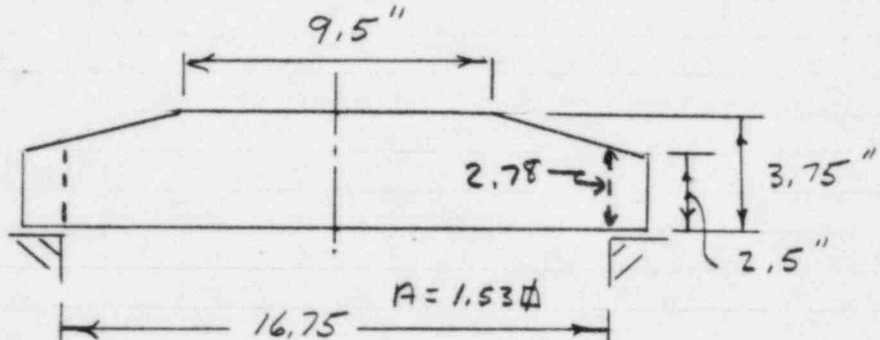

$.68 \times 10^6$ #   3100 psi   pressure surge

7.2×10^6 #   28,600 psi   impact

7.88×10^6 #

STONE & WEBSTER ENGINEERING CORPORATION

CALCULATION SHEET

5010.65

CALCULATION IDENTIFICATION NUMBER				
J.O. OR W.O. NO.	DIVISION & GROUP	CALCULATION NO.	OPTIONAL TASK CODE	PAGE 10-2
12210	NM(C)	2043	SQE	REV. 1

Shear Out

The allowable shear load in the disk at the seat inside diameter where the bending stress is zero

$$= .7(S_u/\sqrt{3}) \cdot \text{shear area} \cdot \text{strain rate factor}$$

$$= .7\left(\frac{70000}{1.73}\right) \cdot (16.75\pi\ 2.78)(2)$$

$$= 8.28 \times 10^6\ \# > 7.88 \times 10^6 \qquad F_S = \underline{1.05}\ \text{OK}$$

Rupture

The disk must absorb the impact energy at strains below the rupture level. The impact energy equals

$$= \frac{417}{32}(45)^2 \frac{12}{2} = 158,000\ \text{in}\#$$

The plastic strain energy of a circular disk from Appendix B, equation 5

$$= \frac{\pi}{2}\left(\frac{\pi}{2} - 1\right) \sigma_y t^2 y_0$$

CALCULATION IDENTIFICATION NUMBER				
J.O. OR W.O. NO.	DIVISION & GROUP	CALCULATION NO.	OPTIONAL TASK CODE	PAGE 10-3
12210	NM(C)	2043	SQE	REV. 1

$$= .89(40000)(3.75)^2 y_o$$

$$= 501{,}000 y_o$$

Equating to the impact energy and solving for the deflection, y_o, at the disk center

$$y_o = 158000 / 501000$$

$$= .32''$$

From Eqn. 6, Appendix B, the maximum strain associated with this deflection is

$$\epsilon = \frac{t}{2}\left(\frac{\pi}{D}\right)^2 y_o \quad = \frac{3.75}{2}\left(\frac{\pi}{16.75}\right)^2 (.32)$$

$$= .021$$

which includes the small contribution from the pressure surge by overstating the incoming energy (mass of disk).

The allowable strain

$$= .7 \times \text{elongation} \quad = .7(.22)$$

$$= .154 > .021$$

$\underline{FS = 7.3}$ OK

CALCULATION IDENTIFICATION NUMBER				PAGE 10-3
J.O. OR W.O. NO.	DIVISION & GROUP	CALCULATION NO.	OPTIONAL TASK CODE	
12210	NM(C)	2043	SQE	REV. 1

$$= .89(40000)(3.75)^2 y_0$$

$$= 501{,}000 y_0$$

Equating to the impact energy and solving for the deflection, y_0, at the disk center

$$y_0 = 158000 / 501000$$

$$= .32''$$

From Eqn. 6, Appendix B, the maximum strain associated with this deflection is

$$\epsilon = \frac{t}{2}\left(\frac{\pi}{D}\right)^2 y_0 \quad = \frac{3.75}{2}\left(\frac{\pi}{16.75}\right)^2 (.32)$$

$$= .021$$

which includes the small contribution from the pressure surge by overstating the impacting energy (mass of disk).

The allowable strain

$$= .7 \times \text{elongation} \quad = .7(.22)$$

$$= .154 > .021 \qquad \underline{FS = 7.3}$$

CALCULATION IDENTIFICATION NUMBER				
J.O. OR W.O. NO.	DIVISION & GROUP	CALCULATION NO.	OPTIONAL TASK CODE	PAGE 10-4
12210	NM(C)	2043	SQE	REV. 1

Hence, the integrity of the disk is demonstrated.

9.2 Rock Shaft (A182 F6a)

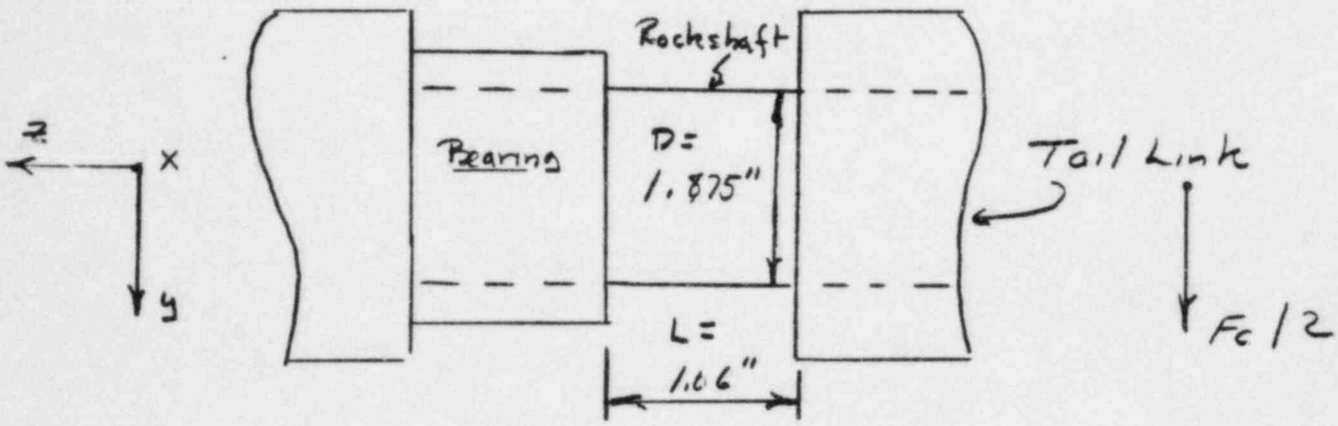

Pre-Impact

The shear stress from the centrifugal force

$= F_c/(2 \cdot \text{area of rock shaft})$

$= 26,300/2(2.8)$

$= 4700$ psi

CALCULATION SHEET

5010.65

CALCULATION IDENTIFICATION NUMBER				
J.O. OR W.O. NO.	DIVISION & GROUP	CALCULATION NO.	OPTIONAL TASK CODE	PAGE 10-5
12210	NMC(c)	2043	SQE	REV. 1

The allowable shear stress

$$= \frac{.7 S_u}{\sqrt{3}} = .7(70000)/1.73$$

$$= 28300 \text{ psi} > 4700 \qquad \underline{FS = 6} \quad OK$$

The bending stress

$$= Mc/I = \frac{26300}{2}(1.06)\frac{1.875}{2}\frac{1}{.61}$$

$$= 21{,}400 \text{ psi}$$

The allowable bending stress

$$= .7 S_u = .7(70000)$$

$$= 49000 > 21{,}400 \text{ psi} \qquad \underline{FS = 2.3} \quad OK$$

Combining via the stress interaction formulas of Reference 9, Appendix F7923

$$R_b = 21{,}400/49000 = .44$$

$$R_s = 4700/28300 = .17$$

Since $R = \sqrt{R_b^2 + R_s^2} = .47 < 1$, integrity under pre-impact loads is demonstrated

CALCULATION IDENTIFICATION NUMBER				
J.O. OR W.O. NO.	DIVISION & GROUP	CALCULATION NO.	OPTIONAL TASK CODE	PAGE 10-6
12210	NM(C)	2043	SQE	REV. 1

Uniform Impact

The rockshaft must carry a kick back load of 240 kips, as given in Table 8.4 for FXK. The resulting stress

$= \frac{FXK}{2} / \text{Area}$

$= \frac{240000}{2} (2.8)$

$= 33{,}600$ psi

The allowable shear stress

$= .7 S_u \cdot \text{strain rate factor} / \sqrt{3}$

$= .7(70000)(2)/1.73$

$= 56{,}600$ psi $> 33{,}600$ $\underline{Fs = 1.7}$ OK

The bending stress

$= MC/I = FXK(2L)(C)/8I$

$= 242000^{*}(1.06)(\frac{1.875}{2})/4(.61)$

$\approx 98{,}600$ psi

* Used actual value from computer run.

CALCULATION SHEET

5010.65

CALCULATION IDENTIFICATION NUMBER				
J.O. OR W.O. NO.	DIVISION & GROUP	CALCULATION NO.	OPTIONAL TASK CODE	PAGE 10-7
12210	NM(C)	2043	SQE	REV. 1

the allowable bending stress

$= .7 S_u \cdot$ strain rate factor

$= .7(70000)(2)$

$= 98{,}000$ psi $< 99{,}000$ allowed $\boxed{NC}$

A non-linear strain analysis is required to demonstrate integrity of the rockshaft.

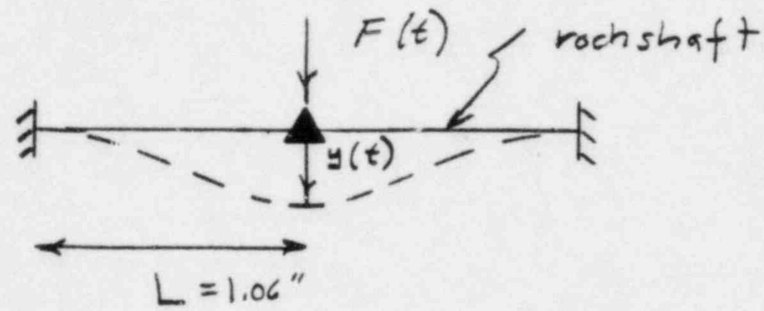

The rockshaft is modelled as shown in the sketch. All the mass of the rock shaft and the tail link bushing are lumped at the point shown by the black triangle, driven by the time varying kickback force F(t), obtained from the kickback loads analysis. Figure 10-1 shows the damped trace. Only the first peak will be used as shown on the Figure. Both the shear and bending strains are

computed as a function of time. Following the procedure of section 9231 of Appendix A, Reference 9, the interactive ratio is formed

$$R = \sqrt{R_s^2 + R_b^2} < 1$$

where, here

R_s = shear strain / allowable

R_b = bending strain / allowable

the differential equation governing the rockshaft response to load is given by

$$m\ddot{y} + ky = F(t)$$

as long as primarily elastic conditions prevail. After essentially plastic conditions are achieved, the equation is switched by FORTRAN logic to

$$m\ddot{y} + R_p = F(t)$$

where R_p is the constant resistance to displacement. The maximum bending moment is given by

$$MOM = \frac{F(2L)}{8} = FL/4$$

The resistance R_p is the value of F when MOM = M_p, the plastic moment. Thus

$$R_p = 4M_p/L$$

For a circular section (Eqn. 4, App. A) this reduces to

$$R_p = \frac{8}{3\pi}\sigma_y A D/L$$

The elastic stiffness, k, for combined shear and bending, since this a short beam, was obtained from the expression for deflection under a concentrated load at the center

$$\delta = \delta_{bending} + \delta_{shear}$$

From reference 15

$$\delta_{bending} = W(2L)^3/192EI = WL^3/24EI$$

For direct shear

$$\tau = \gamma G = \frac{\delta_s}{L} G = W/2A$$

from which is obtained

$$\delta_{shear} = WL/2AG$$

Combining bending with shear

$$\delta = WL^3/24EI + WL/2AG$$

which provides the stiffness

$$k = W/\delta = \frac{1}{L^3/24EI + L/2AG}$$

for elastic conditions.

From Appendix A, the relation between deflection y and the maximum strain is, from eqn. 14 therein

CALCULATION IDENTIFICATION NUMBER				
J.O. OR W.O. NO.	DIVISION & GROUP	CALCULATION NO.	OPTIONAL TASK CODE	PAGE 10-11
12210	NM(C)	2043	SQE	REV. 1

$$\epsilon = \frac{D}{2}\frac{1}{\rho} = \frac{\pi^2}{4}\frac{Dy}{L^2}$$

These equations were coded for computation using the IBM CSMP III simulation program. Details of the coding and results are provided in the following pages. The results show that the interactive strain ratio is less than one, i.e.

$$R = .65 < 1$$ OK

Hence, integrity under uniform impact loading is demonstrated.

FIG. 10-1

(STRESS VECTOR NO. 36) EQULIB CHK RESPONSE FOR ELEMENT NUMBER 30, STRESS TYPE 1 (NOD/DOF X1)

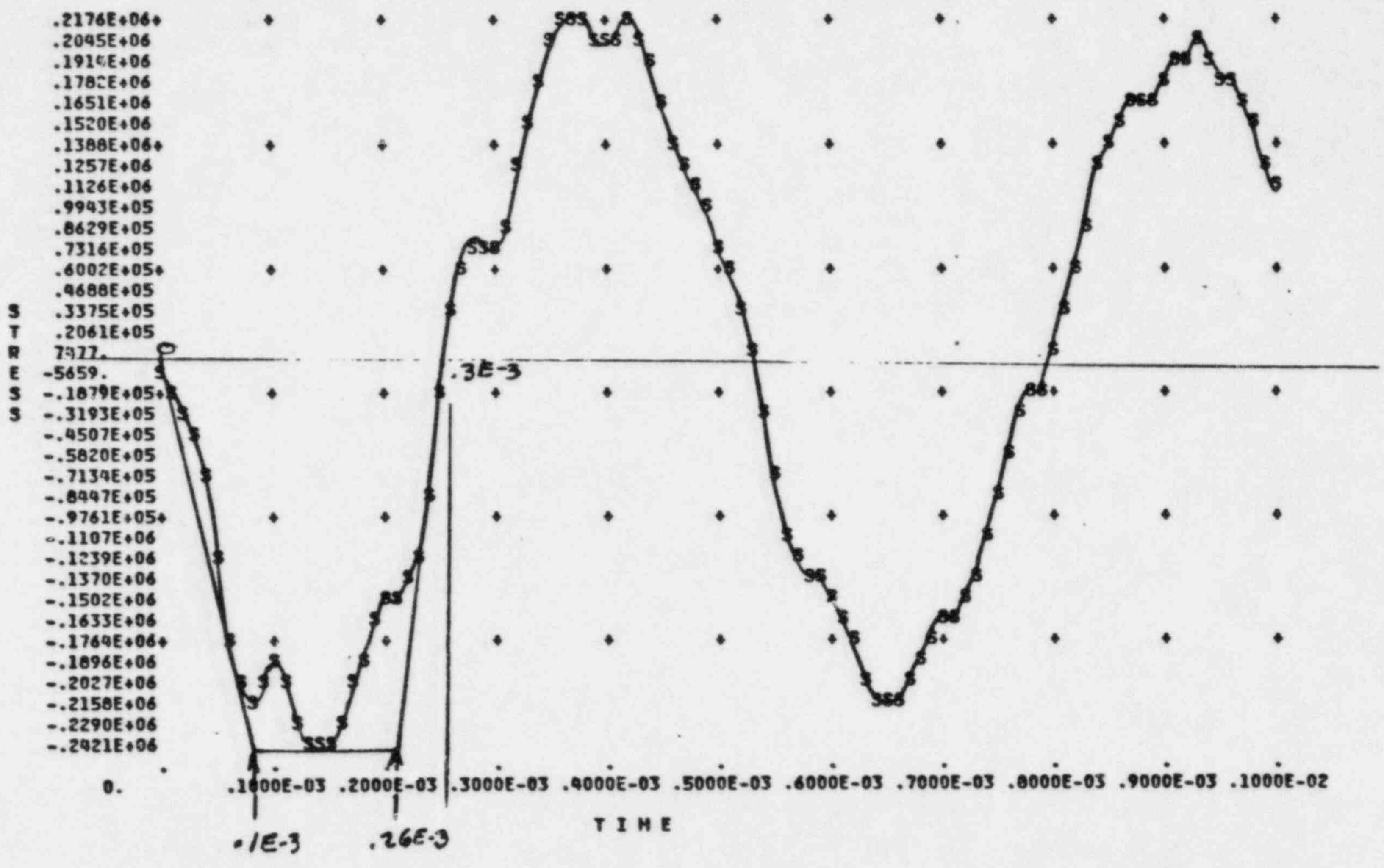

STONE & WEBSTER ENGINEERING CORPORATION

CALCULATION SHEET

J.O. OR W.O. NO.	DIVISION & GROUP	CALCULATION IDENTIFICATION NUMBER: CALCULATION NO.	OPTIONAL TASK CODE	PAGE 10-12 REV. 1

5010.65

STONE & WEBSTER ENGINEERING CORPORATION

CALCULATION SHEET

5010.65

CALCULATION IDENTIFICATION NUMBER				PAGE 10-13 REV. 1
J.O. OR W.O. NO.	DIVISION & GROUP	CALCULATION NO.	OPTIONAL TASK CODE	
12210	NM(C)	2043	5QE	

```
$$$CONTINUOUS SYSTEM MODELING PROGRAM  III   V1M1   TRANSLATOR OUTPUT$$$

TITLE        TIME HISTORY STRAIN IN THE ROCKSHAFT FROM KICKBACK LOAD
TITLE                  1B21*AOV032A CHECK VALVE
TITLE              GSU/RIVER BEND POWER STATION - UNIT 1

* STORED JMG.RS032A:210

FUNCTION TH=(0.,0.),(.1E-3,.242E6),(.26E-3,.242E6),(.3E-3,0.),...
         (.5E-3,0.)
INITIAL
PARAM WTG=71.,E=27.E6,GS=11.E6,L=1.06,A=2.8,IRS=.61,D=1.88
* ROCKSHAFT MATERIAL IS SS A182 F6A, TEMP=500 F
* SIGY=34,700*1.2 = 41,600 PSI FROM APP. F FOR SUPPORTS
PARAM EL=.18,SIGY=41600.,PI=3.14
ALELB=EL
ALELS=ALELB/1.73
CONST G=386.
M=WTG/G
RP=.84*SIGY*A*D/L
EK=PI**2*D/(4.*L**2)
K=1./(L**3/(24.*E*IRS)+L/(2.*A*GS))

DYNAMIC
FT=AFGEN(TH,TIME)
DDY=(FT-RY)/M
PROC RY=FUNC(RP)
RY=K*Y
IF(RY.GT.RP)RY=RP
ENDPROC
DY=INTGRL(0.,DDY)
Y=INTGRL(0.,DY)
BSTRN=EK*Y
SIG1=E*BSTRN
SIG2=MOM*D/(2.*IRS)
MOM=FT*L/4.
SSTRN=Y/L

* 'RATIO' IS CALCULATED IN ACCORDANCE WITH APPENDIX A9231 OF THE
* ASME III B&PV CODE
RATIO=SQRT((BSTRN/ALELB)**2+(SSTRN/ALELS)**2)

TAU1=GS*SSTRN
TAU2=FT/(2.*A)
METHOD RKSFX
* RANGE BSTRN,SSTRN,SIG1,SIG2,TAU1,TAU2,Y,MP,RP,RE,RATIO
TIMER FINTIM=.0004S,PRDEL=.00001,DELT=.0000001
PRINT RATIO,Y,FT,RY
TERMINAL
WRITE(6,10)K
10 FORMAT(/5X,'STIFFNESS OF ROCKSHAFT(K) =',E15.3)
END
STOP

OUTPUT VARIABLE SEQUENCE
ALELB  ALELS  M     RP    EK    K      FT     RY    DDY   DY
Y      BSTRN  SIG1  MOM   SIG2  SSTRN  RATIO  TAU1  TAU2  ZZ1004
```

STONE & WEBSTER ENGINEERING CORPORATION

CALCULATION SHEET

5010.65

CALCULATION IDENTIFICATION NUMBER				
J.O. OR W.O. NO.	DIVISION & GROUP	CALCULATION NO.	OPTIONAL TASK CODE	PAGE 10-14
12210	NM(C)	2043	5QE	REV. 1

TIME HISTORY STRAIN IN THE ROCKSHAFT FROM KICKBACK LOAD
1B21*AOV032A CHECK VALVE
GSU/RIVER BEND POWER STATION - UNIT 1

TIME	RATIO	Y	FT	RY
.0	.0	.0	6.2500E-02	.0
1.00000D-05	5.3960E-05	2.1898E-06	24200.	108.29
2.00000D-05	4.2994E-04	1.7448E-05	48400.	862.86
3.00000D-05	1.4413E-03	5.8491E-05	72600.	2892.6
4.00000D-05	3.3844E-03	1.3735E-04	96800.	6792.3
5.00000D-05	6.5305E-03	2.6502E-04	1.2100E+05	13106.
6.00000D-05	1.1119E-02	4.5121E-04	1.4520E+05	22314.
7.00000D-05	1.7349E-02	7.0406E-04	1.6940E+05	34818.
8.00000D-05	2.5378E-02	1.0299E-03	1.9360E+05	50932.
9.00000D-05	3.5314E-02	1.4331E-03	2.1780E+05	70873.
1.00000D-04	4.7213E-02	1.9160E-03	2.4200E+05	94755.
1.10000D-04	6.1027E-02	2.4766E-03	2.4200E+05	1.2248E+05
1.20000D-04	7.6438E-02	3.1020E-03	2.4200E+05	1.5341E+05
1.30000D-04	9.3037E-02	3.7757E-03	2.4200E+05	1.7353E+05
1.40000D-04	.11057	4.4870E-03	2.4200E+05	1.7353E+05
1.50000D-04	.12901	5.2356E-03	2.4200E+05	1.7353E+05
1.60000D-04	.14838	6.0215E-03	2.4200E+05	1.7353E+05
1.70000D-04	.16866	6.8446E-03	2.4200E+05	1.7353E+05
1.80000D-04	.18986	7.7050E-03	2.4200E+05	1.7353E+05
1.90000D-04	.21198	8.6026E-03	2.4200E+05	1.7353E+05
2.00000D-04	.23501	9.5372E-03	2.4200E+05	1.7353E+05
2.10000D-04	.25895	1.0509E-02	2.4200E+05	1.7353E+05
2.20000D-04	.28382	1.1518E-02	2.4200E+05	1.7353E+05
2.30000D-04	.30960	1.2564E-02	2.4200E+05	1.7353E+05
2.40000D-04	.33630	1.3648E-02	2.4200E+05	1.7353E+05
2.50000D-04	.36391	1.4768E-02	2.4200E+05	1.7353E+05
2.60000D-04	.39245	1.5926E-02	2.4200E+05	1.7353E+05
2.70000D-04	.42176	1.7116E-02	1.8150E+05	1.7353E+05
2.80000D-04	.45119	1.8310E-02	1.2100E+05	1.7353E+05
2.90000D-04	.47990	1.9476E-02	60501.	1.7353E+05
3.00000D-04	.50711	2.0580E-02	.0	1.7353E+05
3.10000D-04	.53212	2.1595E-02	.0	1.7353E+05
3.20000D-04	.55481	2.2516E-02	.0	1.7353E+05
3.30000D-04	.57518	2.3342E-02	.0	1.7353E+05
3.40000D-04	.59322	2.4074E-02	.0	1.7353E+05
3.50000D-04	.60893	2.4712E-02	.0	1.7353E+05
3.60000D-04	.62232	2.5255E-02	.0	1.7353E+05
3.70000D-04	.63339	2.5704E-02	.0	1.7353E+05
3.80000D-04	.64213	2.6059E-02	.0	1.7353E+05
3.90000D-04	.64854	2.6319E-02	.0	1.7353E+05
4.00000D-04	.65269	2.6485E-02	.0	1.7353E+05
4.10000D-04	$\boxed{.65440}$	2.6557E-02	.0	1.7353E+05
4.20000D-04	.65384	2.6534E-02	.0	1.7353E+05
4.30000D-04	.65096	2.6417E-02	.0	1.7353E+05
4.40000D-04	.64575	2.6206E-02	.0	1.7353E+05
4.50000D-04	.63822	2.5900E-02	.0	1.7353E+05

Point Impact

Point impact stresses occur before uniform impact stresses and therefore are treated independently. From Table 8,2, the worst case loads - the rockshaft are 60 kips (FXK) and 160 in-kips (MYK). These combine to load the rockshaft

$$= \frac{FXK}{2} + \frac{MYK}{Grip} \quad (maximum)$$

$$= \frac{60}{2} + 160/16.4$$

$$= 40 \text{ in Kips}$$

Since this is much smaller than the load from uniform kickback, no further analysis is required.

CALCULATION IDENTIFICATION NUMBER				
J.O. OR W.O. NO.	DIVISION & GROUP	CALCULATION NO.	OPTIONAL TASK CODE	PAGE 10-16
12210	NM(C)	2043	SQE	REV. 1

10.3 Tail Link

From Table 8.4, the moment acting on the weakest section of the tail link, where it joins the dish 4.5" from ℄ rockshaft, the bending moment is 960 in-kips from uniform impact. The bending stress is calculated

$$\sigma_b = \frac{MC}{I} = 960000\left(\frac{2.9}{2}\right)/30.$$

$$= 46{,}400 \text{ psi}$$

The allowable tensile stress

$$= .7 S_u (\text{stain rate factor})$$

$$= .7(70000)(2) = 98000 > 46400 \text{ psi} \quad \text{OK}$$

The shear stress acting on this section

$$= 240000/43 = 5600 \text{ psi}$$

the allowable shear stress

$$= .7\left(\frac{70000}{1.73}\right)(\text{strain rate factor})$$

CALCULATION IDENTIFICATION NUMBER				
J.O. OR W.O. NO.	DIVISION & GROUP	CALCULATION NO.	OPTIONAL TASK CODE	PAGE 10-17
12210	NA(C)	2043	SQE	REV. 1

$= 56,600$ psi > 5600 FS=10 OK

Applying section 92B1 of appendix A, Ref. 9,

$$R = \sqrt{R_s^2 + R_b^2} < 1$$

$$= \left[\left(\frac{5600}{56,600}\right)^2 + \left(\frac{46400}{98000}\right)^2\right]^{1/2}$$

$$= .48 < 1$$

FS = 2.1 OK

Hence, the integrity of the tail link is demonstrated. For a strain rate factor of 1 instead of 2, this ratio becomes

$$R = .48(2) = .96 < 1$$

CALCULATION IDENTIFICATION NUMBER				
J.O. OR W.O. NO.	DIVISION & GROUP	CALCULATION NO.	OPTIONAL TASK CODE	PAGE 10-18
12210	NM(C)	2043	SQE	REV 1

10.4 Seat/Disk Interface

The stress in the disk and seat at their interface is calculated using the familiar water hammer equation

$$\Delta\sigma = \frac{\Delta u}{c} E$$

where Δu = the impact speed and c = the sonic speed in steel. Thus

$$\Delta\sigma = \frac{45}{16,400} 27 \times 10^6 = 74,000 \text{ psi compression}$$

The allowable tensile stress

= .7 Su (Strain rate factor)

FS = 1.3

= .7(70000) 2 = 98,000 psi > 74000 OK

Hence, the integrity of the seat/disk interface is established, from which it is concluded that the leakage will be within the make-up capability of the RCIC or HPCS systems.

APPENDIX A

Plastic Strain Energy for Beams of Various Cross-section

PLASTIC STRAIN ENERGY FOR BEAMS OF VARIOUS CROSS-SECTION

Ignoring the initial elastic stage, the plastic strain energy is given by the expression

$$E = \int_0^L M_p d\theta \tag{1}$$

where M_p is the plastic bending moment and $d\Theta$ is the angle through which this moment is rotated. For physical reasons, the integral is always positive.

Referring to Figure 2 showing a differential element in the line

$$M_p = Fa = \sigma_y \; A \; a/2$$

since the line stress is at yield, σ_y (assumed for simplicity). The distance 'a' between the center of area above and below the neutral axis is given by the integral expression (Figure 3).

$$\frac{A}{2}\,\frac{a}{2} = \int_o^\pi z \; dA = \int_o^\pi (r\sin\alpha)\;(rtd\alpha)$$

$$\frac{a}{2} = \frac{2}{A}\, r^2 t \int_o^\pi \sin\alpha d\alpha = -\frac{2r^2t}{A}\cos\alpha\Big|_o^\pi = \frac{4r^2t}{A}$$

$$= \frac{4r^2t}{2\pi rt} = \frac{D}{\pi} \tag{2}$$

Thus, the plastic bending moment becomes

$$M_p = \sigma_y A \frac{D}{\pi} \tag{3}$$

for a thin circular tube. By a similar analysis, it is shown that the plastic moment for a solid circular section is given by

$$M_p = \frac{4}{3} r^3 \sigma_y = \frac{2}{3} \sigma_y A D/\pi \quad (4)$$

For a rectangular section of height, h, and width, b

$$M_p = \frac{1}{4} \sigma_y A h$$

To determine $d\Theta$, assume that the deflection curve shown by the dashed line in Figure 1 is approximated by

$$y = y_o \cos \pi x/L \quad (5)$$

Differentiating twice, we obtain

$$y' = \theta = -y_o(\pi/L) \sin \pi x/L \quad (6)$$

$$y'' = \theta' = 1/\rho = -y_o(\pi/L)^2 \cos \pi x/L \quad (7)$$

where $1/\rho$ = curvature of the beam. Noting that $d\theta = \theta' dx$, the expression for energy given by equation 1 becomes

$$E_B = \int M_p d\theta = \int M_p y_o (\pi/L)^2 \cos \pi x/L \, dx$$

Calling $\pi x/L = \xi$, the integration reads

$$E_B = (\pi/L)\, y_o Mp \int_{-\pi}^{\pi} \cos \xi d\xi$$

Remembering that the integrand is never less than zero since energy is always absorbed, change the limits to $\pi/2$ and zero, and multiply by 4

$$E_B = (4y_o/L)\ \pi\ Mp\ \sin\ \Big|_o^{\pi/2}$$

which yields for the plastic strain energy in bending

$$E_B = 4\ \pi\ Mp\ y_o/L \tag{8}$$

The displacement, y_o, must now be related to strain, ε, in order to determine acceptable damage. Referring to Figure 2

$$\varepsilon = (ds-dx)/dx = ds/dx - 1$$

Since $ds = (\rho + r)\ d\theta$, the expression for strain can be written

$$\varepsilon = (\rho + r)\ d\theta/dx - 1$$

But, from equation 7, $d\theta/dx = 1/\rho$ so that

$$\varepsilon = (\rho + r)/\rho - 1 = r/\rho$$

Replacing $1/\rho$ by its equivalent from equation 7

$$\varepsilon = r\left(\frac{\pi}{L}\right)^2 y_o \cos\frac{\pi x}{L}$$

which has for its maximum

$$\varepsilon = \frac{\pi^2}{2}\ \frac{Dy_o}{L^2} \tag{9}$$

$$\frac{y_o}{L} = \frac{2}{\pi^2}\ \frac{L}{D}\ \varepsilon \tag{10}$$

Now, replacing y_o by ε in equation 8 yields

$$E_B = \frac{8}{\pi}\frac{L}{D} M_p \varepsilon \tag{11}$$

for the strain energy of a beam pinned at both ends.

For a beam fixed at both ends, the assumed deflection curve is

$$y = \frac{y_o}{2}\left(\cos\frac{2\pi x}{L} + 1\right) \tag{12}$$

By a similar analysis to the simply supported case, the plastic strain energy in bending for a beam with both ends fixed

$$E_B = 4\pi\, Mp\, \frac{y_o}{L} \tag{13}$$

$$\varepsilon = \frac{D}{2}\,\frac{1}{\rho} = \pi^2\,\frac{Dy_o}{L} \tag{14}$$

$$\frac{y_o}{L} = \frac{1}{\pi^2}\,\frac{L}{D}\,\varepsilon \tag{15}$$

which yields for the plastic strain energy in terms of strain

$$E_B = \frac{4}{\pi}\, Mp\, \frac{L}{D}\,\varepsilon \tag{16}$$

For a beam with one end fixed and the other end pinned, the assumed deflection curve for uniform loading is given by the elastic curve obtained from any edition of Rourk's Formulas for Stress and Strain

$$y = 3.86\, y_o\left[3\left(\frac{X}{L}\right)^3 - 2\left(\frac{X}{L}\right)^4 - \frac{X}{L}\right] \tag{17}$$

where X is measured from the pinned end. Again, a similar analysis leads to the result for plastic strain energy in bending

$$E_B = 3\pi\, Mp\, \frac{y_o}{L} \tag{18}$$

$$\varepsilon = 1.2\,\pi^2 \,\frac{Dy_o}{L^2} \tag{19}$$

$$\frac{Y_o}{L} = \frac{.83}{\pi^2}\,\frac{L}{D}\,\varepsilon \tag{20}$$

which yields for the plastic strain energy in terms of strain

$$E_B = \frac{2.5}{\pi}\,M_p\,\frac{L}{D}\,\varepsilon \tag{21}$$

CALCULATION SHEET

5010 65

CALCULATION IDENTIFICATION NUMBER				
J.O. OR W.O. NO.	DIVISION & GROUP	CALCULATION NO.	OPTIONAL TASK CODE	PAGE A-7
12210	NM(C)	2043	SQE	

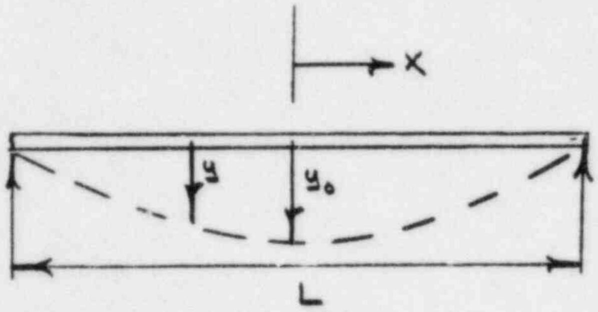

FIGURE 1

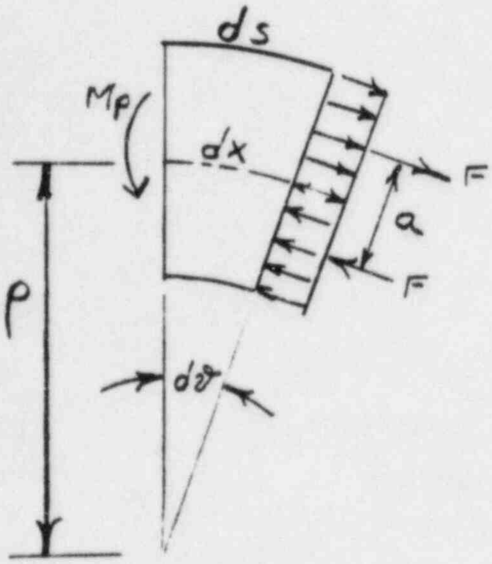

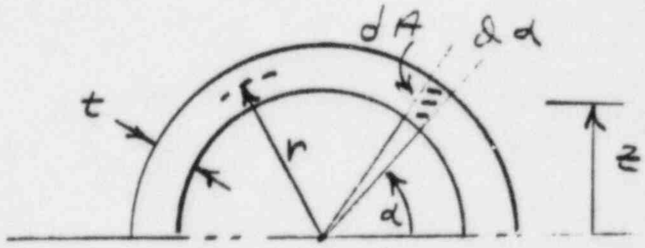

FIGURE 3

FIGURE 2

APPENDIX B

Plastic Strain Energy for a Circular Plate in Bending

PLASTIC STRAIN ENERGY FOR A CIRCULAR PLATE

The strain energy of a plate in bending is derived below for a purely plastic response to a uniform loading. Ignoring the elastic contribution greatly simplifies the analysis and is conservative.

A deflection curve that satisfies the simply-supported boundary conditions is assumed

$$y = y_o \cos \frac{\pi r}{2R} \tag{1}$$

$$y' = y_o \left(\frac{\pi}{2R}\right) \sin \frac{\pi r}{2R}$$

$$y'' = y_o \left(\frac{\pi}{2R}\right)^2 \cos \frac{\pi r}{2R} = \frac{1}{\rho} = \frac{d\theta}{dr} \tag{2}$$

Referring to the Figure, the strain energy is given by

$$E_s = \int M_p \, d\theta \tag{3}$$

summed over the plate where M_p is the moment for fully plastic loading. Referring to the figure, because of symmetry, the plastic moment acting at radius, r, is simply the unit moment, M_p times the circumference at radius, r.

$$M_p = \left(\frac{t}{2}\right)^2 \sigma_y (2\pi r) \tag{4}$$

Inserting into the integral

$$E_s = \int_o^R \left(\frac{t}{2}\right)^2 \sigma_y (2\pi r) \, y_o \left(\frac{\pi}{2R}\right)^2 \cos \frac{\pi r}{2R} \, dr$$

which reduces to

$$E_s = \left(\frac{t}{2}\right)^2 \sigma_y \, y_o 2\pi \int_o^{\pi/2} \xi \cos \xi \, d\xi$$

with $\xi = \frac{\pi r}{2R}$

Integrating,

$$E_s = 2\pi\sigma_y \left(\frac{t}{2}\right)^2 y_o \left[\cos \xi + \xi \sin \xi\right]_o^{\pi/2}$$

$$= \frac{\pi}{2}\left(\frac{\pi}{2} - 1\right) \sigma_y \, t^2 y_o \tag{5}$$

The plastic strain by definition equals

$$\varepsilon = \frac{ds-dr}{dr} = \frac{ds}{dr} - 1$$

$$= \frac{(\rho+t/2)d\theta}{\rho d\theta} - 1 = t/2\rho$$

Since $1/\rho = \theta'$, this becomes

$$\varepsilon = \frac{\pi^2}{8} \frac{t y_o}{R^2} \tag{6}$$

which can be used to eliminate y_o from the energy equation

$$E_s = \frac{2}{\pi}\left(1 - \frac{2}{\pi}\right) \sigma_y \, V\varepsilon \tag{7}$$

where V= volume of the circular plate ($\pi R^2 t$) and ε is the maximum strain.

STONE & WEBSTER ENGINEERING CORPORATION

CALCULATION SHEET

5010.65

CALCULATION IDENTIFICATION NUMBER				
J.O. OR W.O. NO.	DIVISION & GROUP	CALCULATION NO.	OPTIONAL TASK CODE	PAGE B-4
12210	NM(C)	2043	SQE	

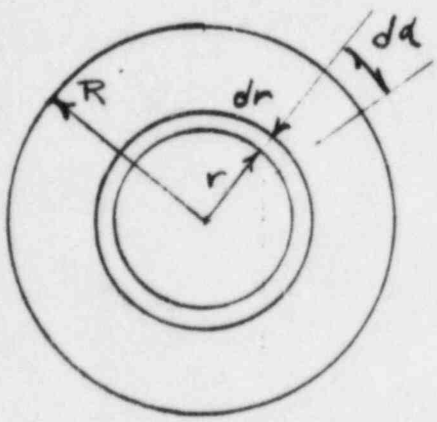

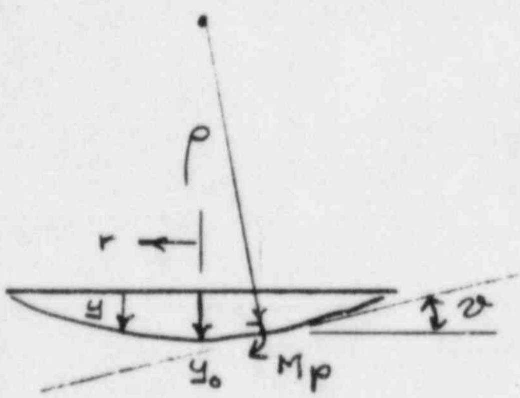

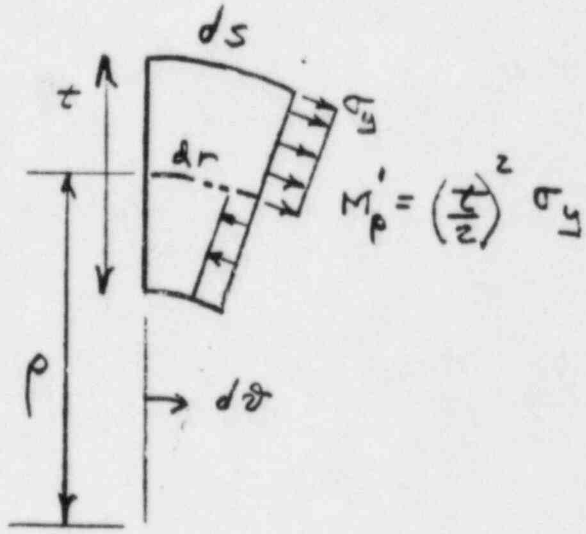

APPENDIX C

Miscellaneous Reference Material

Stone and Webster Engineering Corporation
CALCULATION SHEET

Calculation Identification Number				
J.O./W.O. NO. 12210	DIVISION & GROUP NM(C)	CALCULATION NO. 2043	OPTIONAL CODE SQE	PAGE C-2 0720

REFERENCE 7

122/0- NM(c) S&Z-2043

C-3/20

J. C. WAMBOLD
Assistant Professor,
Department of Mechanical Engineering,
The Pennsylvania State University,
University Park, Pa.

F. D. JU
Professor,
Department of Mechanical Engineering,
The University of New Mexico,
Albuquerque, N. Mex.

Safe Impact Speed for Hollow Circular Cylinders

An analog simulation of stress wave propagation in hollow circular cylinders with, and without, end caps for the purpose of determining safe impact velocity. The results were checked with experimental tests run by Sandia Corporation.

Introduction

THE PRESENT paper deals with problems of axisymmetric elastic wave propagation in moderately thick-walled hollow cylinders with a flat end cap, Fig. 1. The analysis was done to provide design engineers with a program with which to

1 Check the safety of cylinders from fracture due to end-on impact.

2 Predict the safe speed of end-on impact without fracture for various designs to establish the effects of each variable—i.e., material, length, width, etc.

The impact speed is of the order of hundreds fps so that the shear effect[1] is predominant and any initiation of fracture is to be considered failure. Thus the fracture could be caused by the shear wave, as observed from many geological phenomena such as "shear cones" of volcanoes and meteor impact. With the foregoing objectives and restricting this work to polycrystalline material of low ductility, it is postulated that the initiation of fracture will occur before there is time for plastic flow [1][2] and the linear theory of elastic applies.

The mathematical model for the fracture initiation of a closed-end hollow cylinder is essentially the Pochhammer-Chree model [2, 3]. The problem of uncapped hollow circular cylinders was treated by Ghosh [4], McFadden [5], Hermann and Mirsky [6], and more recently, by Gazis [7] whose work Fitch [8] verified with experiments on 5052 aluminum-alloy cylinders.

[1] At high pressure, the shock wave is hydrodynamic in nature. Fracture then is mostly due to the "spalling" effect.

[2] Numbers in brackets designate References at end of paper.

Contributed by the Applied Mechanics Division for publication (without presentation) in the JOURNAL OF APPLIED MECHANICS.

Discussion on this paper should be addressed to the Editorial Department, ASME, United Engineering Center, 345 East 47th Street, New York, N. Y. 10017, and will be accepted until July 20, 1970. Discussion received after the closing date will be returned. Manuscript received by ASME Applied Mechanics, May 12, 1969; final revision, December 31, 1969. Paper No. 70-APM-QQ.

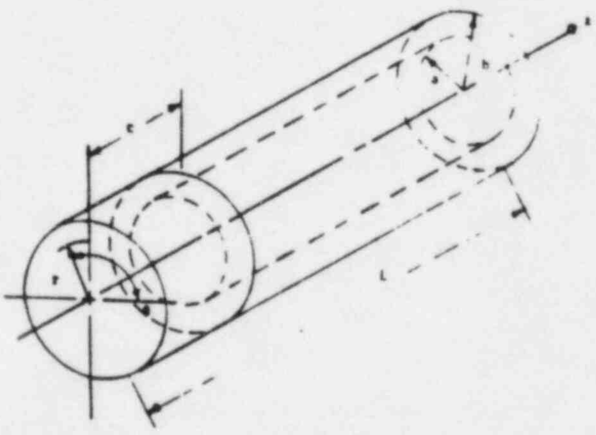

Fig. 1 Region of analysis and definition of coordinate system

The Pochhammer-Chree model may be treated by (a) analytic methods or by (b) numerical methods. The analytical methods may involve the use of transform calculus (e.g., DeVault and Curtis [9]) or where displacements are assumed to be harmonic (e.g., Pochhammer-Chree [2, 3], and Gazis [7]). The analytical methods are generally restricted to pressure bars of relatively simple geometry such as a solid bar on a hollow cylinder.

The numerical methods involve use of (a) the digital computer (e.g., Thorne and Hermann [10]) or (b) the simulation technique. The digital programming, due to intrinsic stability problem has, in the past, introduced artificial damping terms either in the governing differential equation or in the numerical method. The criticism is that in order to gain stability, the basic characteristic of the dynamic system is altered. Lax and Wendroff [12] offered a method of getting stable numerical solutions and later, after this work was started, Clifton [13], using the Lax-Wendroff

122/0- NM(c)- SGE-2043 C4/20

method, offers a method of solving plane problems. Still later, Berthol [14] offers further work on the solutions of two-dimensional wave propagation of finite bars. The present paper employs a simulation technique to solve the problem of closed-end hollow cylinder which does not necessitate the introduction of any artificial damping terms. In addition, and perhaps the main advantage of simulating by analog computer is that the designer can vary parameters to obtain an optimum design. Parameters can be varied on both digital and analog but with the following tradeoff—Berthoff indicates a solution time on the digital of approximately 1 hr, the analog solutions are of the order of 3 sec. Resetting of new parameters takes seconds on the digital and less than 5 min on the analog. Since many solutions are required, the analog offered a great savings in both cost and time.

Mathematical Model

Interior. The basic governing differential equation for the displacement field, $\mathbf{u}(r, z, t)$ in the body is

$$c_d^2 \text{ grad div } \mathbf{u} - 2c_s^2 \text{ curl } \boldsymbol{\omega} = \ddot{\mathbf{u}} \qquad (1)$$

where $\boldsymbol{\omega}(r, z, t)$ is the rotation field such that $\boldsymbol{\omega} = \frac{1}{2}$ curl $\mathbf{u}$, c_d and c_s are the dilatational and shear wave speeds, respectively, and $\ddot{\mathbf{u}} = (\partial^2 \mathbf{u}/\partial t^2)$. In terms of axisymmetric cylindrical coordinates (r, z), equation (1) may be written

$$c_d^{-2}\ddot{u}_r = \frac{1}{r}(ru_{r,r})_{,r} - \frac{u_r}{r^2} + \left(\frac{c_s}{c_d}\right)^2 u_{r,zz} + \left(1 - \frac{c_s^2}{c_d^2}\right) u_{z,rz} \qquad (1a)$$

$$c_d^{-2}\ddot{u}_z = u_{z,zz} + \left(\frac{c_s}{c_d}\right)^2 \frac{1}{r}(ru_{z,r})_{,r} + \left(1 - \frac{c_s^2}{c_d^2}\right) u_{r,rz} + \frac{u_{r,z}}{r} \qquad (1b)$$

where (u_r, u_z) are the radial and longitudinal components of $\mathbf{u}$, the comma in the subscripts denotes partial differentiation with respect to the coordinates following the comma.

Boundaries. On the boundaries, the following constraints must be met, Fig. 1:

On $r = a$, $z > c$, $\sigma_{ri} = 0$ $(i = r, \theta, z)$. Therefore

$$\left[2\alpha^2 u_{r,r} + (1 - \alpha^2)\left(u_{r,r} + \frac{u_r}{r} + u_{z,z}\right)\right] = 0 \qquad (2a)$$

$$[u_{r,z} + u_{z,r}] = 0 \qquad (2b)$$

On $r = b$, $\sigma_{ri} = 0$ $(i = r, \theta, z)$. Therefore

$$\left[2\alpha^2 u_{r,r} + (1 - \alpha^2)\left(u_{r,r} + \frac{u_r}{r} + u_{z,z}\right)\right] = 0 \qquad (3a)$$

$$[u_{r,z} + u_{z,r}] = 0 \qquad (3b)$$

On $z = c$, $r < a$, $\sigma_{zi} = 0$ $(i = r, \theta, z)$. Therefore

$$\left[2\alpha^2 u_{z,z} + (1 - \alpha^2)\left(u_{r,r} + \frac{u_r}{r} + u_{z,z}\right)\right] = 0 \qquad (4a)$$

$$[u_{r,z} + u_{z,r}] = 0 \qquad (4b)$$

At the corner $r = a$, $z = c$, $\sigma_{\hat{r}i} = 0$, $i = \hat{r}, \theta, \hat{z}$ where $\hat{r}$ and $\hat{z}$ are rotated about r by 45 deg. Therefore

$$\sigma_{\hat{r}\hat{r}} = \frac{\sigma_{rr} + \sigma_{zz}}{2} - \sigma_{rz} \quad \text{and} \quad \sigma_{\hat{r}\hat{z}} = \frac{\sigma_{rr} - \sigma_{zz}}{2}$$

This makes the following restrictions on displacements:

$$(1 - \alpha^2)(u_{r,r} + u_{z,z}) + (1 - 2\alpha^2)\frac{u_r}{r} - \alpha^2(u_{r,z} + u_{z,r}) = 0 \qquad (5a)$$

$$u_{r,r} - u_{z,z} = 0 \qquad (5b)$$

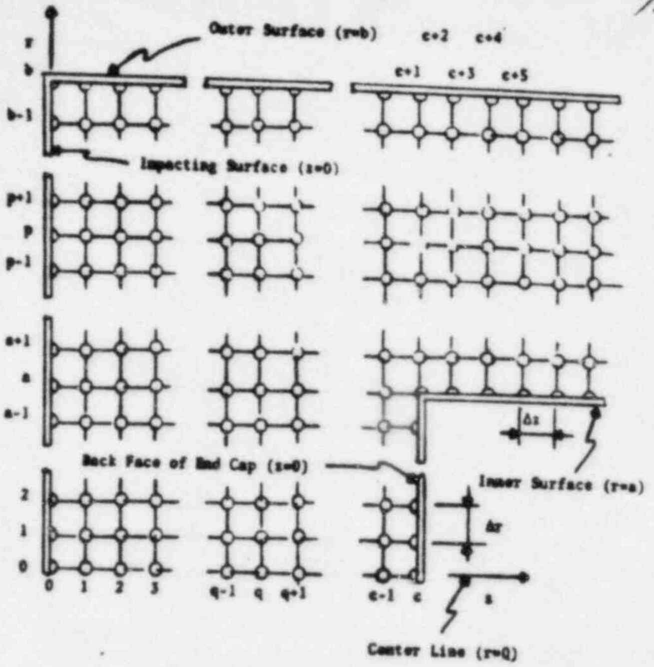

Fig. 2 Finite-difference network

where $\alpha = c_s/c_d$. The equations of motion (1a) and (1b) subject to the boundary values (2)–(5) along with the input loading specification completely define the mathematical model.

Analog Model

Adaptions of Equations to Analog. Before the partial differential equations can be solved by the analog simulation, the problem must be converted to a system of linear difference-differential equations by converting spatial variables (r, z) to discrete variables, while time (t) is retained as the continuous variable. The spatial position in (r, z) is therefore designated as junction points (p, q), respectively, Fig. 2, in a two-dimensional net. The governing equations (1) become the following second-order difference-differential equations.

$$\left(\frac{\Delta r}{c_d}\right)^2 \frac{d^2}{dt^2}(u_r^{p,q}) = 2Au_r^{p,q} + B_1 u_r^{p+1,q} + B_2 u_r^{p-1,q} + D_1(u_r^{p,q+1} + u_r^{p,q-1}) + E_1(u_z^{p+1,q+1} - u_z^{p-1,q+1} - u_z^{p+1,q-1} + u_z^{p-1,q-1}) \qquad (6a)$$

$$\left(\frac{\Delta r}{c_d}\right)^2 \frac{d^2}{dt^2}(u_z^{p,q}) = 2Ku_z^{p,q} + u_z^{p,q+1} + u_z^{p,q-1} + D_2(B_1 u_z^{p+1,q} + B_2 u_z^{p-1,q}) + E_2(u_r^{p+1,q+1} - u_r^{p+1,q-1} - u_r^{p-1,q+1} + u_r^{p-1,q-1}) + M(u_r^{p,q+1} + u_r^{p,q-1}) \qquad (6b)$$

where Δr and Δz are mesh sizes in r, z, respectively, and $u_i^{p,q}$ $(i = r, z)$ is the value of u_i at $r = p\Delta r$ and $z = q\Delta z$.

$$A = 1 + \alpha^2\beta^2 + \tfrac{1}{2}\gamma, \quad \beta \text{ (mesh ratio)} = \frac{\Delta r}{\Delta z},$$

$$\gamma \text{ (radial size ratio)} = \frac{\Delta r}{r}$$

$$B = 1 + \tfrac{1}{2}\gamma, \quad B_1 = 1 - \tfrac{1}{2}\gamma, \quad D_1 = \alpha^2\beta^2, \quad D_2 = \alpha^2\beta^2$$

$$E_1 = \tfrac{1}{4}\beta(1 - \alpha^2), \quad E_2 = \frac{1}{4\beta}(1 - \alpha^2),$$

$$K = 1\alpha^2\beta^{-2}, \quad M = \frac{(1 - \alpha^2)\gamma}{2\beta}$$

12/10- NM(C) SQE- 2043 CJ/20

The boundary conditions are also described by the difference form as

$$u_r^{a+1,q} = u_r^{a-1,q} + (1 - 2\alpha^2)2\gamma_a u_r^{a,q} + \beta u_z^{a,q+1} - \beta u_z^{a,q-1} \quad (7a)$$

$$p = a, \quad q = c$$

$$u_z^{a+1,q} = u_z^{a-1,q} + \beta(u_r^{a,q+1} - u_r^{a,q-1}) \quad (7b)$$

$$u_r^{b+1,q} = u_r^{b-1,q} + (1 - 2\alpha^2)2\gamma_b u_r^{b,q} + \beta u_z^{b,q+1} - \beta u_z^{b,q-1} \quad (8a)$$

$$p = b, \quad q = 0$$

$$u_z^{b+1,q} = u_z^{b-1,q} - \beta(u_r^{b,q+1} - u_r^{b,q-1}) \quad (8b)$$

$$u_r^{p,c+1} = u_r^{p,c-1} - \frac{1 - 2\alpha^2}{\beta}(u_z^{p+1,c} - u_z^{p-1,c} + 2\gamma u_r^{p,c}) \quad (9a)$$

$$p = a, \quad q = c$$

$$u_z^{p,c+1} = u_z^{p,c-1} - \frac{1}{\beta}(u_r^{p+1,c} - u_r^{p-1,c}) \quad (9b)$$

$$u_r^{a+1,c+1} = u_r^{a+1,c-1} - \frac{4(1 - \alpha^2)\Delta r}{\alpha^2 G_1 a} u_r^{a,c} + \frac{2\beta}{G_1}(u_z^{a+1,c+1}) - \frac{G_2}{G_1}(u_r^{a-1,c+1} - u_r^{a-1,c-1}) - \frac{2\beta}{G_1}(u_z^{a-1,c-1}) \quad (10a)$$

$$p = a, \quad q = c$$

$$u_z^{a+1,c+1} = u_z^{a+1,c-1} + \frac{4\beta(1 - 2\alpha^2)}{\alpha^2 a G_1} u_r^{a,c} - \frac{G_2}{G_1}(u_z^{a+1,c+1}) - \frac{2\beta}{G_1}(u_r^{a-1,c+1} - u_r^{a-1,c-1}) + \frac{G_2}{G_1}(u_z^{a-1,c-1}) \quad (10b)$$

where

$$G_1 = 1 + \beta^2 + \frac{2\beta}{\alpha^2}(1 - \alpha^2) \qquad \gamma_a = \gamma \text{ with } r = a$$

$$G_2 = 1 + \beta^2 - \frac{2\beta}{\alpha^2}(1 - \alpha^2) \qquad \gamma_b = \gamma \text{ with } r = b$$

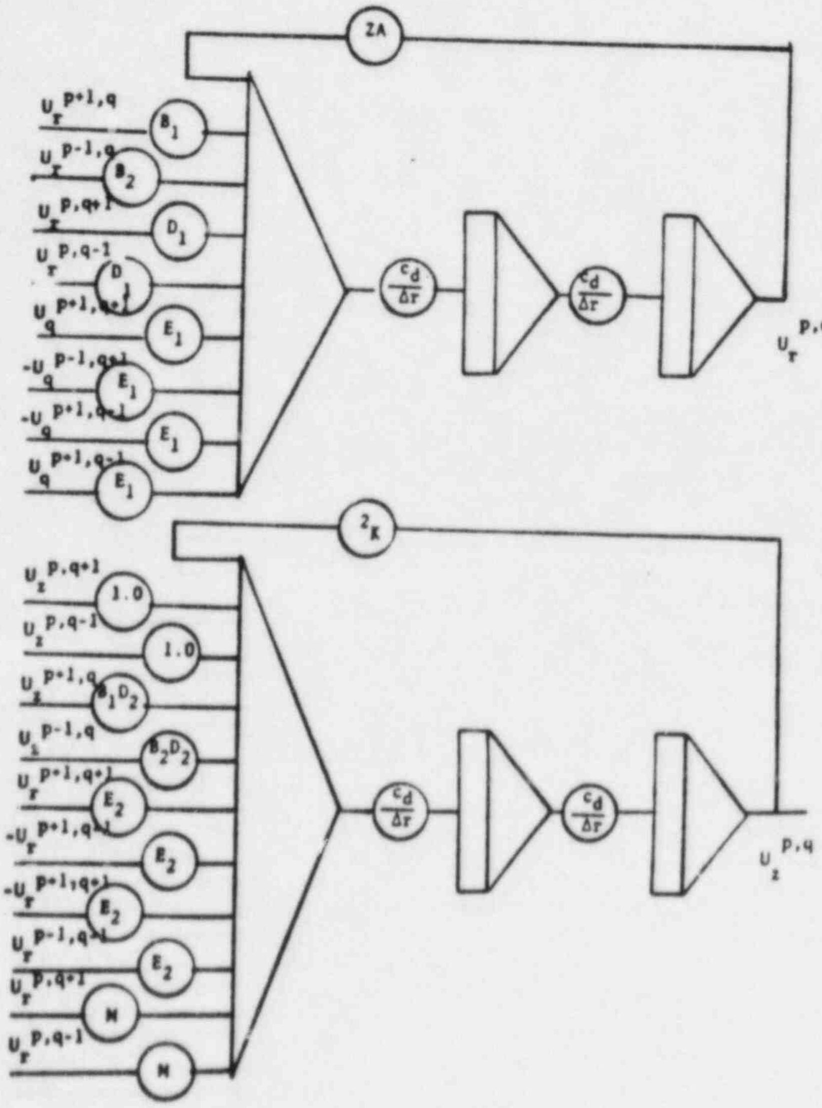

NOT BEING USED

Fig. 3 Analog circuit for interior node point p, q, equation (6). The foregoing equation can also be used on the boundaries if the points outside are artificially created by summing and multiplying interior points as indicated by the boundary equations (7)–(10).

C6/20

122/0 -NM(c)-50Z2043

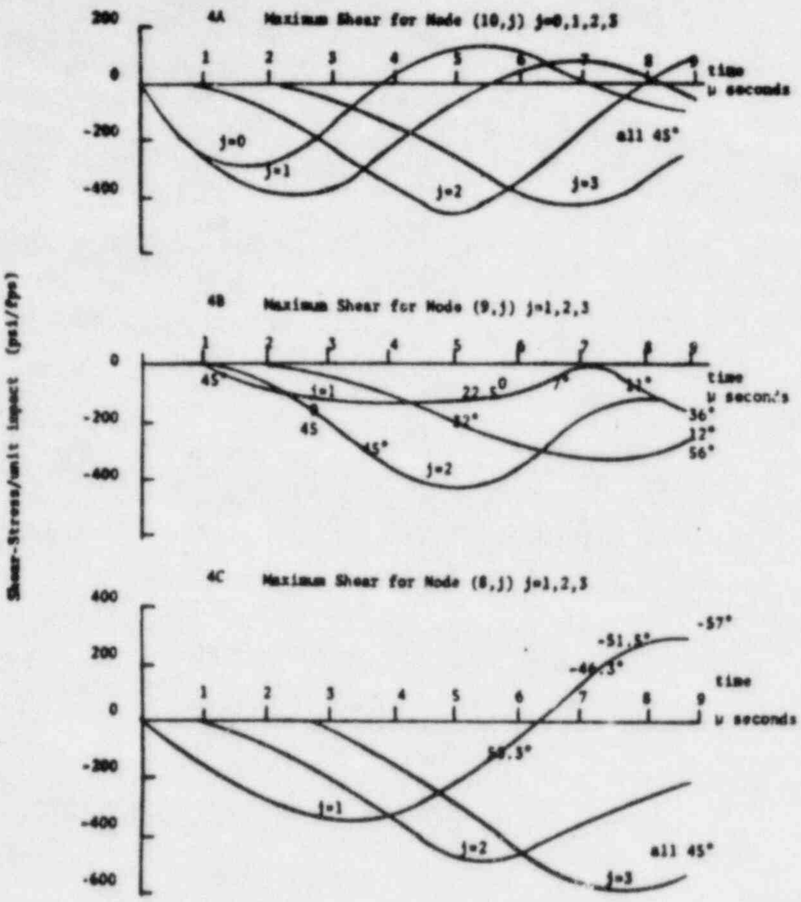

Fig. 4 Stress-time history for maximum shear of problem 3; $\Delta r = 0.1$, $\beta = 1/2$ (refer to Fig. 2 for node numbers)

General Program. The boundary conditions (7)–(10) are combined with the governing difference-differential equations (6) to give a pair of difference-differential equations at each junction point, which relates the radial and axial acceleration there with the surrounding displacements. Thus, by summing the proper surrounding displacement and by integrating twice, the radial and axial accelerations, velocities, and displacements are obtained,[3] Fig. 3.

After one decides on the sizes (end cap thickness, inside and outside diameters), mesh size, and material in terms of modulus of elasticity (E), Poisson's ratio (ν), and density (ρ), the data are put into a digital program and the pot setting for the problem will be given.

Using these pot settings (if digital set pots are available, they can be set directly as was done by the authors) in the analog circuits, one obtains the solution in terms of outputs of 1 volt = $1.2\Delta r\sqrt{\frac{(1-\nu-2\nu^2)}{E}}$ in. (fps of impact) with 10 volts of initial velocity applied to the front surface. Real time is equal to $\Delta r\sqrt{\frac{(1-\nu-2\nu^2)}{E}}\, X$ (computer time).

Table 1 Maximum shear stresses

Position		Problem I		Problem II		Problem III	
Radial	Axial	Stress	Time	Stress	Time	Stress	Time
1.0	0.2	400	2.54	400	3.50	400	3.40
1.0	0.4	-	-	500	4.90	460	4.90
1.0	0.6	300	5.53	380	7.36	410	7.00
1.0	0.8	-	-	320	9.80	-	-
0.9	0.2	-	-	-	-	160	4.20
0.9	0.4	-	-	-	-	440	4.90
0.9	0.6	-	-	-	-	360	7.36
0.8	0.2	-	-	280	3.86	360	5.50
0.8	0.4	-	-	-	-	480	5.06
0.8	0.6	480	5.01	480	7.01	500	7.50
0.8	0.8	540	5.50	-	-	-	-

Shear Stress in psi/fps of impact speed
Time in Microseconds

Discussion and Results

To check for convergence and stability, the problem was run three times, each run with a finer mesh size. All runs were made for model size of $b = 1.0$ in., $a = 0.8$ in., $c = 0.4$ in., a time scaling of $(\Delta z/c_d)$ and stainless steel material. All of the results[4] are summarized in Tables 1 and 2, where problem 3 is the finest mesh, problem 2 is the next, and problem 1 the largest mesh. For problem 3, maximum shear stress-time curves at several critical points are shown in Fig. 4. The results indicate that for low velocity levels the critical shear stress is reached on the inside surface and thus the initiation of a crack at this point, Fig. 4(c). Then at about a 50 percent increase in velocity, the point of initiation of a crack is transferred to the outside surface, Fig. 4(a).

It should be noted that these results apply to a cylinder with

[3] Complete simulation program is referred to Ju and Wambold [15].

[4] The analog simulation was performed on the computer at Holloman AFB.

122/v - NM(c) S&E 2043 C 7/20

Fig. 5 Fracture initiation in a cylinder as a result of end-on impact. Tests were performed at Sandia Corporation, Albuquerque, N. Mex.

the end cap used and that a different end cap could alter the results. The results of velocity magnitude (given in Table 2) and the locations of fracture were in agreement with experiment.[5] Fig. 5 shows a fractured cylinder[4] as a result of end-on impact. For 1018 and 4130 steel, the experimental results give a threshold velocity of 244 and 242, respectively, for visible fracture initiation. The fracture velocity as predicted by the analog simulation are 150 and 220 fps, respectively. The velocities predicted by this work are lower limits since the Tresca's failure theory (maximum shear stress) is generally considered conservative for fracture initiation. In fact, the higher velocity required to initiate fracture on the outside surface is generally needed. Thus, if a high degree of safety is not required, the safe velocity could be taken as the one related to the outside surface fracture velocity rather than that causing fracture on the inside surface.

Having established the feasibility of this technique, one can now take the general program developed and test a particular model to establish a safe impact speed or for a given impact speed find the geometrical and the mechanical characteristics of the model for safe impact without fracture.

In design, a voltage representing the safe impact velocity may be referenced on a comparator and compared to points of maximum stress giving a "go–no-go" test. Thus the design engineer would have an immediate answer as to the safety of his design.

[4] Re: Sandia Corporation.

[5] Impact fracture of the capped cylinders was performed at Sandia Corporation, Albuquerque, N. Mex.

Table 2 Predicted maximum safe impact velocities for cylinders made of several stainless steels

Material	Shear Strength Range*	Maximum Impact Velocity Range for Outside Surface	Maximum Impact Velocity Range for Inside Surface
Am-350	107 to 120 kpsi	260 to 300 fps	220 to 240 fps
17-1PH	110 to 136 kpsi	275 to 340 fps	220 to 270 fps
17-4PH	123 kpsi	308 fps	250 fps
AISI	80 to 100 kpsi	200 to 250 fps	160 to 200 fps

*Values from Military Handbook Five

References

1 Kolsky, H., *Stress Waves in Solids*, Dover, 1952, p. 195.
2 Pochhammer, L., *J. Reine Angew. Math.*, Vol. 81, 1876, p. 324.
3 Chree, C., *Transactions of the Cambridge Philosophical Society*, Vol. 14, 1889, p. 250.
4 Ghosh, J., *Bulletin of the Calcutta Mathematical Society*, Vol. 14, 1923–1924, p. 31.
5 McFadden, A., *Journal of the Acoustical Society of America*, Vol. 26, 1954, p. 714.
6 Herrmann, G., and Mirsky, I., Journal of Applied Mechanics, Vol. 23, Trans. ASME, Vol. 78, 1956, p. 563.
7 Gasis, D. C., *Journal of the Acoustical Society of America*, Vol. 31, 1959, pp. 563 and 573.
8 Fitch, A. H., *Journal of the Acoustical Society of America*, Vol. 35, 1963, p. 706.
9 DeVault, G. P., and Curtis, C. W., "Elastic Cylinder With Free Lateral Surface and Mixed Time-Dependent End Conditions," *Journal of the Acoustical Society of America*, Vol. 34, No. 4, Apr. 1962, pp. 421–432.
10 Thorne, B. J., and Hermann, W., "Toody, A Computer Program for Calculating Problems of Motion in Two Dimension," Report No. SC-RR-66-602 Sandia Corporation, July 1967.
11 Love, A. E. H., *Mathematical Theory of Elasticity*, Dover, 4th ed., 1944, p. 143.
12 Lax, P. D., and Wendroff, B., "Difference Schemes With High Order of Accuracy for Solving Hyperbolic Equations," *Comm. Pure Applied Mathematics*, Vol. 17, 1964, pp. 381–398.
13 Clifton, R. J., "A Difference Method for Plane Problems in Dynamic Elasticity," *Quarterly of Applied Mathematics*, Vol. 25, 1967, pp. 97–116.
14 Bertholf, L. D., "Numerical Solutions for Two-Dimensional Elastic Wave Propagation in Finite Bars," Journal of Applied Mechanics, Vol. 34, Trans. ASME, Vol. 89, Series E, 1967, p. 725.
15 Ju, F. D., and Wambold, J. C., "Analog Model of Wave Propagation in Open and Closed-End Cylinders," SC-CR-67-2627, Sandia Corporation Report, Apr. 1967.

Stone and Webster Engineering Corporation
CALCULATION SHEET

Calculation Identification Number				
J.O./W.O. NO. 12210	DIVISION & GROUP NM(C)	CALCULATION NO. 2043	OPTIONAL CODE SQE	PAGE C-8 0720

REFERENCE 13

122/0- NM (C) SQI-2042   C-9/20
REF. 13

STONEWBST CHI

ELAN P2 MTL
EB. 14/84
'SG 5072

12210-ND(B)-224-100-PX-1007-PA   Pg 110
REF 5.2

TN.: MR. R. J. MCMORLAND

SUBJECT: PURCHASE ORDER NOS.: RBS-228.211-049 + RBS-228.221-068
VALVES GENERAL - CAT. I AND II
RIVER BEND STATION - UNIT 1
GULF STATES UTILITIES CO.

THESE ARE THE ANSWERS TO YOUR QUESTIONS IN YOUR TWX RBTX-84-049:

1) CLOSED ANGLE OF DISC = 10 DEGREES.
FULL OPEN ANGLE OF DISC = 61 DEGREES.

2) MINIMUM PIPE VELOCITY REQUIRED FOR FULL DISC LIFT -

ITEM 79 V = 49 X SQUARE ROOT OF FLUID SPECIFIC VOLUME. FO-101 A & B

ITEM 57 V = 52 X SQUARE ROOT OF FLUID SPECIFIC VOLUME. V + F C

FLOW TO KEEP DISC AT CRACK OPEN POSITION IS INDETERMINATE (UNSTABLE).

3) PLOT SMOOTH CURVE FROM FOLLOWING -

DISC ANGULAR POSITION PERCENT OF FULL OPEN	VALVE CV PERCENT OF FULL OPEN ($C_v = 7000$)
0	0
10	14
30	40
50	64
75	86
100	100

4) TO BE DETERMINED BY TEST LATER.

5) MASS OF DISC = 205 LBS
MASS OF HANGER = 24 LBS.

REFER TO DRAWING: C.G. OF DISC PLUS HANGER IS LOCATED 10.6 INCHES BELOW AND .38 INCHES TO THE RIGHT OF PIVOT CENTRELINE WITH DISC CLOSED.

6) M.I. DISC W.R.T. PIVOT = 30161
M.I. HANGER W.R.T. PIVOT = 1019

REGARDS
J M FARRELL, ENG.
LX NO.: 05-826599

TONEWBST CHI

VELAN P2 MTL

Stone and Webster Engineering Corporation
CALCULATION SHEET

Calculation Identification Number				
J.O./W.O. NO. 12210	DIVISION & GROUP NM(C)	CALCULATION NO. 2043	OPTIONAL CODE SQE	PAGE C-10 of 20

REFERENCE 14

12 2/1 - NM(c) - SQE 2043 4-11/20

-REF.-14

ATWOOD & MORRILL CO., INC.
SALEM, MASS. 01970

ENGINEERING DESIGN REPORT

Report No. 300-15202-00 Pg 1/13

Date April 17, 1984

CI 8404270002

TITLE

12210-NP(B)-228-800-PX-1007-FQ

REFS-5

20" - 900# FEEDWATER CHECK VALVE

VALVE DATA FOR PERFORMING CLOSURE TIME ANALYSIS

FOR

Stone & Webster Engineering Corporation
Cherry Hill, N.J. 08034

P.O. No. RBS-228.218-062-30
Atwood & Morrill S.O. No. 15202-01

Original Issue (Rev. 0)			Revisions (1)	(2)	(3)	(4)
Signature	Title	Date	Initials Date			
Originator: Carl Belinger Jr.	DESIGN ENG	4/17/84	- - - -	- - - -	- - - -	- - - -
Reviewer: (MANAGEMENT) A Ramaropoulos	ENG SECT MGR	4/17/84	- - - -	- - - -	- - - -	- - - -
Reviewer:			- - - -	- - - -	- - - -	- - - -
Engineering Management:			- - - -	- - - -	- - - -	- - - -

122/0-NM(1) SOF-2043 C/12/20

PROC. NO. 30C-15202-00

12210-NP(B)-228-800-PX-1007-PA Pg 114

REF 55

REVISION SHEET		
Rev. No.	Date	Revision
0	4/17/84	Original Issue

12210-NP(B)-22B-800-PX-1007-FA
REF 5.5

115

TABLE OF INFORMATION

1.) The Center of Gravity of the disc about the shaft centerline is: $CG_x = 1.21$ in. and $CG_y = 9.65$ in. (See Fig. 1).

2.) The Mass of the disc is 12.95 slugs.

3.) The Mass moment of inertia of the disc about the shaft centerline is 12.16 slug - ft^2.

4.) Disc angle versus fluid velocity - See Fig. 3.

12210-NP(B)-228-F007 PX-1007-#A
REF 55
Pg 116

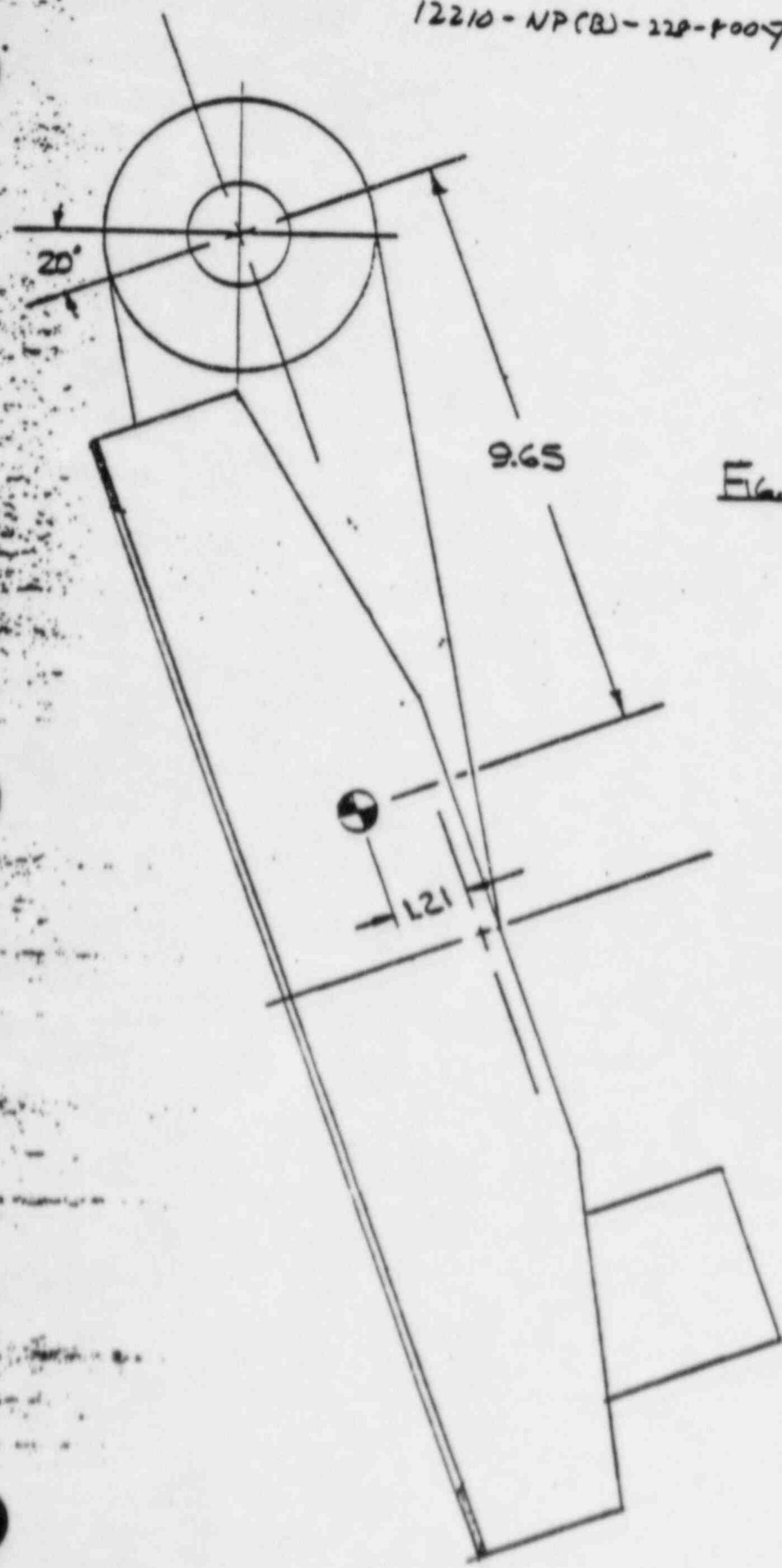

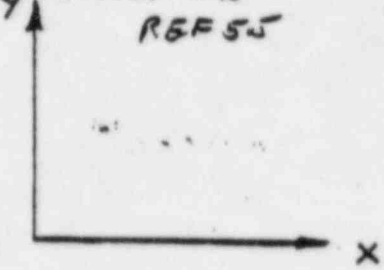

Fig. 1: 20"-900# Disc - Closed Position On 20° Seat
Scale: 3/8" = 1"

PROC. NO 300-15202-00

12210 - NP(B)-228-800 - DX-1007-FA
REF 55

Pg 117

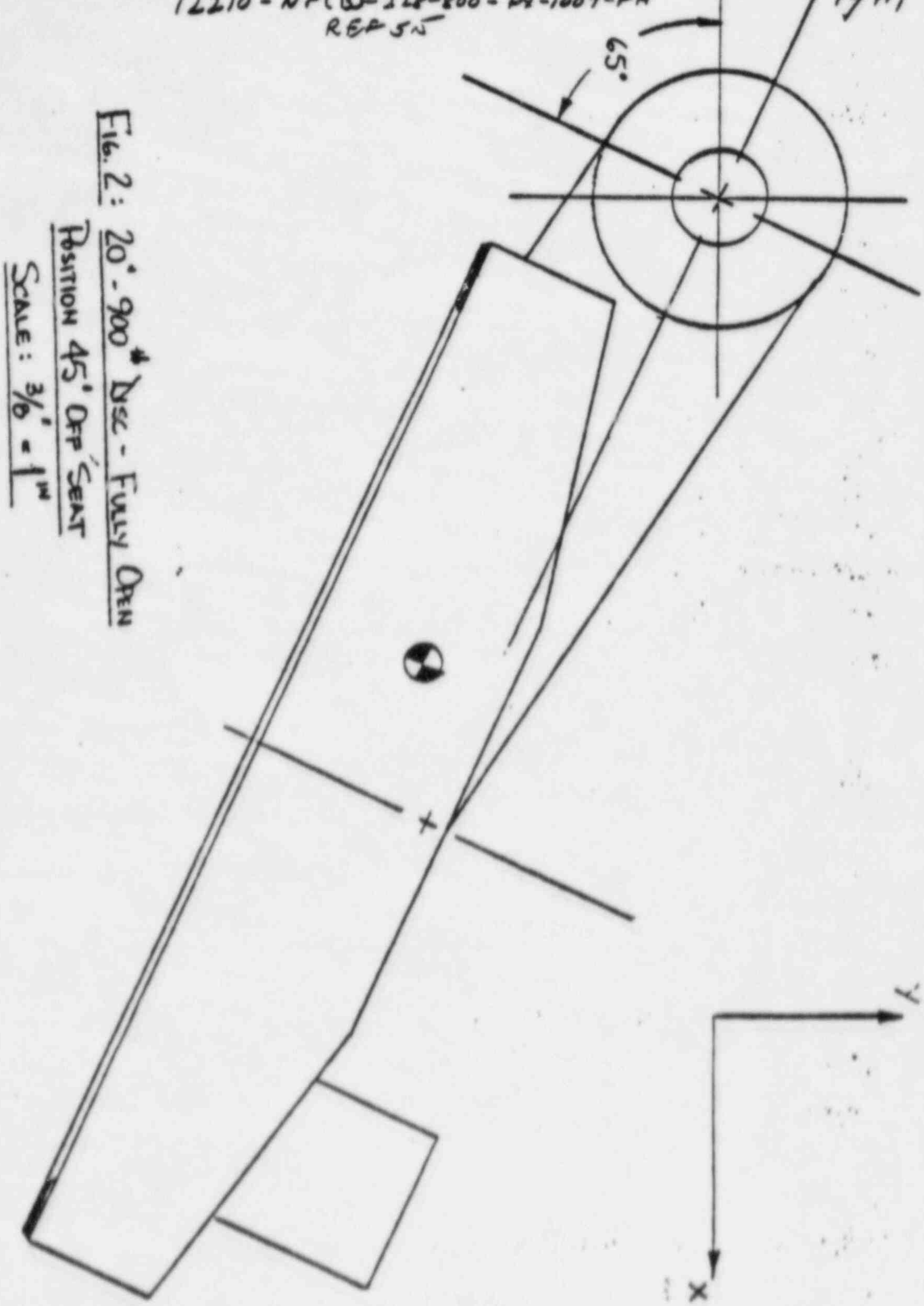

Fig. 2: 20"-900# Disc - Fully Open
Position 45° Off Seat
Scale: 3/16" = 1"

PROC. NO. 300-1520

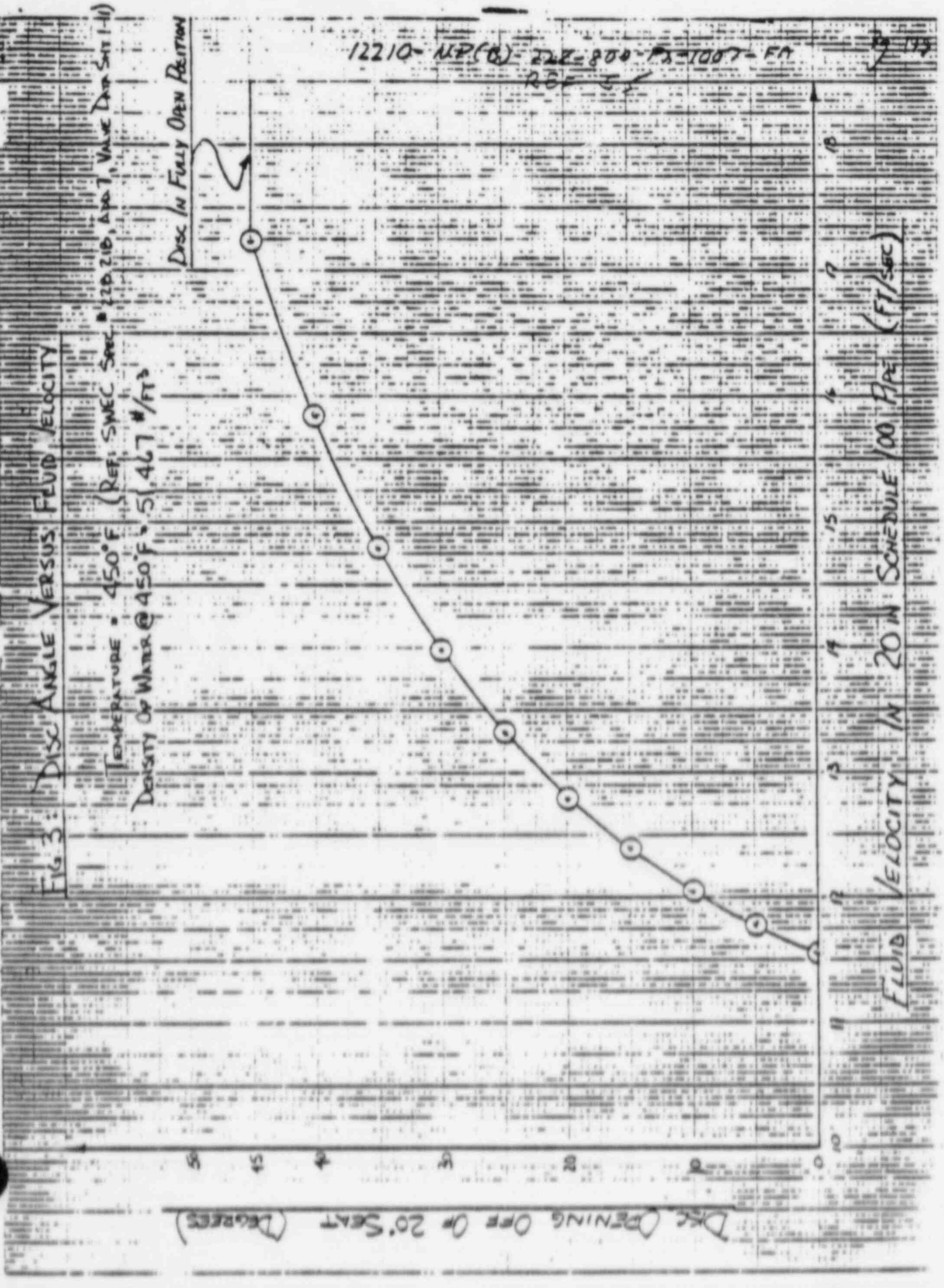

LAST PAGE

REFERENCE 16

12210-NMC(L) SQE-2048

C-10/20

EM*-2697

INTEROFFICE CORRESPONDENCE

TO:	LOCATION	SUBJECT / REFERENCE / J.O. NO.
Q. LY	6Y	FW CHECK VALUE MEASUREMENTS /12210
FROM: J. MACINTOSH	LOCATION SEG/4	

MESSAGE: —

ATTACHED PLEASE FIND TABLE AND DRAWING OF FEEDWATER CHECK VALUE 1B21*AOV032B WHICH WAS MEASURED IN PLACE. DIMENSIONS GIVEN ARE APROXIMATE DUE TO ACCESSIBILITY OF VALUE. NO SEAT BEARING AREA COULD BE OBTAINED.

CC. D. BRAY

10/17/84 DATE

J MacIntosh SIGNATURE

4555 TELEPHONE

REPLY:

thank you very much

10/20/84 DATE

[signature] SIGNATURE

3655 TELEPHONE

A 040 138

122/0-NM(C) SQE-2043 C 19/20

Page 2 of 3

Stone and Webster Engineering Corporation
CALCULATION SHEET

Calculation Identification Number				
J.O. OR W.O. NO. 14764.07	DIVISION & GROUP NM(C)	CALCULATION NO. 2043	OPTIONAL CODE SQE	PAGE 15

Dimensions

TABLE 4.3	Atwood/Morrill Check Valve 1B21*ACV032A,B	MEASURED	REF.	Velan Check Valve 1B21*F010A,B	REF.
Diam of Disk(in)	~~18.75~~	19"	12	17.6	11
Dist from Rockshaft to Disk Center	12.3	14"	2	11.7	3
Diam of Pin	---	1 7/8"	--	2.6	3
Diam of Rockshaft	2.7	4 9/16"	2	2.0	3
Gap between Tail Disk & Bearing	.1 or less	SEE DWG	2	.1 or less	3
Dist between CG of Disk & Pin Seat(boss)	2.2	CANNOT MEAS.	12	1.5	11
Clearance - Disk/Tlk	--	NA	--	.5 (7)	
Thickness of Disk	3.75 ctr, 1.9 rim	2 1/2	12	3.6 ctr, 2.75 rim	11
Seat Annulus	.5+	CANNOT MEAS.	2	.56	3
Tail Link Section	4.5 x 2.0	SEE DWG	2	1.8 x 5.0	3
Tail Link Grip	14.4	16 3/8"	2	6.1	3
Seat Inside Diam	15.75	CANNOT MEAS.	2	15.75	3
Diam of Tlk Boss	---	NA	--	4.0	3

Material Properties at 500F (Ref. 9, Appendix I)

TABLE 4.4	Sy (ksi)	Su (ksi)	Elong.* (%)	E (psi*e-6)	Sm (ksi)	
CS SA 216 WCC	40	70	22	27	21.6	
CS SA 105	36	70	22	27	19.5	
SS SA 564 630	105	135	16	27	42.8	
SS A 182 F6a	40	70	25 *Ref.10	27	22.0	

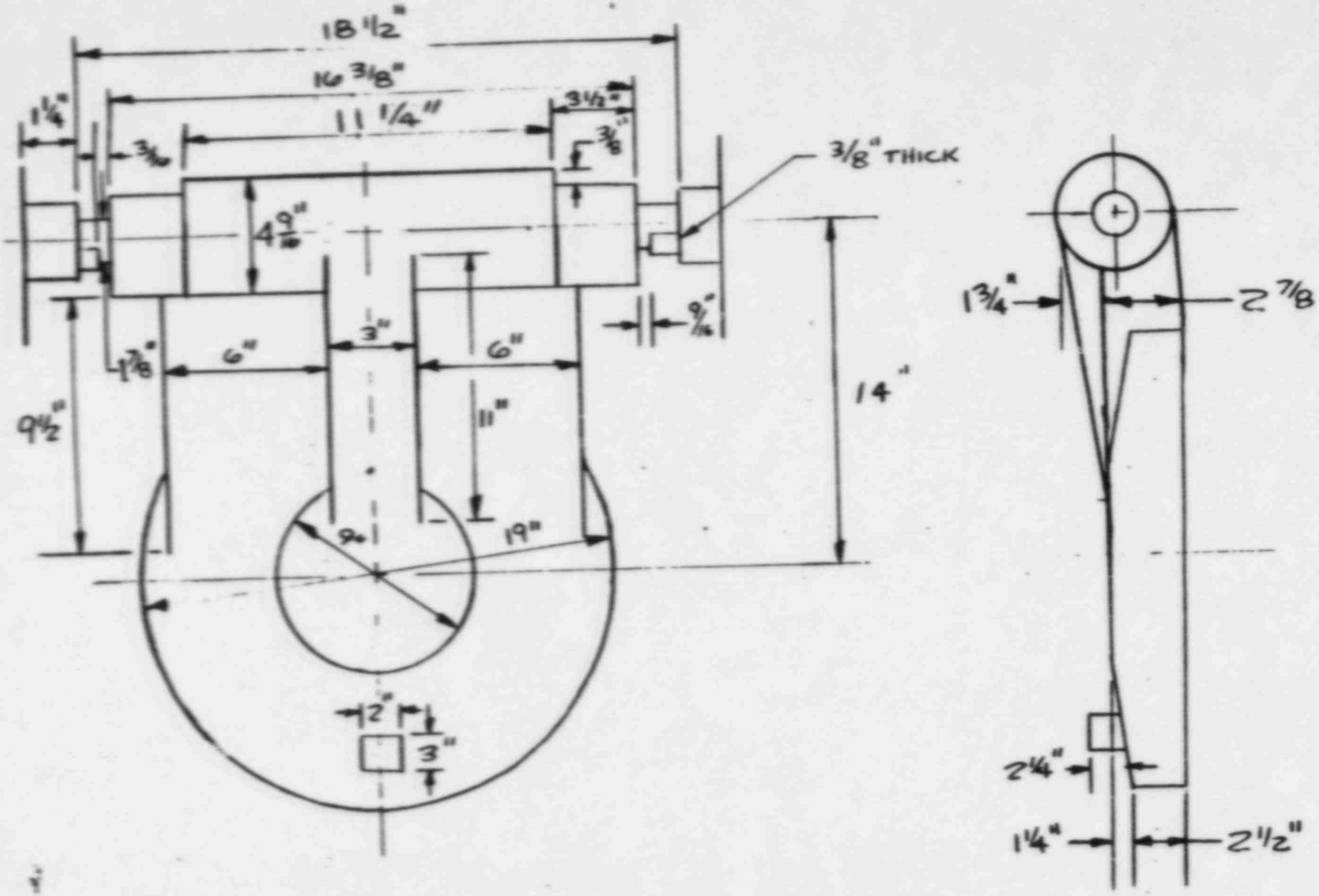

NTS FEEDWATER VALVE

Stone and Webster Engineering Corporation
CALCULATION SHEET

Calculation Identification Number				
J.O./W.O. NO. 12210	DIVISION & GROUP NM(C)	CALCULATION NO. 2043	OPTIONAL CODE SQE	PAGE D-1 of 9

APPENDIX D

Computer Log and Microfiche

Inform impact of 1821 & ADV F 032 A

D-2/9

COMPUTER LOG

7729

S & W AUTH. NO. 4737
CALCULATION NO. 2043
CDC CHARGE NO. B3881 WC
ORDER NO. 12210

RUN NO.	JOB NO. *	FICHE LOC.		PREPARED BY		REVIEWED BY		COMP. **	COMMENTS
		PAGE	SECT	SIGNATURE	DATE	SIGNATURE	DATE		
3WA	949			Carl Ebeck	10/9/84	Joe Fein	10/3/84	CDC	HOC superceded by TDA
3WB	2663			Carl Ebeck	10/9/84	"	"	CDC	Dyre1 superceded by TDB
TDA	3014			Carl Ebeck	10/9/84	"	"	CDC	HOC
TDB	3015			Carl Ebeck	10/9/84	"	"	CDC	Dyre1

* COMPUTER GENERATED JOB NUMBER

** COMPUTER USED (S&W OR CDC)

POINT IMPACT [illegible]LYSIS OF 1B21W AOV7022A

COMPUTER LOG

D-3/9

7729

S&W AUTH. NO. 4737
CDC CHARGE NO. B3BB1WC

CALCULATION NO. SQE-2043
JOB ORDER NO. 12210

RUN NO.	JOB NO. *	FICHE LOC. PAGE	FICHE LOC. SECT	PREPARED BY SIGNATURE	PREPARED BY DATE	REVIEWED BY SIGNATURE	REVIEWED BY DATE	COMP. **	COMMENTS
3AA	3334			[illegible]	10/30/84	[illegible]	10/30/84		HGR 7.4 PT a (10/26/84)
3AA	422			"	"	"	"		DYN 1 7.4 PT a (10/27/84)
3AB	3336			"	"	"	"		HGR 7.4 PT b (10/26/84)
3AB	424			"	"	"	"		DYN 1 7.4 PT b (10/27/84)
3AC	114			"	"	"	"		HGR 7.4 PT C (10/26/84)
3AC	3337			"	"	"	"		DYN 1 7.4 PT C (10/29/84)
3AD	[illegible]			"	"	"	"		HGR 7.4 PT D (10/28/84)
3AD	429			"	"	"	"		DYN 1 7.4 PT D (10/27/84)
3AE	3367			"	"	"	"		HGR 7.4 PT E (10/26/84)
3AE	3533			"	"	"	"		DYN 7.4 PT E (10/29/84)
3AF	116			"	"	"	"		HGR 1 7.4 PT F (10/28/84)
3AF	432			"	"	"	"		DYN 1 7.4 PT F (10/27/84)

* COMPUTER GENERATED JOB NUMBER

** COMPUTER USED (S&W OR CDC)

PT impact [illegible]) → [illegible] (CONT.)

D-4/9

COMPUTER LOG

7729

S & W AUTH. NO. 4737 CALCULATION NO. SQE-2043
CDC CHARGE NO. 83881WC JOB ORDER NO. 12210

RUN NO.	JOB NO. *	FICHE LOC.		PREPARED BY		REVIEWED BY		COMP. **	COMMENTS
		PAGE	SECT	SIGNATURE	DATE	SIGNATURE	DATE		
3A6	3376			[illegible]	10/29/84	[illegible]	10/30/84		HGX 7ie PT G (10/26/84)
3B	435								DYKE 1 7is PT G (10/27/84)

* COMPUTER GENERATED JOB NUMBER

** COMPUTER USED (S&W OR CDC)

COMPUTER LOG

VELAN CHECK VA[illegible] 1821#F010A
FOR UNIFORM IMPACT ANALYSIS

D-5/9

7729

S & W AUTH. NO. 4737
CDC CHARGE NO. 83281 WC
CALCULATION NO. 12210-SQ-I-20 #3
JOB ORDER NO. 12210

RUN NO.	JOB NO. *	FICHE LOC.		PREPARED BY		REVIEWED BY		COMP. **	COMMENTS
		PAGE	SECT	SIGNATURE	DATE	SIGNATURE	DATE		
11A				[illegible]	11/8/84	[illegible]	11/8/84	CDC	HGL RUN TAPE # A10514
11B								CDC	ZYRE1

* COMPUTER GENERATED JOB NUMBER

** COMPUTER USED (S&W OR CDC)

VERAN 1B2[illegible] [illegible]OA CHECK VALVES (F010A)
POINT IMPACT ANALYSIS

D-6/9

COMPUTER LOG

7729

S&W AUTH. NO. 4737
CDC CHARGE NO. B388 [illegible]

CALCULATION NO. 12210-S&I 2C-43
JOB ORDER NO. 12210

RUN NO.	JOB NO. *	FICHE LOC.		PREPARED BY		REVIEWED BY		COMP. **	COMMENTS
		PAGE	SECT	SIGNATURE	DATE	SIGNATURE	DATE		
1aa				Cam Chau k [illegible]	11/5/84	J McGuinn	11/8/84	CDC	H&R 70K PT a TAPE # 12556
1ba				Cam Chau k [illegible]	11/6/84	"	"	"	DYRE1 70K PT a
1ab				Cam Chau k [illegible]	11/7/84	"	"	"	H&R 70K PT b TAPE # 12557
1bb				Cam Chau k [illegible]	11/7/84	"	"	"	DYRE 1 70K PT b
1ac				Cam Chau k [illegible]	11/7/84	"	"	"	H&R 70K PT C TAPE # 12562
1bc				Cam Chau k [illegible]	11/7/84	"	"	"	DYRE 1 70K PT C
1ad				"	"			"	H&R 70K PT D TAPE # 12569
1bd				"	"			"	DYRE1 70K PT D
1ae				"	"			"	H&R 70K PT e TAPE # 12650
1be				"	"			"	DYRE 1 70K PT e
1af				"	"			"	H&R 70K PT f TAPE # 12672
1bf				"	"			"	DYRE1 70K PT f

* COMPUTER GENERATED JOB NUMBER

** COMPUTER USED (S&W OR CDC)

VELAN F010

D-7/9

COMPUTER LOG

7729

S & W AUTH. NO. 4737
CDC CHARGE NO. B3881WC

CALCULATION NO. 12210-SQE-2043
JOB ORDER NO. 12210

RUN NO.	JOB NO. *	FICHE LOC.		PREPARED BY		REVIEWED BY		COMP. **	COMMENTS
		PAGE	SECT	SIGNATURE	DATE	SIGNATURE	DATE		
1a9/				[illegible]	11/7/84	[illegible]	11/8/84	CDC	HDR FOR F 9 TAPE # 12 676
1b9/									

* COMPUTER GENERATED JOB NUMBER

** COMPUTER USED (S&W OR CDC)

CL8412130001

STONE & WEBSTER ENGINEERING CORPORATION

CALCULATION TITLE PAGE

5010.54 (FRONT)

CLIENT & PROJECT				PAGE 1 OF 104 145 WITH 38 PAGES OF APPENDIX
GULF STATES UTILITIES - RIVER BEND UNIT 1				
CALCULATION TITLE (indicative of the Objective): FEEDWATER CHECK VALVE INTEGRITY FOLLOWING PIPE RUPTURE (O.C.)				QA CATEGORY (✓) ☒ I - NUCLEAR SAFETY RELATED ☐ II ☐ III ☐ ____ OTHER
CALCULATION IDENTIFICATION NUMBER				Calculation Status
J. O. OR W.O. NO.	DIVISION & GROUP	CURRENT CALC. NO.	OPTIONAL TASK CODE	
12210	NM(C)	2043	SQE	FINAL

APPROVALS - SIGNATURE & DATE [signature] 10/30/84

PREPARER(S)/DATE(S)	REVIEWER(S)/DATE(S)	INDEPENDENT REVIEWER(S)/DATE(S)	REV. NO. OR NEW CALC NO.	SUPERSEDES CALC. NO. OR REV. NO.	CONFIRMATION *REQUIRED (✓) YES	NO
J. M. Gwinn [signature] 10/30/84	[signature] CAM T. LY 10/29/84	S.M. Feldman [signature] 10/30/84 S.M. FELDMAN	New	N/A		✓
J. M. Gwinn [signature] 12/7/84	[signature] CAM T. LY 12/7/84	S.M. Feldman [signature] 12-10-84 S.M. FELDMAN	1	Rev. 0		✓
J.M. Gwinn [signature] 6/2/85	[signature] CAM T. LY 7/3/85	S.M. Feldman [signature] S.M. FELDMAN 7/3/85	2	1		✓

REV. 1 APPROVAL [signature] 12/10/84

*As listed in this block.

Rev. 2 APPROVAL [signature] 7/3/85

CALCULATION DISTRIBUTION			LOADS TRANSMITTALS		
GROUP	NAME & LOCATION	COPY SENT (✓)	GROUP	NAME & LOCATION	COPY SENT (✓)
Project Files	DDMartin (4R)				
Fire Files (microfilm)	Boston 401 Summer Street				
PPF	Site				
EQ (SEISMIC)	N. MUNI (6Y)				
EMD/B03	J. GWINN 2V6/9				
EMD/CHDC	S. FELDMAN (2AR)				

STONE & WEBSTER ENGINEERING CORPORATION

CALCULATION SHEET

5010.65

CALCULATION IDENTIFICATION NUMBER				
J.O. OR W.O. NO.	DIVISION & GROUP	CALCULATION NO.	OPTIONAL TASK CODE	PAGE ____

page D-8

microfiche

STONE & WEBSTER ENGINEERING CORPORATION

CALCULATION SHEET

5010.65

CALCULATION IDENTIFICATION NUMBER				
J.O. OR W.O. NO.	DIVISION & GROUP	CALCULATION NO.	OPTIONAL TASK CODE	PAGE E107-38
12210	NM(C)	2043	SQE	

APPENDIX E

VOID PAGES

Stone and Webster Engineering Corporation
CALCULATION SHEET

Calculation Identification Number				
J.O./W.O. NO. 12210	DIVISION & GROUP NM(C)	CALCULATION NO. 2043	OPTIONAL CODE SQE	PAGE 9-1 of 16

9. INTEGRITY OF VELAN CHECK VALVE 1B21*F010

VOID

Stone and Webster Engineering Corporation
CALCULATION SHEET

Calculation Identification Number				
J.O./W.O. NO. 12210	DIVISION & GROUP NM(C)	CALCULATION NO. 2043	OPTIONAL CODE SQE	PAGE 19

5. SUMMARY OF RESULTS

VOID

TABLE 5.1		AOVF32			F010		
		Calculated	Allowable	FS	Calculated	Allowable	FS
Disk	-shear #	7.88E6	8.28E6	1.05	4.2E6	7.8E6	1.9
	-strain %	2.3	15.4	6.7	2.9	15.4	5.3
Rockshaft	-stress ksi	N/A	N/A		28.5	54.6	1.9
	-ratio	.35	1.0	2.9	N/A	N/A	
Tail Link	-stress ksi	N/A	N/A		68.1	70.0	1.03
	-ratio	.89	1.0	1.1	N/A	N/A	
Pin	-stress ksi	N/A	N/A	N/A	4.8	28.8	6.0
Stud	-stress ksi	N/A	N/A	N/A	41.0	49.	1.2
Seat/Disk Interface	-stress ksi	74.	98.	1.3	98.8	70.	1.4

Stone and Webster Engineering Corporation
CALCULATION SHEET

Calculation Identification Number				
J.O. OR W.O. NO. 12210	DIVISION & GROUP NM(C)	CALCULATION NO. 2043	OPTIONAL CODE SQE	PAGE 24

VOID

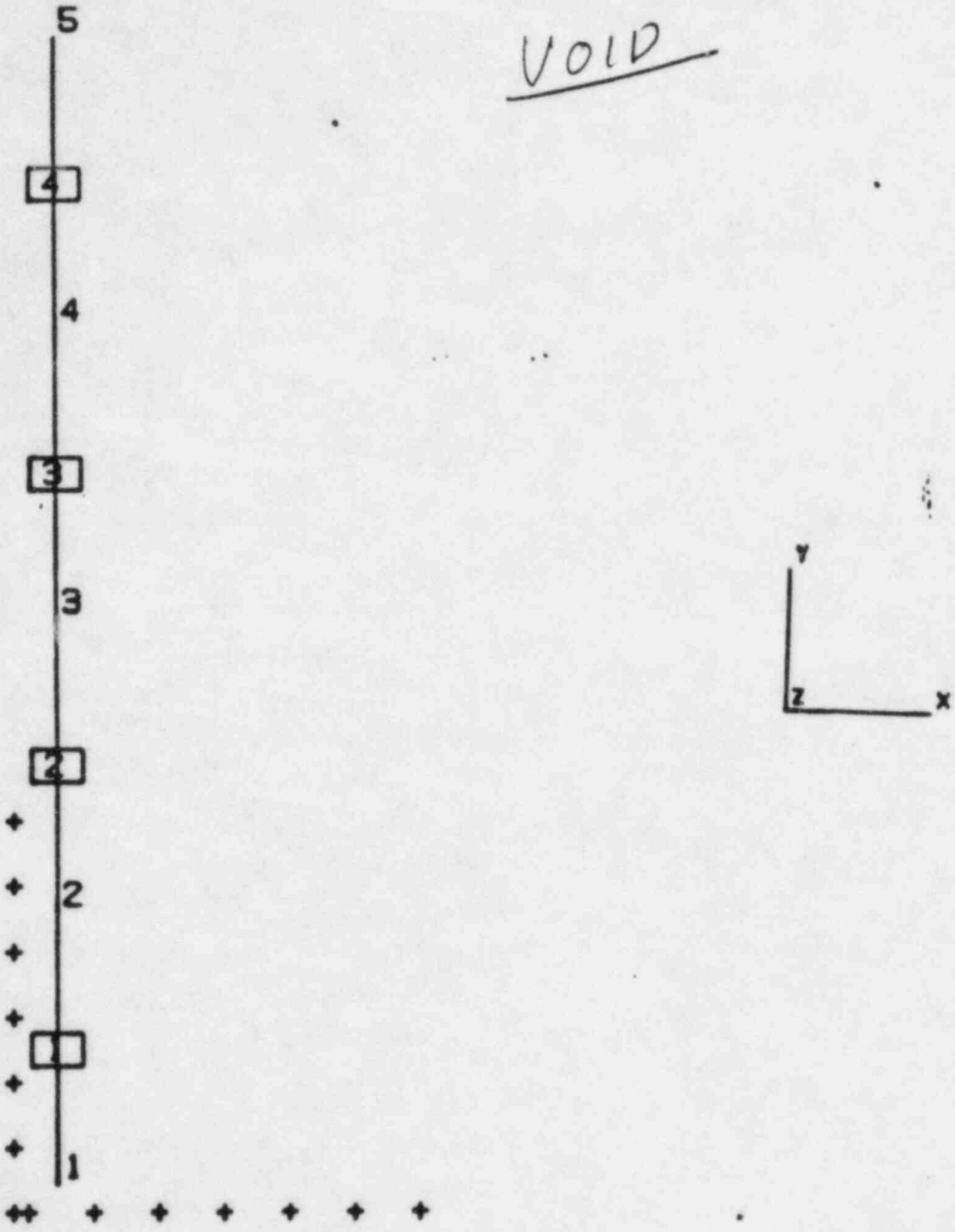

UNIFORM IMPACT MODEL OF CHECK VALVE 1B21*F010A TAIL-LINK

CALCULATION IDENTIFICATION NUMBER				
J.O. OR W.O. NO.	DIVISION & GROUP	CALCULATION NO.	OPTIONAL TASK CODE	PAGE 9-2
12210	NM(C)	2043	SQE	

9.1 Disk (SA 105)

VOID

Loading

Uniform impact of the disk on the seat generates a reaction of 3.57×10^6 #, as given by FXK in Table 8.5. In reality, the impact speed varies linearly with the distance from the rockshaft but the total is the same for a constant impact speed equal to the average speed at the disk center of mass. Acting simultaneously with impact is the pressure surge from rapidly closing the check valve. The maximum pressure is used although it occurs several milliseconds after impact.

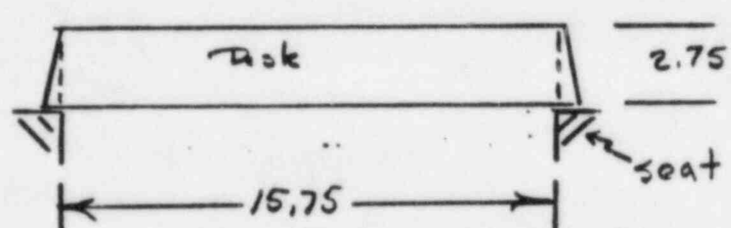

$.62 \times 10^6$ # ↓ 3200 psi

3.57×10^6 # ↓ 18,300 psi

4.2×10^6 # 21,500 psi

STONE & WEBSTER ENGINEERING CORPORATION

CALCULATION SHEET

A 5010.65

CALCULATION IDENTIFICATION NUMBER				
J.O. OR W.O. NO.	DIVISION & GROUP	CALCULATION NO.	OPTIONAL TASK CODE	PAGE 9.3
12210	NM(C)	2043	SQE	

Shear Out

VOID

The allowable shear load in the disk at the inside diameter of the seat where the bending stress in the disk is zero, is given by

$$P_u = .7 \frac{\sigma_u}{\sqrt{3}} \cdot \text{shear area} \cdot \text{strain rate factor}$$

$$= .7 \left(\frac{70000}{1.7}\right) \left(15.75\pi \; 2.75\right)(2)$$

$$= 7.7 \times 10^6 \,\#$$

since $7.7 \times 10^6 \,\# > 4.2 \times 10^6 \,\#$,
the integrity of the disk in shear out is demonstrated.

Rupture

The disk must absorb the impact energy at strains below the rupture level. The impact energy

$$= \frac{190}{32} (60)^2 \frac{12}{2} = 128,000 \text{ in}\#$$

where effective disk weight $= 185 + \frac{20}{4} = 190^{\#}$

STONE & WEBSTER ENGINEERING CORPORATION

CALCULATION SHEET

5010.65

CALCULATION IDENTIFICATION NUMBER				
J.O. OR W.O. NO.	DIVISION & GROUP	CALCULATION NO.	OPTIONAL TASK CODE	PAGE 9.4
12210	NA(C)	2043	SQE	

VOID

The plastic strain energy of a circular disk from Appendix E

$$= \frac{\pi}{2}\left(\frac{\pi}{2}-1\right)\sigma_y t^2 y_0$$

$$= .89\,(36000)(2.75)^2 y_0 \quad = 244,000\, y_0$$

Equating to the impact energy and solving for the deflection at the center of the disk

$$y_0 = \frac{128,000}{244,000} = .53''$$

From Appendix B, the maximum strain associated with this deflection is

$$\epsilon = \frac{t}{2}\left(\frac{\pi}{D}\right)^2 y_0 = \frac{2.75}{2}\left(\frac{\pi}{15.75}\right)^2(.53)$$

$$= .029 \text{ in/in}$$

which neglects the deflection of the disk from the pressure, it being in the elastic range and therefore negligible.

STONE & WEBSTER ENGINEERING CORPORATION

CALCULATION SHEET

5010.65

CALCULATION IDENTIFICATION NUMBER				
J.O. OR W.O. NO. 12210	DIVISION & GROUP N/M(C)	CALCULATION NO. 2043	OPTIONAL TASK CODE SQE	PAGE 9-5

VOID

The allowable strain

$= .7 \cdot \text{Elongation} = .7(.22) = .154 > .029$ OK

which shows that the disk will not rupture under impact loading.

9.2 Pin (SA105)

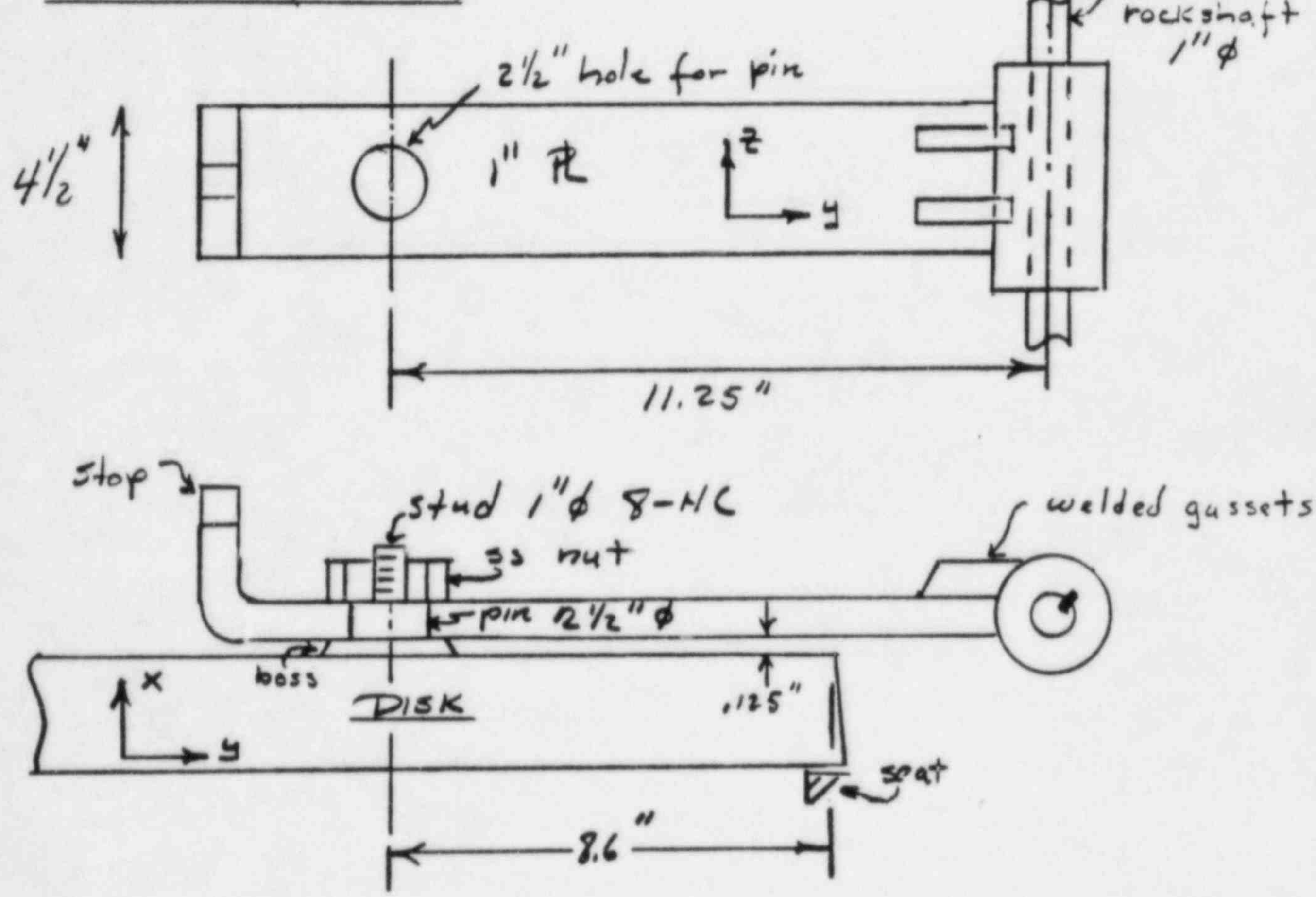

STONE & WEBSTER ENGINEERING CORPORATION

CALCULATION SHEET

5010.65

CALCULATION IDENTIFICATION NUMBER				
J.O. OR W.O. NO.	DIVISION & GROUP	CALCULATION NO.	OPTIONAL TASK CODE	PAGE 9-6
12610	NMP(C)	2043	SQE	

VOID

The pin and stud are ~~integral~~ and welded to the disk. A ss nut locked to the stud keeps the tail link tight to the boss.

Pre-impact

The centrifigal force, Fc, is reacted by shear on the pin. The shear stress on the pin

$= F_c / \text{Area of pin}$

$= 21500/4.5 = 4800$ psi

the allowable shear stress

$= .7 S_u/\sqrt{3} \quad = .7(70000)/1.7$

$= 28300$ psi > 4800 OK

the centrifigal force is eccentric to the tail link, generating a moment which is reacted by the stud in tension and the boss in compression

$$= F_c\left(\frac{2.75}{2} + .125 + \frac{1}{2}\right)$$

STONE & WEBSTER ENGINEERING CORPORATION

CALCULATION SHEET

5010 65

CALCULATION IDENTIFICATION NUMBER				
J.O. OR W.O. NO. 12210	DIVISION & GROUP NM(C)	CALCULATION NO. 2043	OPTIONAL TASK CODE SQE	PAGE 9.7

VOID

$= 21{,}500(2.0)$ ~~= 43,000 in#~~

The distance between the edge of the boss and the ℄ stud = 3.5/2 = 1.75 in. Dividing into the moment yields the force on the stud

$= 43{,}000/1.75 = 24{,}600\#$

which corresponds to a tensile stress

$= 24{,}600/.60$

$= 41{,}000$ psi

The allowable stress

$= .7\,S_u = .7\,(70000)$

$= 49{,}000$ psi $> 41{,}000$ OK

Hence, the integrity of the pin is demonstrated for pre-impact loads.

CALCULATION IDENTIFICATION NUMBER				
J.O. OR W.O. NO.	DIVISION & GROUP	CALCULATION NO.	OPTIONAL TASK CODE	PAGE 9-8
12210	N/M(C)	2043	SQE	

VOID

Uniform Impact

From Table 9.5, a force FXK = 55 Kips acts in compression at the disk center which is in no way carried by the pin or stud. Also acting is a moment MZK = 100 ink which is not real since the plastic moment, from appendix

$$= \frac{1}{4} \sigma_y A t = \frac{1}{4} (36000)(4.5)(1) = 40500$$

$$= 40,500 \text{ in\#}$$

is exceeded. What really happens is the tail link deflects in bending until it strikes the disk, 1/8" away, thus limiting the strain.

Point Impact

These forces and moments from Table 9.? are much lower than those resulting from pressure impact and uniform impact, because of the flexibility of the tail link in bending and

torsion. Hence, integrity of the pin is demonstrated for paint impact loading.

VOID

9.3 Tail Link

Pre-Impact

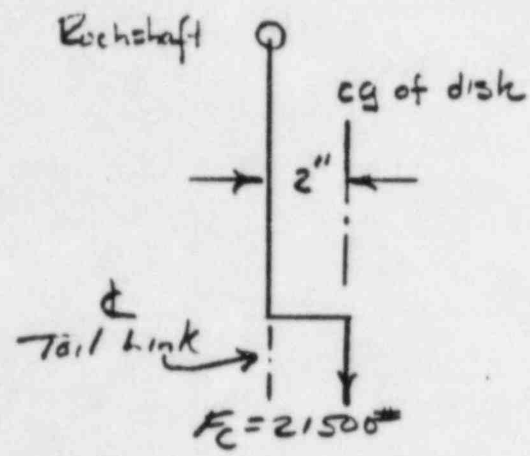

The centrifugal force, F_c, loads the tail link in direct tension and bending, Assuming that the nut makes the full tail link section effective in bending, the total tensile stress

$$= \frac{F_c}{2} + F_c(2''\text{arm})\, c/I$$

$$= \frac{21,500}{2} + 21500(2)(.5)/.375$$

$$= 10,800 + 57,300 = 68,100 \text{ psi}$$

which is greater than the tensile allowable, but less than the ultimate stress of 70,000 psi.

5010.65

CALCULATION IDENTIFICATION NUMBER				
J.O. OR W.O. NO.	DIVISION & GROUP	CALCULATION NO.	OPTIONAL TASK CODE	PAGE 9-10
12210	NM(C)	20Y3	SQE	

VOID

Referring to Ref. 1, it is observed that this stress lasts for one or two milliseconds which is not of sufficient duration to develop the strain necessary for failure.

The deflection of the disk off the seat just prior to impact

$$= PL/AE = 21500(11.25)/4.5 \times 27E6$$

$$= .002 \text{ inches}$$

which is insignificant compared to the allowable deflection of .25". Hence, the integrity and operability of the tail link under pre-impact loading is demonstrated.

CALCULATION IDENTIFICATION NUMBER				
J.O. OR W.O. NO.	DIVISION & GROUP	CALCULATION NO.	OPTIONAL TASK CODE	PAGE 9-11
12210	NM(C)	2043	59E	

VOID

Uniform Impact

The worst case bending for the tail link is caused by deflection of the disk center following impact with the seat, calculated in section 9.1 to be .64 inches including the contribution from the pressure surge. From Appendix A, the

plastic strain corresponding to a deflection, y_0, of a simply supported beam of length = 2×11.25

$$\epsilon = \frac{\pi^2}{2} \frac{D y_0}{L^2} = \frac{\pi^2}{2} \frac{(1)(.64)}{(2 \times 11.25)^2}$$

$$= .0062 < .7(22) = .154 \quad \text{OK}$$

Since this occurs after the initial kickback loads, the contribution from shear is negligible.

CALCULATION SHEET

5010.65

CALCULATION IDENTIFICATION NUMBER				
J.O. OR W.O. NO.	DIVISION & GROUP	CALCULATION NO.	OPTIONAL TASK CODE	PAGE
12210	NM(C)	2043	SQE	9-12

The worst case shear loads from Table [illegible] are [illegible] kips at the [illegible] shaft end and [illegible] 55 kips at the pin end. Maximum shear stress

VOID

= 55000/area = [illegible]

= 12,200 psi

The allowable shear stress

$= .7\,S_u/\sqrt{3} = .7(70000)/1.7$

$= 28{,}300 > 12{,}200$ psi (OK)

Hence, integrity of the tail link is demonstrated for uniform impact loading.

Point Impact

Point impact loads, as seen from Table 8.5, are much smaller than pre- or uniform impact. Hence, integrity for point impact loads is demonstrated.

CALCULATION IDENTIFICATION NUMBER				
J.O. OR W.O. NO.	DIVISION & GROUP	CALCULATION NO.	OPTIONAL TASK CODE	PAGE 9-13
12210	NM(C)	20V3	SQE	

9.4 Rock shaft

VOID

Pre-impact

The rock shaft reacts the centrifigal force in double shear. The stress

$= 21,500/2(\text{Area})$

$= 21,500/2(.79) = 13,600$ psi

which is below the allowable

$= .7(105000)/\sqrt{3}$

$= 42500 > 13600$ psi OK

Uniform Impact

From Table 8.5, the kickback load is 45 kips in double shear, resulting in a stress

$= \frac{45000}{2}/\text{area} = \frac{45000}{2}/.79$

$= 28,500$ psi

5010.65

CALCULATION IDENTIFICATION NUMBER				
J.O. OR W.O. NO.	DIVISION & GROUP	CALCULATION NO.	OPTIONAL TASK CODE	PAGE 9-14
12210	NM(C)	2043	SQE	

the allowable shear stress VOID

$= .7 S_u/\sqrt{3} = .7(135{,}000)/1.7$

$= 54{,}600$ psi $> 28{,}500$ OK

Point Impact

Referring to Table 8.3 shows that the point impact loads on the rockshaft are much smaller than the loads from pre-impact and uniform impact.

~

Hence, the rockshaft integrity is demonstrated for all critical loads.

CALCULATION IDENTIFICATION NUMBER				PAGE 9-15
J.O. OR W.O. NO. 12210	DIVISION & GROUP NM(C)	CALCULATION NO. 20V3	OPTIONAL TASK CODE SQE	

9.5 Seat/Disk Interface ~~VOID~~

The stress caused by impact in the seat and disk material at the interface is calculated from the hammer equation.

$$\Delta\sigma = \frac{\Delta u}{c} E$$

where c is the speed of sound in steel.
Thus

$$\Delta\sigma = \frac{60}{16,400} 27E6 = 98,800 \text{ psi}$$

The allowable stress for

$$= .7 S_u (\text{strain rate factor})$$

$$= .7 (70000)(2) = 98000 \text{ psi}$$

Although slightly above the allowable, it is below ultimate and since this stress acts for a time less than 1/2 millisecond (Fig. 8.2), very little damage to the

STONE & WEBSTER ENGINEERING CORPORATION

CALCULATION SHEET

APPENDIX E PAGE E 190,
39

A 5010.65

CALCULATION IDENTIFICATION NUMBER				
J.O. OR W.O. NO.	DIVISION & GROUP	CALCULATION NO.	OPTIONAL TASK CODE	PAGE 9-16
12210	NM(B)	2043	SQE	

seat/disk interface is indicated. Hence, the leakage will remain within acceptable limits.

VOID

Calculation Identification Number				
J.O./W.O. NO. 12210	DIVISION & GROUP NM(C)	CALCULATION NO. 2043	OPTIONAL CODE SQE	PAGE 10-1 of 19

10. INTEGRITY OF ATWOOD/MORRILL CHECK VALVE 1B21*AOV032

VOID

5010.65

CALCULATION IDENTIFICATION NUMBER				
J.O. OR W.O. NO.	DIVISION & GROUP	CALCULATION NO.	OPTIONAL TASK CODE	PAGE 10-2
12210	NM(C)	2043	SQE	

10.1 Disk (SA216 WCC)

VOID

Loading

Uniform impact of the disk on the seat generates a reaction of 7.2×10^6 #, as given by FxK in Table 5.4. Acting simultaneously with impact is the pressure surge from rapidly closing the check valve.

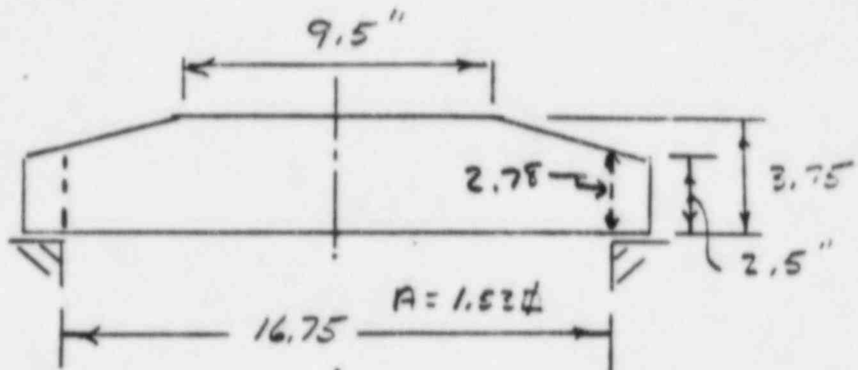

68×10^6 #   3100 psi   pressure surge effect

7.2×10^6 #   28,600 psi   impact

7.88×10^6 #   31,700 psi Total

CALCULATION SHEET

5010.65

CALCULATION IDENTIFICATION NUMBER				
J.O. OR W.O. NO.	DIVISION & GROUP	CALCULATION NO.	OPTIONAL TASK CODE	PAGE 10-3
12210	NM(C)	2043	SQE	

VOID

Shear Out

The allowable shear load in the disk at the seat inside diameter where the bending stress is zero

$$= .7(S_u/\sqrt{3}) \cdot \text{shear area} \cdot \text{strain rate factor}$$

$$= .7\left(\frac{70000}{1.73}\right)\cdot(16.75\pi\ 2.75)(2)$$

$$= 8.28\times10^6 \# > 7.88\times10^6$$ OK

Rupture

The disk must absorb the impact energy at strains below the rupture level. The impact energy

$$= \frac{4.7}{32.2}(45)^2\frac{12}{2} = 158{,}000 \text{ in\#}$$

The plastic strain energy of a circular disk from Appendix E

$$= \frac{\pi}{2}\left(\frac{\pi}{2}-1\right)\sigma_y t^2 y_0$$

A 5010 65

CALCULATION IDENTIFICATION NUMBER				
J.O. OR W.O. NO.	DIVISION & GROUP	CALCULATION NO.	OPTIONAL TASK CODE	PAGE 10-4
12210	NM(C)	2043	SQT	

$$= .89(36000)(3.75)^2 y_0$$

VOID

$$= 450000 y_0$$

Equating to the impact energy and solving for the deflection, y_0, at the disk center

$$y_0 = 158000 / [illegible]$$

$$= [illegible]''$$

From Appendix B, the maximum strain associated with this deflection is

$$\epsilon = \frac{t}{2}\left(\frac{\pi}{r_0}\right)^2 y_0 = \frac{3.75}{2}\left(\frac{\pi}{\sqrt{[illegible]}}\right)^2 ([illegible])$$

$$= .023$$

which includes the small contribution from the pressure surge by overstating the impact energy (mass of disk).

The allowable strain

$$= .7 \times \text{elongation} = .7(.22)$$

$$= .154 > .023$$

(5K)

CALCULATION IDENTIFICATION NUMBER				
J.O. OR W.O. NO.	DIVISION & GROUP	CALCULATION NO.	OPTIONAL TASK CODE	PAGE 10-5
12210	NM(c)	2043	SQE	

Hence, the integrity of the disk is demonstrated.

9.2 Rock Shaft (A182 F6a)

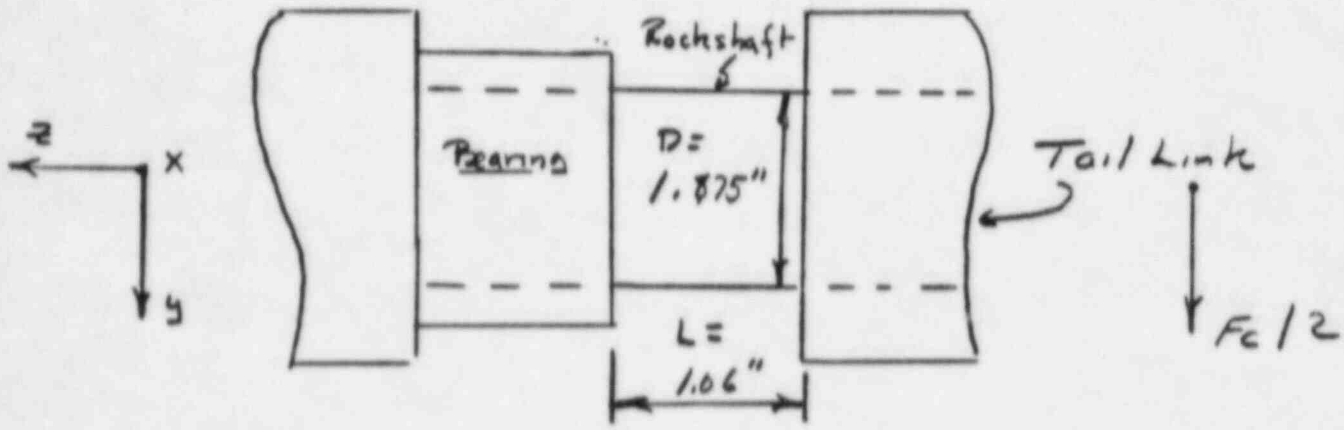

Pre-Impact

The shear stress from the centrifigal force

= Fc /(2 • area of rock shaft)

= 26,300/ 2 (2.8)

= 4700 psi

CALCULATION IDENTIFICATION NUMBER				
J.O. OR W.O. NO.	DIVISION & GROUP	CALCULATION NO.	OPTIONAL TASK CODE	PAGE 10-6
12210	NM(c)	2043	SQI	

The allowable shear stress VOID

$$= \frac{.7 S_u}{\sqrt{3}} = .7(70000)/1.7$$

$$= 28300 \text{ psi} > 4700$$ OK

The bending stress

$$MC/I = \frac{26300}{2}(1.06)\frac{1.5}{2}\frac{1}{.51}$$

$$= 21{,}400 \text{ psi}$$

The allowable bending stress

$$= .7 S_u = .7(70000)$$

$$= 49000 > 21{,}400 \text{ psi}$$ OK

Combining via the stress interaction formula of Reference 7, Appendix F7231

$$R_b = 21{,}400/49000 = .44$$

$$R_s = 4700/28300 = .17$$

Since $R = \sqrt{R_b^2 + R_s}$ = .47 < 1, integrity under pre-impact loads is demonstrated

5010.65

CALCULATION IDENTIFICATION NUMBER				
J.O. OR W.O. NO.	DIVISION & GROUP	CALCULATION NO.	OPTIONAL TASK CODE	PAGE 10-7
12210	NMS(C)	2043	SQE	

Uniform Impact

VOID

The rockshaft must carry a kick back load of 240 kips, as given in Table 8.4 for FXK. The resulting stress

$= \frac{FXK}{2} / \text{Area}$

$= \frac{240000}{2} (2.8)$

$= 33,600$ psi

The allowable shear stress

$= .7 Su \cdot \text{strain rate factor} / \sqrt{3}$

$= .7 (70000)(2)/1.7$

$= 57,600$ psi $> 33,600$ OK

The bending stress

$= MC/I = FXK(2L)(C)/8I$

$= 242000^{*}(1.06)(\frac{1.875}{2})/4(.61)$

$= 99,000$ psi

* Used actual value from computer run.

The allowable bending stress

= .7 S_u · strain rate factor

= .7(70000)(2)

= 98,000 psi < 99,000 $\boxed{NG}$

A non-linear strain analysis is required to demonstrate integrity of the rockshaft.

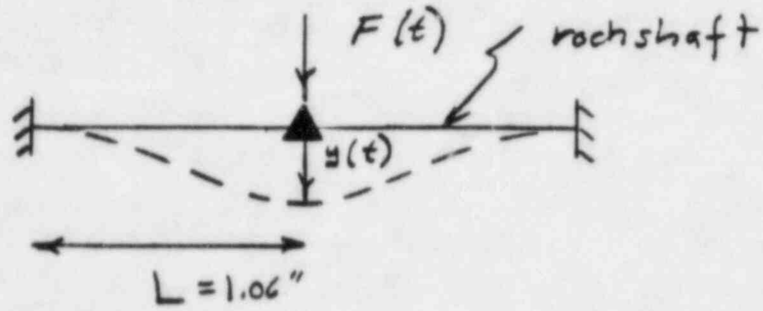

The rockshaft is modelled as shown in the sketch. All the mass of the rock shaft and the tail link bushing are lumped at the point shown by the black triangle, driven by the time varying kickback force F(t), obtained from the kickback loads analysis. Figure — shows the damped trace. Only the first peak will be used as shown on the Figure. Both the shear and bending strains are

CALCULATION IDENTIFICATION NUMBER				
J.O. OR W.O. NO.	DIVISION & GROUP	CALCULATION NO.	OPTIONAL TASK CODE	PAGE 10-9
12210	NM(C)	2043	SQI	

computed as a function of time. Following the procedure of section 9231 of Appendix A, Reference 9, the interactive ratio is formed

$$R = \sqrt{R_s^2 + R_b^2} < 1$$

VOID

where, here

R_s = shear strain / allowable

R_b = bending strain / allowable

the differential equation governing the rockshaft response to load is given by

$$m\ddot{y} + ky = F(t)$$

as long as primarily elastic conditions prevail. After essentially plastic conditions are achieved, the equation is switched by Fortran logic to

$$m\ddot{y} + R_p = F(t)$$

CALCULATION IDENTIFICATION NUMBER				
J.O. OR W.O. NO.	DIVISION & GROUP	CALCULATION NO.	OPTIONAL TASK CODE	PAGE 10-10
12210	NM(C)	2043	S&E	

where R_p is the constant resistance to displacement. The maximum bending moment is given by

VOID

$$MOM = \frac{F(2L)}{8} = FL/4$$

The resistance R_p is the value of F when MOM = M_p, the plastic moment. Thus

$$R_p = 4M_p/L$$

For a circular section (App. F), this reduces to

$$R_p = \frac{8}{3\pi}\sigma_y A D$$

The elastic stiffness, k, for combined shear and bending, since this a short beam, was obtained from the expression for deflection under a concentrated load at the center

VOID

$$\delta = \delta_{bending} + \delta_{shear}$$

From reference 15

$$\delta_{bending} = W(2L)^3/192EI = WL^3/24EI$$

For direct shear

$$\tau = \gamma G = \frac{\delta_s}{L} G = W/A$$

from which is obtained

$$\delta_{shear} = WL/AG$$

Combining bending with shear

$$\delta = WL^3/24EI + WL/AG$$

which provides the stiffness

$$k = W/\delta = \frac{1}{L^3/24EI + L/AG}$$

for elastic conditions.

From Appendix A, the relation between deflection y and the maximum strain is

CALCULATION IDENTIFICATION NUMBER				
J.O. OR W.O. NO.	DIVISION & GROUP	CALCULATION NO.	OPTIONAL TASK CODE	PAGE 10-12
12210	NM(C)	2043	SGZ	

$$\epsilon = \frac{D}{2}\frac{1}{\rho} = \frac{\pi^2}{4}\frac{Dy}{L^2}$$

VOID

These equations were coded for computation using the IBM CSMP III simulation program. Details of the coding and results are provided in the following pages. The results show that the interactive strain ratio is less than one, i.e.

$$R = .35 < 1$$

OK

Hence, integrity under uniform impact loading is demonstrated.

(STRESS VECTOR NO. 36) EQULIB CHK RESPONSE FOR ELEMENT NUMBER 38, STRESS TYPE 1 (NOD/DOF X1)

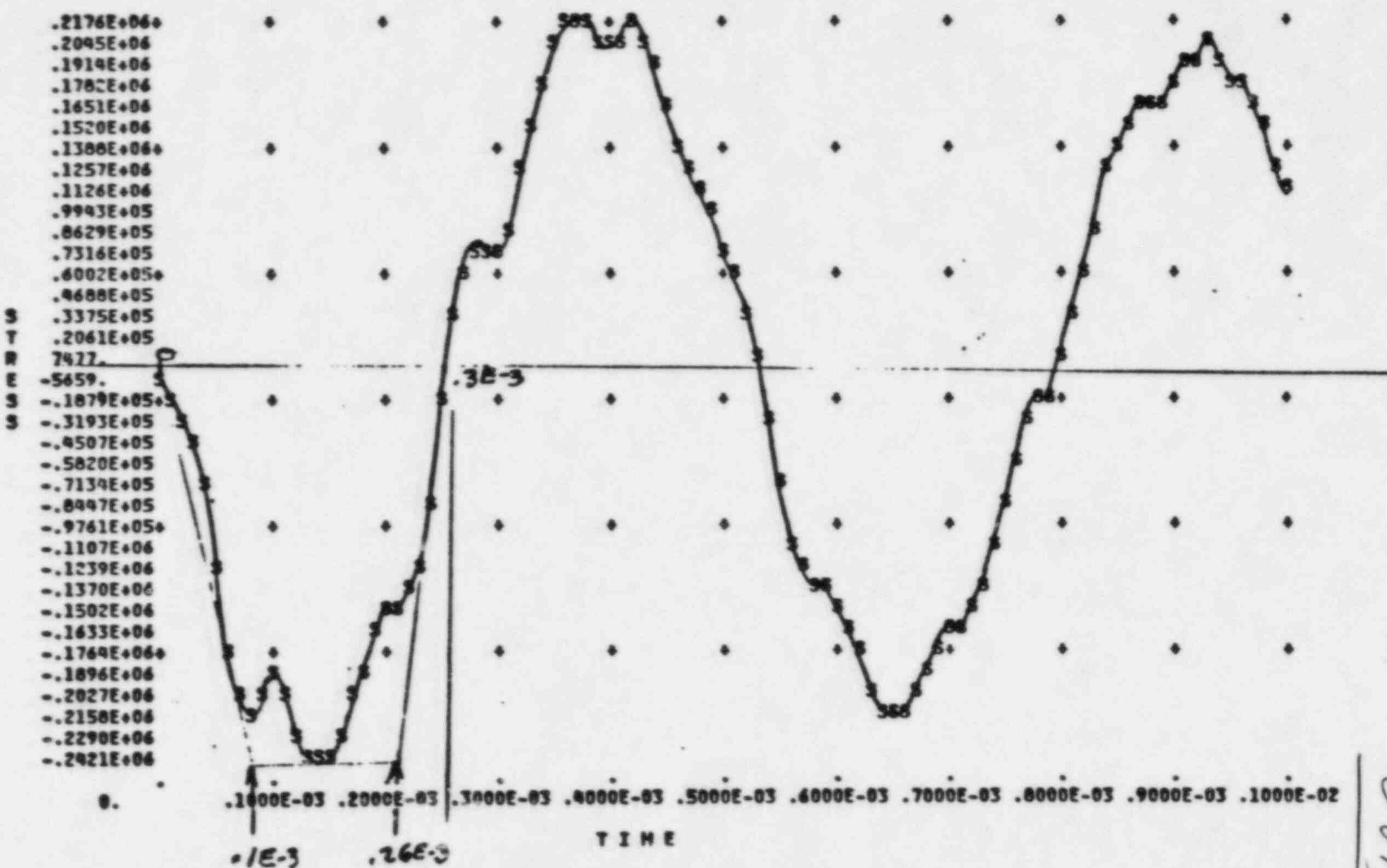

Void

STONE & WEBSTER ENGINEERING CORPORATION
CALCULATION SHEET

APPENDIX II PAGE II-32-38

J.O. OR W.O. NO.	DIVISION & GROUP	CALCULATION NO.	OPTIONAL TASK CODE	PAGE
				10-13

CALCULATION IDENTIFICATION NUMBER

CALCULATION IDENTIFICATION NUMBER				
J.O. OR W.O. NO.	DIVISION & GROUP	CALCULATION NO.	OPTIONAL TASK CODE	PAGE 11-14

VOID

```
***CONTINUOUS SYSTEM MODELING PROGRAM  III   V1M1   TRANSLATOR OUTPUT***

TITLE          TIME HISTORY STRAIN IN THE ROCKSHAFT FROM KICKBACK LOAD
TITLE                     1B21*AOV032A CHECK VALVE
TITLE                GSU/RIVER BEND POWER STATION - UNIT 1

* STORED JMG.RS032A:210

FUNCTION TH=(0.,0.),(.1E-3,.242E6),(.26E-3,.242E6),(.3E-3,0.),...
          (.8E-3,0.)
INITIAL
PARAM WTG=71.,E=27.E6,GS=11.E6,L=1.06,A=2.8,IRS=.61,D=1.88
PARAM EL=.25,SIGY=40000.
ALELB=.7*EL
ALELS=ALELB/1.7
CONST G=386.
M=WTG/G
MP=.21*SIGY*A*D
RP=4.*MP/L
EK=(3.14/L)**2*D/(4.*L**2)
K=1./(L**3/(24.*E*IRS)+L/(2.*A*GS))

DYNAMIC
FT=AFGEN(TH,TIME)
PROC DDY=FUNC(MP)
DDY=(FT-K*Y)/M
IF(MOM.GT.MP)DDY=(FT-RP)/M
ENDPROC
DY=INTGRL(0.,DDY)
Y=INTGRL(0.,DY)
BSTRN=EK*Y
SIG1=E*BSTRN
SIG2=MOM*D/(2.*IRS)
MOM=FT*L/4.
SSTRN=Y/L
RE=K*Y

* 'RATIO' IS CALCULATED IN ACCORDANCE WITH APPENDIX A9231 OF THE
* ASME III B&PV CODE
RATIO=SQRT((BSTRN/ALELB)**2+(SSTRN/ALELS)**2)

TAU1=GS*SSTRN
TAU2=FT/(2.*A)
METHOD RKSFX
* RANGE BSTRN,SSTRN,SIG1,SIG2,TAU1,TAU2,Y,MP,RP,RE,RATIO
TIMER FINTIM=.0003,PRDEL=.00001,DELT=.0000001
PRINT BSTRN,SSTRN,Y,FT
NOSORT
IF(Y.LT.0.)CALL FINISH
TERMINAL
WRITE(6,10)K
10 FORMAT(/5X,'STIFFNESS OF ROCKSHAFT(K) =',E15.3)
WRITE(6,11)RATIO
11 FORMAT(/5X,'INTERACTIVE STRAIN RATIO =',F15.3)
END
STOP

OUTPUT VARIABLE SEQUENCE
ALELB  ALELS  M    MP    RP    EK   K      DDY    DY    Y
BSTRN  SIG1   FT   MOM   SIG2  RE   SSTRN  RATIO  TAU1  TAU2
```

5010.65

CALCULATION IDENTIFICATION NUMBER				
J.O. OR W.C. NO.	DIVISION & GROUP	CALCULATION NO.	OPTIONAL TASK CODE	PAGE 10-15

VOID

TIME HISTORY STRAIN IN THE ROCKSHAFT FROM KICKBACK LOAD
1B21*AOV032A CHECK VALVE
GSU/RIVER BEND POWER STATION - UNIT 1

TIME	BSTRN	SSTRN	Y	FT
.0	.0	.0	.0	6.2500E-02
1.000000D-05	7.9778E-06	2.0504E-06	2.1735E-06	24200.
2.000000D-05	6.3804E-05	1.6399E-05	1.7383E-05	48400.
3.000000D-05	2.1416E-04	5.5043E-05	5.8346E-05	72600.
4.000000D-05	5.0321E-04	1.2933E-04	1.3709E-04	96800.
5.000000D-05	9.7136E-04	2.4966E-04	2.6464E-04	1.2100E+05
6.000000D-05	1.6542E-03	4.2516E-04	4.5067E-04	1.4520E+05
7.000000D-05	2.5802E-03	6.6315E-04	7.0294E-04	1.6940E+05
8.000000D-05	3.6209E-03	9.3064E-04	9.8648E-04	1.9360E+05
9.000000D-05	4.7149E-03	1.2118E-03	1.2845E-03	2.1780E+05
1.000000D-04	5.9104E-03	1.5191E-03	1.6102E-03	2.4200E+05
1.100000D-04	7.2476E-03	1.8626E-03	1.9745E-03	2.4200E+05
1.200000D-04	8.7349E-03	2.2450E-03	2.3797E-03	2.4200E+05
1.300000D-04	1.0372E-02	2.6658E-03	2.8257E-03	2.4200E+05
1.400000D-04	1.2159E-02	3.1251E-03	3.3126E-03	2.4200E+05
1.500000D-04	1.4096E-02	3.6229E-03	3.8403E-03	2.4200E+05
1.600000D-04	1.6183E-02	4.1592E-03	4.4087E-03	2.4200E+05
1.700000D-04	1.8419E-02	4.7339E-03	5.0180E-03	2.4200E+05
1.800000D-04	2.0805E-02	5.3472E-03	5.6681E-03	2.4200E+05
1.900000D-04	2.3341E-02	5.9990E-03	6.3590E-03	2.4200E+05
2.000000D-04	2.6027E-02	6.6894E-03	7.0908E-03	2.4200E+05
2.100000D-04	2.8863E-02	7.4183E-03	7.8634E-03	2.4200E+05
2.200000D-04	3.1849E-02	8.1857E-03	8.6769E-03	2.4200E+05
2.300000D-04	3.4985E-02	8.9917E-03	9.5312E-03	2.4200E+05
2.400000D-04	3.8271E-02	9.8362E-03	1.0426E-02	2.4200E+05
2.500000D-04	4.1706E-02	1.0719E-02	1.1362E-02	2.4200E+05
2.600000D-04	4.5292E-02	1.1641E-02	1.2339E-02	2.4200E+05
2.700000D-04	4.9008E-02	1.2596E-02	1.3352E-02	1.8150E+05
2.800000D-04	5.2458E-02	1.3483E-02	1.4292E-02	1.2100E+05
2.900000D-04	5.4773E-02	1.4078E-02	1.4922E-02	60501.
3.000000D-04	5.5739E-02	1.4326E-02	1.5185E-02	.0

$$$ SIMULATION HALTED FOR FINISH CONDITION TIME 3.0000E-04

STIFFNESS OF ROCKSHAFT(K) = 0.495E+08

INTERACTIVE STRAIN RATIO = 0.348

CALCULATION IDENTIFICATION NUMBER				
J.O. OR W.O. NO.	DIVISION & GROUP	CALCULATION NO.	OPTIONAL TASK CODE	PAGE 10-16
12210	NPM (C)	2042	SGE	

Point Impact

VOID

Point impact stresses occur before uniform impact stresses and therefore are treated independently. From Table 8,2, the worst case loads on the rockshaft are 100 kips (FXK) and 290 in kips (MYK). These combine to load the rockshaft

$$= \frac{FXK}{2} + \frac{MYK}{Grip} \quad (\text{maximum})$$

$$= 50 + 290/16.4$$

$$= 68 \text{ in Kips}$$

Since this is much smaller than the load from uniform kickback, no further analysis is required.

STONE & WEBSTER ENGINEERING CORPORATION

CALCULATION SHEET

Appendix E Page E 36 of 38

5010 65

CALCULATION IDENTIFICATION NUMBER				
J.O. OR W.O. NO.	DIVISION & GROUP	CALCULATION NO.	OPTIONAL TASK CODE	PAGE 10-11
12210	NM(C)	2043	SQE	

10.3 Tail Link

VOID

From Table 8.4, the moment acting on the weakest section of the tail link, where it joins the disk 4.5" from ℄ rock shaft, the bending moment is 960 inch-kips. The bending stress is calculated as

$$\sigma_b = \frac{Mc}{I} = 960000\left(\frac{2.9}{2}\right)/16.$$

$$= 87000 \text{ psi}$$

The allowable tensile stress

$$= .7 S_u (\text{strain rate factor})$$

$$= .7(70000)(2) = 98000 > 87000 \text{ psi} \quad \text{OK}$$

The shear stress acting on this section

$$= 240000/43 = 5600 \text{ psi}$$

The allowable shear stress

$$= .7\left(\frac{70000}{1.7}\right)(\text{strain rate factor})$$

= 57,000 psi > 5600 Void (5.13)

Applying section 9.2.3.1 of appendix A, Ref. 9,

$$R = \sqrt{R_t^2 + R_b^2} < 1$$

$$= \left[\left(\frac{5600}{57000}\right)^2 + \left(\frac{87000}{98000}\right)^2\right]^{1/2}$$

$$= .89 < 1$$ OK

Hence, the integrity of the tail link is demonstrated.

CALCULATION IDENTIFICATION NUMBER				
J.O. OR W.O. NO.	DIVISION & GROUP	CALCULATION NO.	OPTIONAL TASK CODE	PAGE 10-19
12210	NM(C)	2043	SQE	

10.4 Seat/Disk Interface VOID

The stress in the disk and seat at their interface is calculated using the familar water hammer equation

$$\Delta\sigma = \frac{\Delta u}{c} E$$

where Δu = the impact speed and c = the sonic speed in steel. Thus

$$\Delta\sigma = \frac{45}{16,400} 27\times10^6 = 74,000 psi \text{ compression}$$

The allowable tensile stress

= .7 Su (Strain rate factor)

= .7(70000) 2 = 98,000 psi > 74000

Hence, the integrity of the seat/disk interface is established, from which it is concluded that the leakage will be within acceptable limits.

STONE & WEBSTER ENGINEERING CORPORATION

CALCULATION SHEET

5010.65

CALCULATION IDENTIFICATION NUMBER				
J.O. OR W.O. NO. 15471.10	DIVISION & GROUP NM(C)	CALCULATION NO. 2043	OPTIONAL TASK CODE SQE	PAGE F-1 of

REV. 2

APPENDIX F

Confirmation of Conclusion

CALCULATION IDENTIFICATION NUMBER				
J.O. OR W.O. NO.	DIVISION & GROUP	CALCULATION NO.	OPTIONAL TASK CODE	PAGE
12210	NM(C)	2043	3Q1E	F-2

F.1 OBJECTIVE

The objective of this Appendix is to confirm the conclusions of Section 5 above.

F.2 METHOD

Inelastic systems and component analyses are carried out using the ANSYS computer program(Ref.18), for comparision of stresses to ASME III Class 1 allowables for faulted service. The stress/strain relationship was approximated by a bilinear curve(Fig.F-1) adjusted for strain rate and temperature effects. The pin and stud are not considered since original stresses therein were below ASME III allowables. Deflection of the disks from their centered position on the seat is not significant.

The dynamic loading just before impact is purely centrifugal, reacted by the rockshaft, stud and tail link. The resulting forces on the rockshaft and stud, the stress in the tail link were calculated by the ANSYS(Ref.18) program. Shear stresses in the rockshaft and stud were obtained manually.

A second run was coded to calculate the force on the rockshaft and the stress in the disk from impact of the F010 tail link on its disk. Shear stress in the rockshaft was, again, determined manually.

A third run was coded for computation of the seat force/deflection curve and the seat stress arising from impact.

A fourth run was coded to compute AOVF032 disk stress and seat force generated by impact and pressure surge, using the seat force/deflection curve obtained from the third program.

The acceptance criteria given in Section 1 was considered satisfied if all calculated stresses are below ASME III(Ref.9) Class 1 allowables for faulted service(App.F).

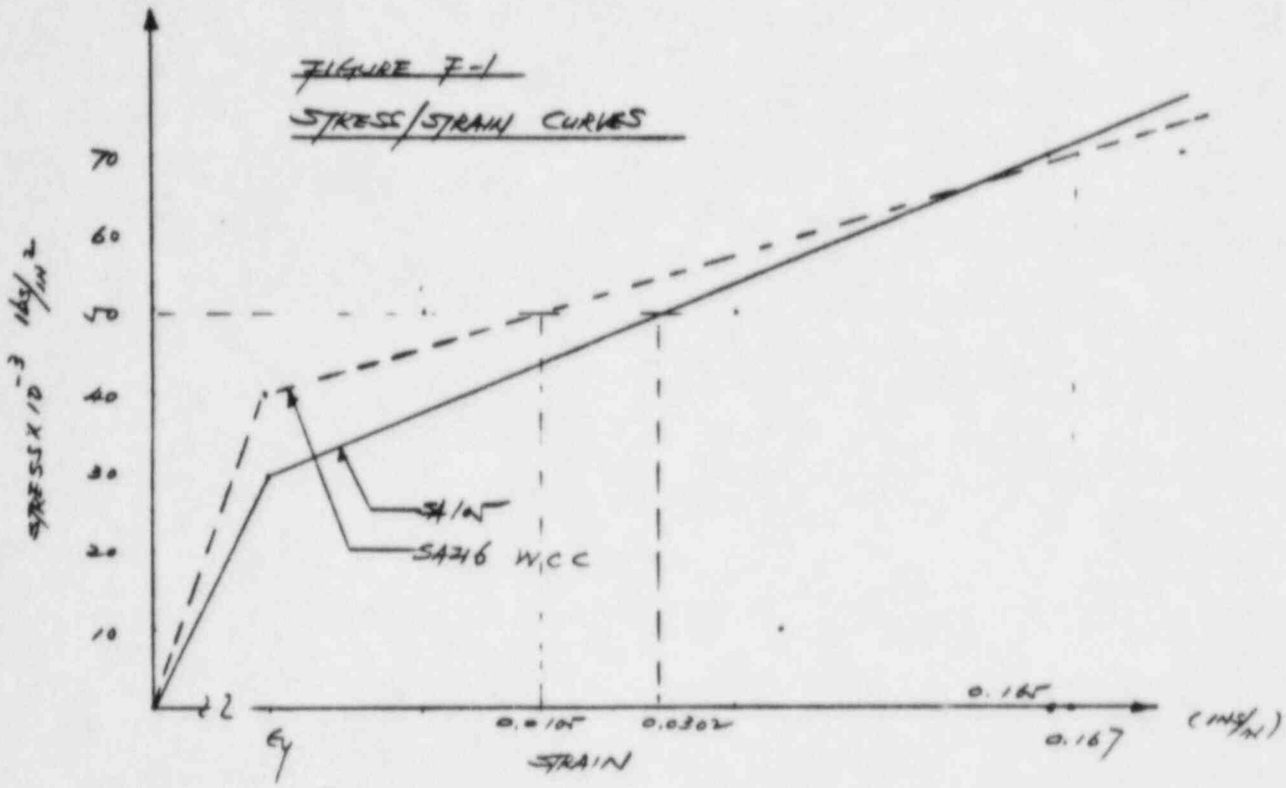

F.3 ASSUMPTIONS

1) The clearance between the tail link bushing and the stud on the disk is sufficient to preclude transfer of significant moment at the instant of impact. This allows analysis of the disk and tail link to be carried out independently.
(confirmation not required)

2) The clearance between the AOVF032 rockshaft and integral tail link is sufficient to preclude transfer of any significant force to the rockshaft from impact of the disk assembly at point not on its center of percussion.

F.4 DESIGN INPUT

Same as Section 4 above.

CALCULATION IDENTIFICATION NUMBER				
J.O. OR W.O. NO.	DIVISION & GROUP	CALCULATION NO.	OPTIONAL TASK CODE	PAGE
12210	NA1(C)	2043	SQE	F-4

F.5 SUMMARY OF RESULTS

TABLE F5.1	AOVF32				F010			
	Calc'd	Allow.	FS	PG#	Calc'd	Allow.	FS	PG#
Disk -stress ksi	38.7	49.	1.27	F-17	46.	49.	1.2	F-15
Rockshaft -stress ksi	4.4	28.3	6.5	F-8	3.7	28.3	7.7	F-6
Tail Link -stress ksi	N/A	N/A	-	-	32.6	49.0	1.5	F-8
Seat -stress ksi	46.6	49.	1.0	F-23	45.	49.	1.09	F-25

F.6 CONCLUSIONS

The results of Section F.5 confirms the conclusion of Section 6 above, that both valves will withstand rapid closure and that the pressure boundary will be maintained.

F.7 REFERENCES(added to the list in Section 7)

18. ANSYS Engineering Analysis System User's Manual, Revision 4, 3-1-1983, SWEC Program ST-348.04/1C

F8.0 TAIL LINK / ROCKSHAFT

Two loading conditions are considered below: pre-impact and impact. Critical elements are the stress in the rockshaft, the stress in the tail link section itself & the stress in the stud which secures the dish to the tail link.

F010 VALVE

Pre-Impact, (Run# 1)

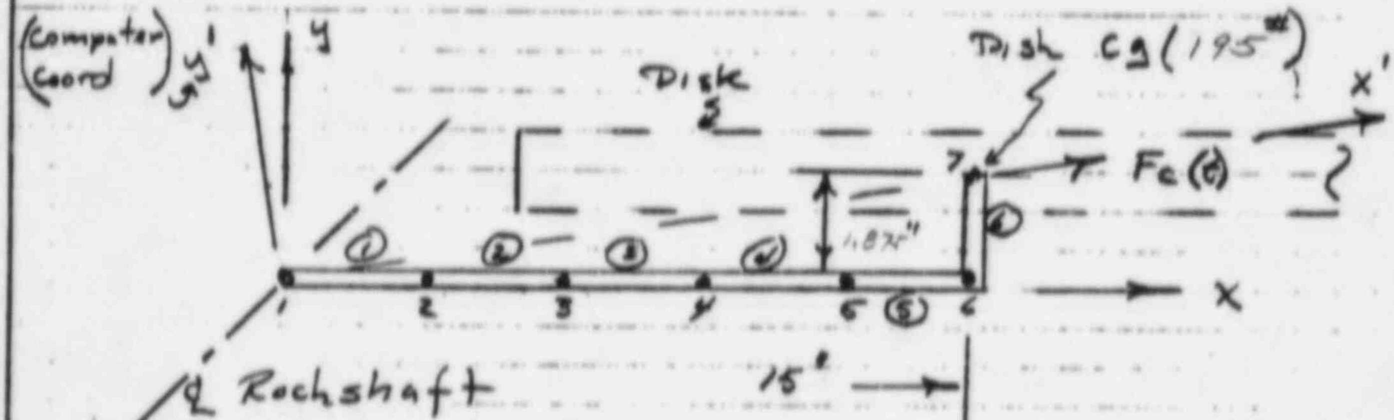

The dish is accelerated about the rockshaft by the reversed flow until impact with the seat. The variation of centrifugal force, Fc, with time was obtained from the time history angular velocity derived in Ref. 1.

CALCULATION IDENTIFICATION NUMBER				PAGE
J.O. OR W.O. NO.	DIVISION & GROUP	CALCULATION NO.	OPTIONAL TASK CODE	
12210	NM(C)	2043	SDE	F-6

The tail link was modelled for ANSYS (Ref. 18) computation as shown in the sketch. All of the disk weight (260#) plus 1/2 the tail link weight was lumped at node 7.

Results were as follows, from run# 1 :

Maximum stress intensity in the tail link

= 29300 psi < 49000 FS = 1.7

OK

(Maximum deflection of the disk from its centered position

= .044" << .625

which demonstrates its insignificance.)

Rockshaft

Stress in double shear

= 20500/2.8(2) = 3,660 psi < $\frac{49000}{1.8}$ = 28300 FS = 7.7

OK

STONE & WEBSTER ENGINEERING CORPORATION

CALCULATION SHEET

5010.65

CALCULATION IDENTIFICATION NUMBER				
J.O. OR W.O. NO.	DIVISION & GROUP	CALCULATION NO.	OPTIONAL TASK CODE	PAGE
12210	NM(C)	2043	SQE	F-7

Impact, (Run # 2)

At impact, the critical elements are stress in the tail link and the rockshaft. The same model as described above was used for ANSYS computation except that dish mass is not included and the stud was replaced by a zero gap element of stiffness equal to 1.5E7, the elastic stiffness of the disk. This is conservative because, since the disk is actually deflecting, it's stiffness as seen by the tail link is reduced.

The maximum reaction at the rockshaft, from the computer run, was 23800#, which results in a shear stress

$$= \frac{23800}{2(2.8)} = 4,300 \text{ psi} < \frac{49000}{\sqrt{3}} < 28300$$

FS = 6.6

OK

STONE & WEBSTER ENGINEERING CORPORATION

CALCULATION SHEET

5010.65

CALCULATION IDENTIFICATION NUMBER				
J.O. OR W.O. NO.	DIVISION & GROUP	CALCULATION NO.	OPTIONAL TASK CODE	PAGE
12210	NM(C)	2043	SQE	F-8

From the computer run, the maximum stress in the tail link

$= 33\,600$ psi < 49010 $F_S = 1.5$

OK

<u>AOVF32 VALVE</u> (No tail link)

<u>Pre-Impact</u>

From Table 8.1, the maximum force on the rock shaft results in a shear stress

$$= \frac{24400}{2(2.8)} = 4400 < 28300 \quad FS = 6.5$$

OK

<u>Impact</u>

The clearance between the disk attachment and the rockshaft precludes any significant reaction.

CALCULATION IDENTIFICATION NUMBER				
J.O. OR W.O. NO.	DIVISION & GROUP	CALCULATION NO.	OPTIONAL TASK CODE	PAGE
12210	NM(C)	2043	50E	F-9

F9.0 DISK ANALYSIS

Pre-impact loads on the disk are not significant, and therefore not addressed. At impact, the critical stresses are bending and membrane as a plate and the local stresses from contact with the seat. However, the disk material being the same as the seat, it is expected that the local stresses will be similar to those computed for the seat in section 10.

Figures F.2 and F.3 show the nodes and elements of the disk as modelled for ANSYS computations. Attached to the rim nodes are elements which represent the non-linear force/deflection character of the seat, obtained from the seat analysis in Section F.10, reduced by a factor of 2 (to account for the contribution from local yielding of the disk.

Stone and Webster Engineering Corporation
CALCULATION SHEET

Calculation Identification Number				
J.O./W.O. NO.	DIVISION & GROUP	CALCULATION NO.	OPTIONAL CODE	PAGE
12210	NM(C)	2043	SQE	F-10

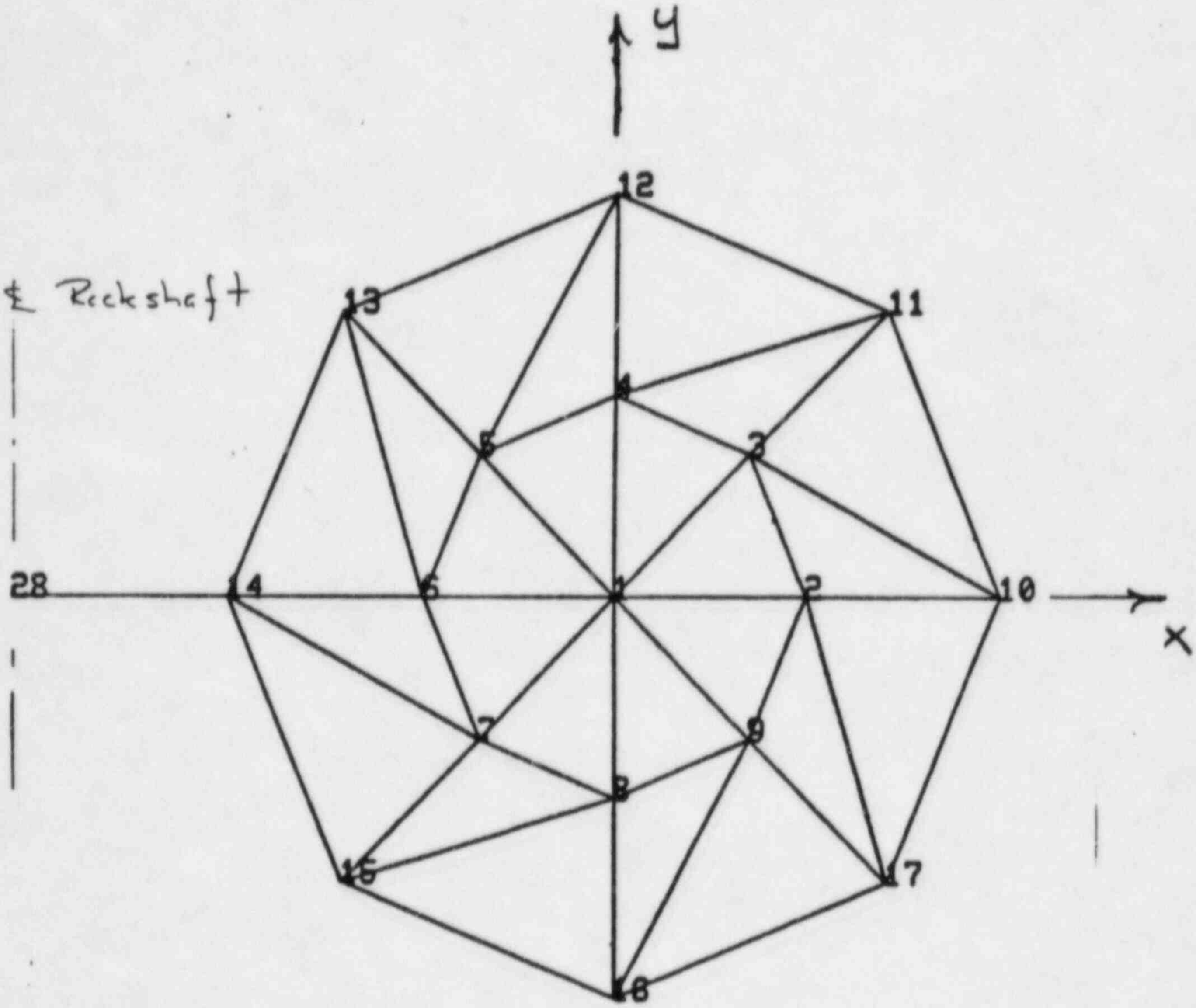

Figure F-2 ANSYS Computer Model for Tail-Link/Disk Impact Loads(Nodes)

Stone and Webster Engineering Corporation
CALCULATION SHEET

Calculation Identification Number				
J.O./W.O. NO.	DIVISION & GROUP	CALCULATION NO.	OPTIONAL CODE	PAGE
12210	EM(C)	2043	SQE	F-11

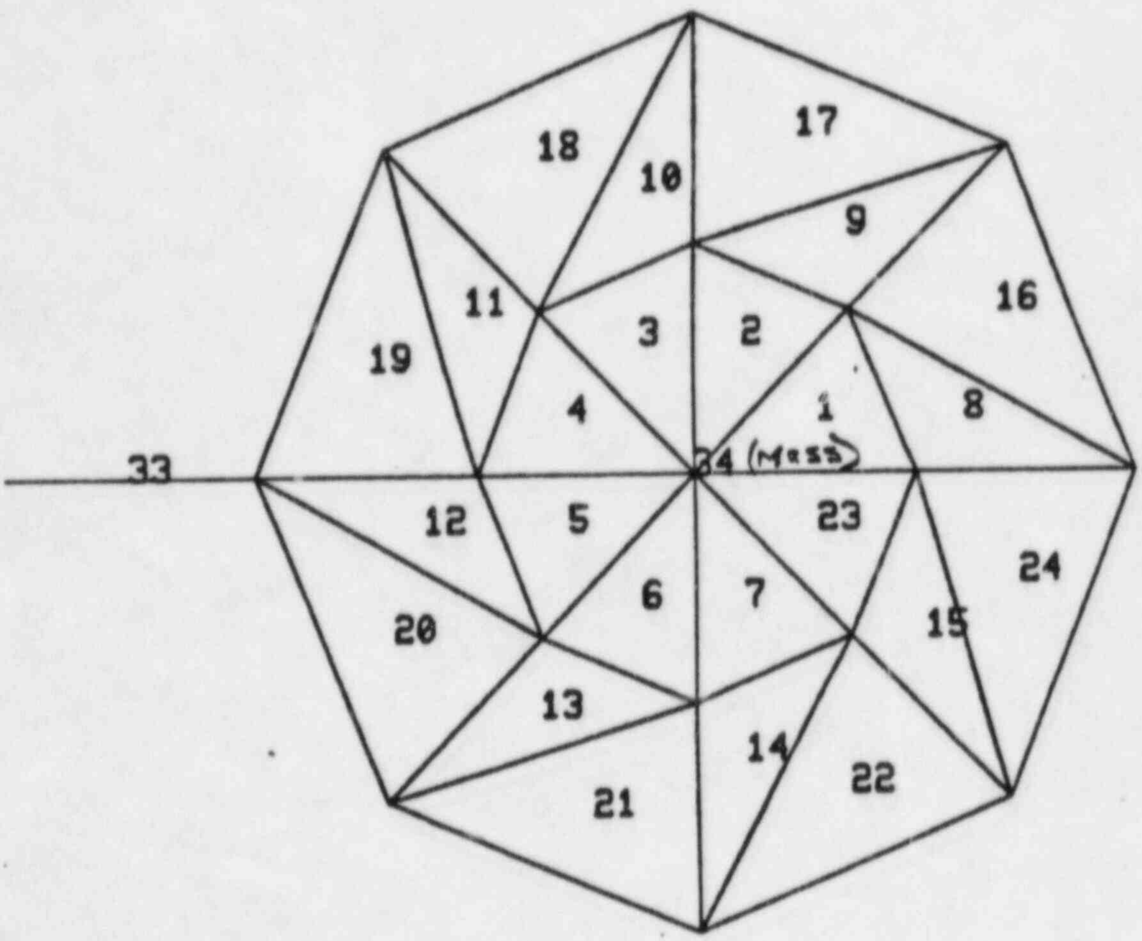

Figure F-3 ANSYS Computer Model for Tail-Link/Disk Impact Loads(Elements)

STONE & WEBSTER ENGINEERING CORPORATION

CALCULATION SHEET

5010.65

CALCULATION IDENTIFICATION NUMBER				
J.O. OR W.O. NO.	DIVISION & GROUP	CALCULATION NO.	OPTIONAL TASK CODE	PAGE
12210	NM(C)	2043	SQE	F-12

Stresses are printed for element 23, representing the worst case for the center elements, and for element 24, representing the worst case for the rim elements.

The seat force is printed out for later use in calculating the seat stress.

The seat analysis of section F.10 shows that after the seat force from disk impact is 1.2E6 #, the stiffness of the seat is greatly reduced by plasticity. This was not modelled in the ANSYS run because two non-linearities, gap stiffness representing the seat and the disk material, occurring in the same time frame could not be made to converge. Thus, the seat force from the ANSYS runs is greatly overstated.

STONE & WEBSTER ENGINEERING CORPORATION

CALCULATION SHEET

5010.65

CALCULATION IDENTIFICATION NUMBER				
J.O. OR W.O. NO.	DIVISION & GROUP	CALCULATION NO.	OPTIONAL TASK CODE	PAGE
12210	NM(C)	2043	SQE	F-13

F010 DISK (Run # 6)

The F010 disk is a 2.75 inch circular plate 17.5 inches in diameter, modelled as a 2.75" circular plate 16.8 inches in diameter to simulate the effective seat diameter. Actual seat diameter is 15.75".

Initial nodal velocities input to ANSYS from Ref. 1 are shown in Table F-2.

STONE & WEBSTER ENGINEERING CORPORATION

CALCULATION SHEET

A 5010.65

CALCULATION IDENTIFICATION NUMBER				
J.O. OR W.O. NO.	DIVISION & GROUP	CALCULATION NO.	OPTIONAL TASK CODE	PAGE
12210	NM(C)	2043	SQE	F-14

F010 58R/S	NODE NUMBER								
	14	13, 15	6	5, 7	1, 4, 8, 12, 16	3, 9	2	11, 17	10
Radius (in)	3.9	6.	8.1	9.3	12.3	15.3	16.5	18.2	20.7
Vel. (ips)	226	348	470	539	713	887	957	1060	1200

TABLE F-2 - INITIAL NODAL VELOCITIES FOR ANSYS INPUT

CALCULATION IDENTIFICATION NUMBER				
J.O. OR W.O. NO.	DIVISION & GROUP	CALCULATION NO.	OPTIONAL TASK CODE	PAGE
12210	NM(C)	2043	8ΦE	F-15

Maximum stress intensity in the disk, as computed by the ANSYS program, element 24

= 40,000 psi < 49000

FS = 1.23

OK

from disk response as a plate. Local stress from impact is expected to be similar to the local stress in the seat, as described in section 10 below.

Maximum seat force from the ANSYS run, variable 21

= 2.1 E6 #

STONE & WEBSTER ENGINEERING CORPORATION

CALCULATION SHEET

5010.65

CALCULATION IDENTIFICATION NUMBER				
J.O. OR W.O. NO.	DIVISION & GROUP	CALCULATION NO.	OPTIONAL TASK CODE	PAGE
12210	NM(C)	2043	39E	F-16

AOVF032 DISK (Run# 5)

the AOVF032 disk is a tapered circular plate of 19" diameter, 2.5" thick at the rim and 3.75" diameter at the center. It was modelled as a 3" circular plate to simulate the average thickness of the outer elements in the model, with a concentrated mass at its center

$$= 260 - 3\pi 8.8^2(.283) = 260 - 207$$

$$= 53^{\#} (.138 \text{ in/slugs})$$

the 17.6" dimension is the estimated diameter of the seat pressure. the seat ID is 16.75".

Initial modal velocities obtained from Ref. 1 are shown in Table F-3.

STONE & WEBSTER ENGINEERING CORPORATION

CALCULATION SHEET

A 5010.65

CALCULATION IDENTIFICATION NUMBER				PAGE
J.O. OR W.O. NO.	DIVISION & GROUP	CALCULATION NO.	OPTIONAL TASK CODE	
12210	NM(C)	2043	5QE	F-17

Maximum stress intensity in the disk, as computed by the ANSYS program, element 24

= 38,700 psi < 49000 FS = 1.27 OK

from disk response as a plate. Local stress from impact is expected to be similar to the local stress in the seat, as described in section 10 below.

Maximum seat force from the ANSYS run, variable 21

= 2.0E6 #

AOVF32 42 Rad/sec	NODE NUMBER								
	14	13, 15	6	5, 7	1, 4, 8, 12, 16	3, 9	2	11, 17	10
Radius (in)	5	7.6	9.5	10.8	14	172	18.5	20.4	23
Vel. (ips)	210	307	400	533	588	722	777	911	966

TABLE F-3 - INITIAL NODAL VELOCITIES FOR ANSYS INPUT

CALCULATION IDENTIFICATION NUMBER				PAGE
J.O. OR W.O. NO.	DIVISION & GROUP	CALCULATION NO.	OPTIONAL TASK CODE	
12210	NM(C)	2043	SQE	F-19

F.10 SEAT ANALYSIS

A 12° sector of the seat annulus was modelled for ANSYS computation of stress intensity and deflection as a function of the impact pressure. Figure F-4 shows the elements while Figures F-5 and F-6 identify the nodes on the left and right hand faces respectively.

The loading was on elements 12, 18 and 24 in the Z direction, varied from .5E6 to 2E6 # over an area of 22.3 in^2.

Deflection was calculated as the average of nodes 25, 26, 29, 30, 73-76. Maximum stress was selected from the loaded elements and adjacent elements 10-12, 17, 18 & 24.

Stone and Webster Engineering Corporation
CALCULATION SHEET

Calculation Identification Number				
J.O./W.O. NO. 12210	DIVISION & GROUP NM(C)	CALCULATION NO. 2043	OPTIONAL CODE SQE	PAGE F-20

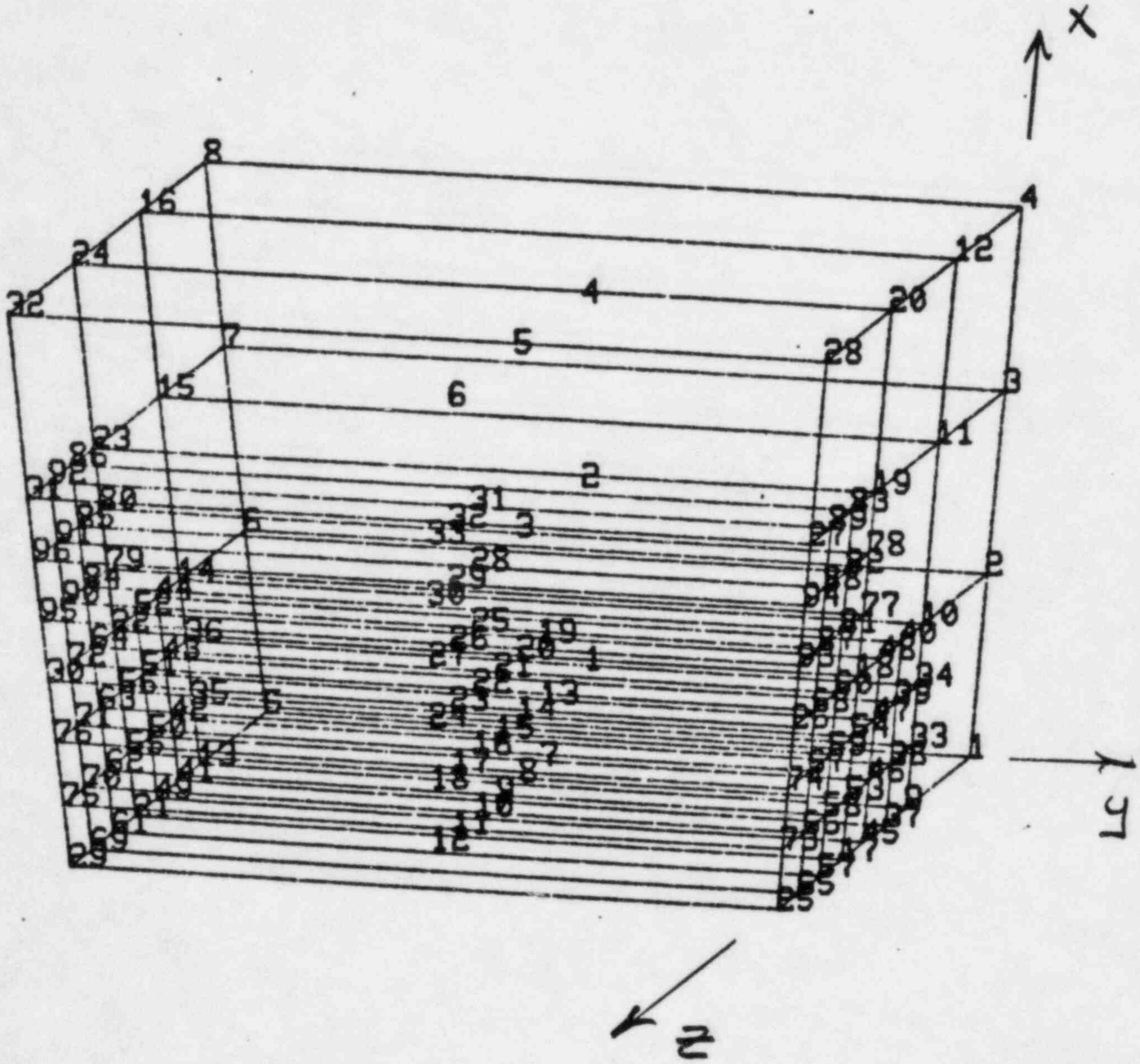

Figure F-4 Computer Model for Seat Analysis

Stone and Webster Engineering Corporation
CALCULATION SHEET

Calculation Identification Number				
J.O./W.O. NO. 12210	DIVISION & GROUP NM(C)	CALCULATION NO. 2043	OPTIONAL CODE SQE	PAGE F-21

32			24			16	8
31	92	86	23			15	7
96	91	85	80				
95	90	84	79				
30	72	64	22	52	44	14	6
76	71	63	56	51	43	36	
75	70	62	55	50	42	35	
29	69	61	21	49	41	13	5

Figure F-5 - Nodes for Left Face of Model

Stone and Webster Engineering Corporation
CALCULATION SHEET

Calculation Identification Number				
J.O./W.O. NO.	DIVISION & GROUP	CALCULATION NO.	OPTIONAL CODE	PAGE
12210	NM(C)	2043	SQE	F-22

28			20			12	4
27	89	83	19			11	3
94	88	82	78				
93	87	81	77				
26	68	60	18	48	40	10	2
74	67	59	54	47	39	34	
73	66	58	53	46	38	33	
25	65	57	17	45	37	9	1

Figure F.6 - Nodes for Right Face of Model

A0VF032 SEAT (Run # 302)

Results of the seat analysis are summarized in Table F-4 below.

From the dish analysis of Section F.9, the maximum seat force is calculated

$$= 2.0E6 \ \#$$

which is overstated because the seat stiffness, as shown in that Table, drops drastically below its elastic value after the seat force is above 1.2E6 #. Hence, the actual seat force is closer to

$$1.2E6 + \frac{(2.0-1.2)E6}{4} = 1.4 \ E6^{\#} \ *$$

which corresponds to a seat stress from the Table by interpolation.

$$= 46{,}600 \text{ psi} < 49{,}000 \qquad FS = 1.05$$

OK

* SEE PAGE F-27 FOR ALTERNATE CALCULATION

CALCULATION IDENTIFICATION NUMBER				
J.O. OR W.O. NO.	DIVISION & GROUP	CALCULATION NO.	OPTIONAL TASK CODE	PAGE F-24
12210	NM(C)	2043	5QE	

Total Force ~# ($x10^{-6}$)	812,270	1,001,430	1,224,000	1,446,500	1,669,000	1,891,600	2,114,100	2,225,400
Element Pressure (ksi)	36.5	45	55	65	75	85	95	100
Average Displ. (in.)	.225E-2	.2926E-2	.4429E-2	.7219E-2	.1162E-1	.1792E-1	.2674E-1	.3602E-1
Stiffness (#/in)	3.61E8	3.42E8	2.76E8	2.00E8	1.44E8	1.06E8	7.91E7	6.18E7
Stress (ksi)	34.3	43.5	45.8	47.4	49.3	51.5	54	56.5

TABLE F-4 - RESULTS OF ANSYS SEAT ANALYSIS FOR 2OVF 032

(Radial Free)

STONE & WEBSTER ENGINEERING CORPORATION

CALCULATION SHEET

5010.65

CALCULATION IDENTIFICATION NUMBER				
J.O. OR W.O. NO.	DIVISION & GROUP	CALCULATION NO.	OPTIONAL TASK CODE	PAGE
12210	NM(C)	2043	SOE	F-25

F010 SEAT (Run # 4)

Results of the ANSYS seat analysis are summarized in Table F-10.2 below.

From the disk analysis of Section F.9, the maximum seat force = 2.0 E6#, which results in a seat stress

= 45,000 psi < 49 ksi FS= 1.09 OK

obtained by interpolation of Table F-4.

Total Force ~# ($x10^{-6}$)	578,600	778,890	890,160	1,001,430	1,112,700	1,335,240	1,557,780	2,003,860
Element Pressure (ksi)	26	35	40	45	50	60	70	90
Average Displ. (in.)	.1072E-2	.1513E-2	.2082E-2	.2985E-2	.4325E-2	.6917E-2	1.0647E-2	1.773E-2
Stiffness (lb/in)	5.4E8	5.1E8	4.3E8	3.4E8	2.6E8	1.9E8	1.5E8	1.1E8
Stress (ksi)	25.9	32.3	33.5	34.5	35.7	37.5	40.0	44.1

TABLE F-5 - RESULTS OF ANSYS SEAT ANALYSIS FOR F010

(Radial Held)

ATTACHMENT TO APPENDIX F

ALTERNATE CALCULATION FOR AOV7032 SEAT FORCE

THIS ATTACHMENT IS INTENDED TO SUBSTANTIATE THE REASONNING FOR ADJUSTING THE MAX. SEAT FORCE IN PAGE F-23 AS FOLLOWS

FROM PAGE F24, THE LIMIT FORCE IS APPROXIMATELY :

$F_y = \underline{812,300 \ \#}$

FROM PAGE F23, THE MAX. ELASTIC SEAT FORCE IS

$F_e = \underline{2.0E6 \ \#}$

FROM EQ. III.7, THE WORKING DUCTILITY RATIO IS

$$\mu = \left(1 - \frac{1}{\xi}\right) + \left[\frac{1}{\xi}\left(\frac{1}{\xi} - 1 + \left(\frac{D}{C}\right)^2\right)\right]^{1/2}$$

WHERE ξ = RATIO OF PLASTIC STIFFNESS AND ELASTIC STIFFNESS

$= \frac{k_2}{k_1} = \frac{5E7}{3.6E8} = \underline{0.139}$

D = DEMAND LOAD = F_e = 2.0E6 # $\Rightarrow \frac{D}{C} = \underline{2.5}$

C = CAPACITY = F_y = 8.123 E5 #

$$\mu = \left(1 - \frac{1}{0.139}\right) + \left[\frac{1}{0.139}\left(\frac{1}{0.139} - 1 + (2.5)^2\right)\right]^{1/2}$$

$\mu = \underline{3.3}$

FROM EQ. III.3 THE DYNAMIC IMPACT LOAD, IF THE SEAT IS MODELED AS ELASTO-PLASTIC ELEMENT IS

$F_d = F_y[1 + \xi(\mu - 1)]$

$= 8.123E5[1 + 0.139(3.3 - 1)]$

$= \underline{1.07E6 \ \#} < \underline{1.4 \ E6}$ AS USED IN THIS CALCULATION (SEE F-23)

THEREFORE IT'S CONSERVATIVE TO USE 1.4E6 #

K•E 10 X 10 TO THE CENTIMETER 18 X 25 CM
KEUFFEL & ESSER CO. MADE IN U.S.A.

46 1512

A = 0.7418 IN²

AOVF 32

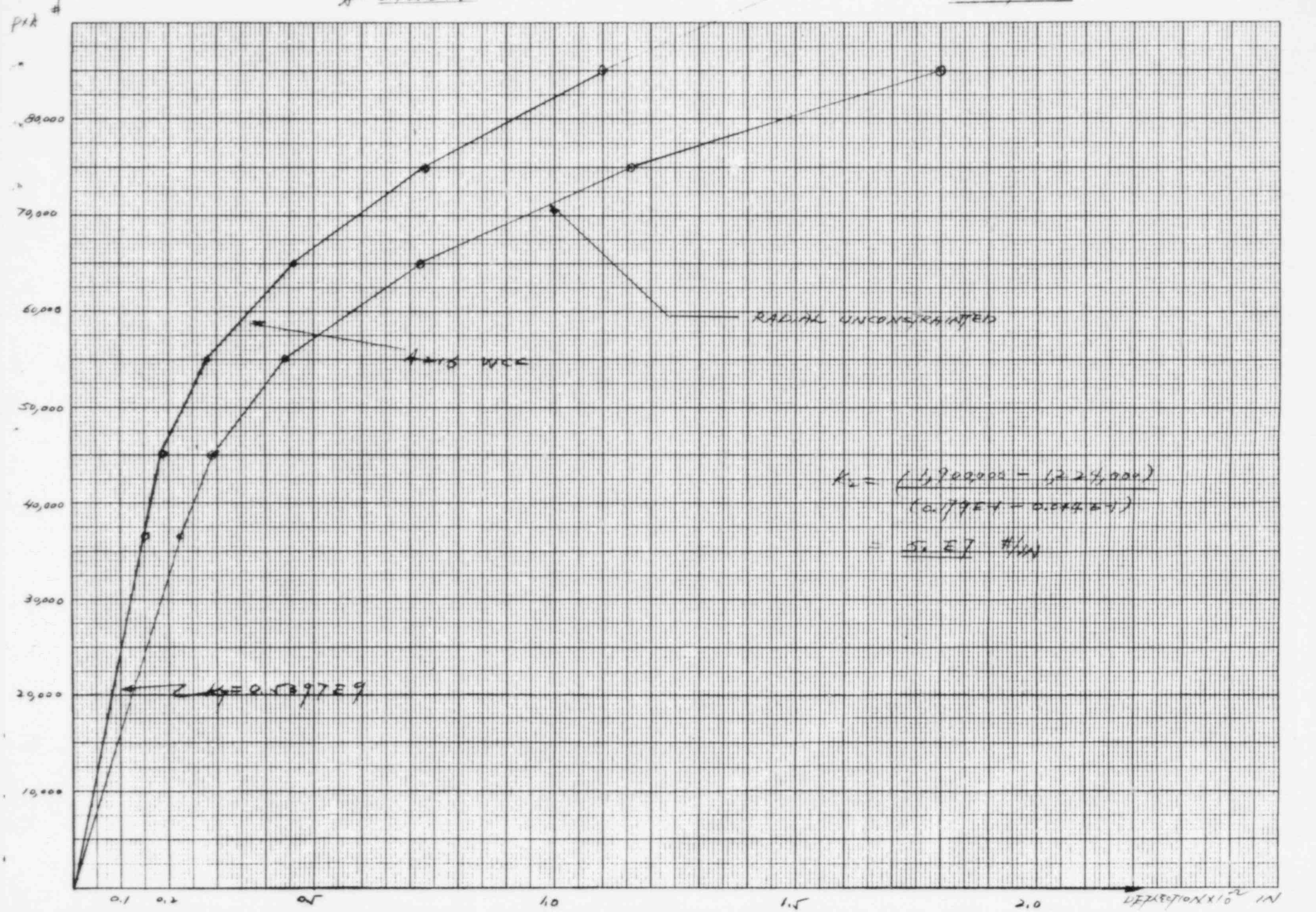

SITUATION A MASS m IS DROPED VERTICALLY DOWNWARD FROM A HEIGHT h AND IS STOPPED BY THE ELASTO-PLASTIC ELEMENT REPRESENTED AS A SPRING MASS SYSTEM. THE MASS OF THE ELASTO-PLASTIC ELEMENT IS LUMPED AS M_e

METHOD ENERGY METHOD

ANALYSIS

I. MATERIAL IS PERFECT-PLASTIC

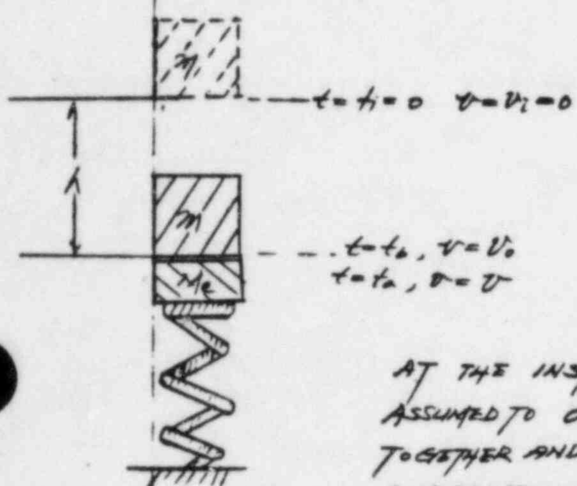

FROM THE TIME t_i THAT THE MASS m IS BEGINNING TO FALL, THE VELOCITY THEN IS ZERO. AFTER MOVING A DISTANCE h THE VELOCITY INCREASES TO V_0. FROM FIG. THE K.E. OF THIS MASS, m, JUST PRIOR TO IMPACT, IS

$$(K.E)_0 = \frac{1}{2} m v_0^2 \quad ------ (1)$$

THE K.E. IS GAINED FROM THE POTENTIAL ENERGY

$$\frac{1}{2} m v_0^2 = mgh \quad ----- (2)$$

AT THE INSTANT OF IMPACT, LOCAL INELASTIC DEFORMATION IS ASSUMED TO OCCUR, AFTER WHICH BOTH MASSES ARE ASSUMED TO MOVE TOGETHER AND SPRING COMPRESSION TAKES PLACE. FROM MOMENTUM CONSERVATION, ONE HAS

$$m v_0 = (m + M_e) v \quad ----- (3)$$

$$v = \frac{m v_0}{(m + M_e)} = \frac{1}{(1+\frac{M_e}{m})} v_0$$

LET $\quad C = \dfrac{1}{(1+\frac{M_e}{m})}$

$\therefore \quad v = C v_0 \quad ------ (4)$

THE TOTAL KINETIC ENERGY OF BOTH BODIES AT THE TIME LOCAL INELASTIC DEFORMATION IS COMPLETE

$$(K.E)_a = \frac{1}{2}(m + M_e) v^2 \quad ---- (5)$$

$$= \frac{1}{2}(m+M_e) c^2 v_0^2 = \frac{1}{2} m (1+\frac{M_e}{m}) c^2 v_0^2$$

$$(K.E)_a = \frac{1}{2} m c v_0^2 \quad ---- (6)$$

FROM (2), (6) BECOMES

$$(K.E)_a = mgh\,C \quad ------ (7)$$

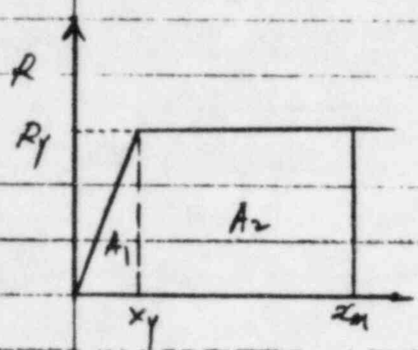

THE TOTAL WORK DONE IN COMPRESSING THE SPRING IS EQUAL TO THE TOTAL K.E. AVAILABLE AT THE TIME LOCAL INELASTIC DEFORMATION IS COMPLETE PLUS THE POTENTIAL ENERGY AVAILABLE RESULTING FROM THE DISPLACEMENT OF SPRING WILL COMPRESS

$$\tfrac{1}{2}(m+M_e)v^2 + (m+M_e)g\,x_m$$
$$= mghc + (m+M_e)g\,X_m$$
$$= mghc + m\left(1+\tfrac{M_e}{m}\right)g\,X_m$$
$$= mghc + \frac{mg\,X_m}{c} \quad \text{----- (8)}$$

THE INTERNAL STRAIN ENERGY IS

$$(P.E) = A_1 + A_2 = R_y x_m - R_y\frac{x_y}{2} \quad \text{--- (9)}$$

BY ENERGY BALANCE, THE TOTAL STRAIN ENERGY STORED IN THE SPRING MUST EQUAL THE TOTAL WORK DONE.

$$R_y X_m - R_y\frac{x_y}{2} = mghc + mg\,x_m/c \quad \text{---- (10)}$$

BUT

$$R_y = kx_y \quad \& \quad X_m = \mu x_y = \mu\frac{R_y}{k} \quad \text{... (11)}$$

$$\left(\frac{\mu}{k}\right)R_y^2 - \frac{R_y^2}{2k} = mghc + mg\frac{\mu}{ck}R_y$$

$$\left[\frac{\mu}{k} - \frac{1}{2k}\right]R_y^2 = mghc + mg\frac{\mu}{ck}R_y$$

$$\left(\frac{2\mu-1}{2k}\right)R_y^2 = mghc + mg\frac{\mu}{ck}R_y$$

$$R_y^2 - mg\frac{2\mu}{(2\mu-1)}R_y - \frac{2mgkhc}{(2\mu-1)} = 0$$

LET $\quad a = \dfrac{mg}{(2\mu-1)}$

$$R_y^2 - 2a\mu R_y - 2akhc = 0$$

$$\therefore \quad R_y = a\mu + \sqrt{(a\mu)^2 + 2akhc}$$

$$\boxed{R_y = a\mu\left[1 + \sqrt{1 + \frac{2khc}{\mu^2 a}}\right]} \quad \text{--- (12)}$$

CLY

THE PERIOD OF THE SYSTEM IS

$$T = 2\pi\sqrt{\frac{m+M_e}{k}} \quad \text{-----} \quad (13) \Rightarrow \frac{k}{(m+M_e)} = \frac{4\pi^2}{T^2}$$

$$R_y = \frac{mg\,\mu}{(3\mu-1)}\left[1+\sqrt{1+\frac{2kh_c(3\mu-1)}{\mu^2 mg}}\right]$$

$$= mg\frac{\mu}{(3\mu-1)}\left[1+\sqrt{1+\frac{2kh(3\mu-1)}{\mu^2(m+M_e)g}}\right] \qquad \text{NOTE } h = \frac{V_0^2}{2g}$$

$$= mg\frac{\mu}{(3\mu-1)}\left[1+\sqrt{1+\frac{2kV_0^2(3\mu-1)}{2\mu^2(m+M_e)g^2}}\right]$$

$$= mg\frac{\mu}{(3\mu-1)}\left[1+\sqrt{1+\frac{4\pi^2 V_0^2(3\mu-1)}{\mu^2 T^2 g^2}}\right]$$

$$\boxed{R_y = mg\left(\frac{\mu}{3\mu-1}\right)\left[1+\sqrt{1+\left(\frac{3\mu-1}{\mu^2}\right)\left(\frac{2\pi V_0}{gT}\right)^2}\right]}$$

IF $\left(\frac{3\mu-1}{\mu^2}\right)\left(\frac{2\pi V_0}{gT}\right)^2 \gg 1$

THEN $1+\sqrt{1+\left(\frac{3\mu-1}{\mu^2}\right)\left(\frac{2\pi V_0}{gT}\right)^2} = \left(\frac{2\pi V_0}{gT}\right)\left(\frac{3\mu-1}{\mu}\right)\sqrt{\frac{1}{3\mu-1}}$

$$\therefore \quad \boxed{R_y = \frac{2\pi m V_0}{T}\sqrt{\frac{1}{3\mu-1}}}$$

BUT $I = mV_0$ = MOMENTUM

$$w = \frac{2\pi}{T} = \sqrt{\frac{k}{m+M}}$$

$$\boxed{R_y = \frac{I w}{\sqrt{3\mu-1}}}$$

IN ELASTIC IMPACT, ONE HAS

$$R_e = I w$$

$$\Rightarrow \quad \boxed{\frac{R_y}{R_e} = \frac{1}{\sqrt{3\mu-1}}}$$

I. MATERIAL IS ELASTO PLASTIC

II.1 DERIVATION OF ABSORBED ENERGY, E_a, I.E. THE INTERNAL STRAIN ENERGY

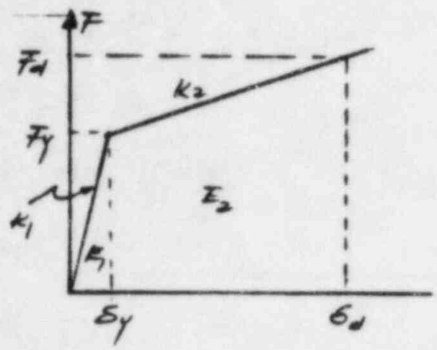

THE ENERGY ABSORBED BY A DEFORMATION OF THE TARGET IS

$$E_a = \int_0^{\delta_d} F_R(x)\,dx \quad ----- \quad (II.1)$$

THE INTERGATION TERM IN THE ABOVE EQUATION CAN BE CARRIED OUT IF WE ASSUME THE MATERIAL OF THE TARGET HAS A BILINEAR FORCE-DISPLACEMENT RELATION AS SHOWN, WHERE

k_1 = ELASTIC STIFFNESS, kips/in

k_2 = PLASTIC STIFFNESS, kips/in

F_y = YIELD FORCE, kips

F_d = LOAD AT MAX. DISPLACEMENT, δ_d, kips

δ_y = YIELD DISPLACEMENT, IN.

δ_d = MAX. DISPLACEMENT, IN.

INTERGRATE THE ABSORBED ENERGY PIECEWISELY OVER THE FORCE-DEFLECTION CURVE, ONE HAS:

$$E_a = E_1 + E_2 = \int_0^{\delta_y} F_R(x)_1\,dx + \int_{\delta_y}^{\delta_d} F_R(x)_2\,dx \quad ---- \quad (II.2)$$

SINCE $\quad F_R(x)_1 = k_1 x \quad ----- \quad (II.3)$

& $\quad F_R(x)_2 = F_y + k_2(x-\delta_y) \quad ----- \quad (II.4)$

$$\Rightarrow \quad E_a = \int_0^{\delta_y} k_1 x\,dx + \int_{\delta_y}^{\delta_d} [F_y + k_2(x-\delta_y)]\,dx \quad ------- \quad (II.5)$$

$$= k_1\frac{\delta_y^2}{2} + F_y(\delta_d-\delta_y) + k_2\left(\frac{\delta_d^2}{2} - \delta_y\delta_d\right) - k_2\left(\frac{\delta_y^2}{2} - \delta_y^2\right)$$

$$= k_1\frac{\delta_y^2}{2} + F_y\delta_d - F_y\delta_y + k_2\frac{\delta_d}{2}(\delta_d - 2\delta_y) + k_2\frac{\delta_y^2}{2}$$

$$= k_1\frac{\delta_y^2}{2} + k_1\delta_y\delta_d - k_1\delta_y\delta_y + k_2\frac{\delta_d^2}{2} - k_2\delta_d\delta_y + k_2\frac{\delta_y^2}{2}$$

$$= k_1\frac{\delta_y^2}{2} + k_1\delta_y\delta_d - k_1\delta_y^2 + k_2\frac{\delta_d^2}{2} - k_2\delta_d\delta_y + k_2\frac{\delta_y^2}{2}$$

$$= -(k_1-k_2)\frac{\delta_y^2}{2} + (k_1-k_2)\delta_y\delta_d + k_2\frac{\delta_d^2}{2}$$

$$= -(k_1\delta_y - k_2\delta_y)\frac{\delta_y}{2} + \frac{\delta_d}{2}[2k_1\delta_y - 2k_2\delta_y + k_2\delta_d]$$

$$= -(k_1\delta_y - k_2\delta_y)\frac{\delta_y}{2} + \frac{\delta_d}{2}[(k_1\delta_y - k_2\delta_y) + (k_1\delta_y + k_2(\delta_d-\delta_y))]$$

$$= -(k_1\delta_y - k_2\delta_y)\frac{\delta_y}{2} + \frac{\delta_d}{2}[(k_1\delta_y - k_2\delta_y) + F_d]$$

$$E_a = \frac{1}{2}\delta_y(k_1-k_2)(\delta_d-\delta_y) + \frac{1}{2}F_d\delta_d \qquad (II.6)$$

USING THE DEFINITION OF DUCTILITY RATIO $\mu = \frac{\delta_d}{\delta_y}$

$$\Rightarrow \quad E_a = \frac{1}{2}\delta_y^2(k_1-k_2)(\mu-1) + \frac{1}{2}\delta_y F_y \mu \quad \text{------- (II.7)}$$

II.2. DERIVATION OF IMPACT LOAD BY APPLYING RAYLEIGH'S PRINCIPAL

WHEN THE TOTAL KINETIC ENERGY OF THE TWO BODIES IS TRANSFORMED INTO THE POTENTIAL ENERGY OF THE COMPRESSED SPRING, THE WEIGHT COMES TO REST AND THE FORCE COMPRESSING THE SPRING ATTAINS IT'S MAX. VALUE.

ACCORDING TO RAYLEIGH'S PRINCIPLE, ONE HAS :

$$(K.E.)_{(m+M)_{max}} = (P.E)_{s,max} \quad \text{---------- (II.8)}$$

$$\frac{1}{2}(m+M)v^2 = \frac{1}{2}\delta_y^2(k_1-k_2)(\mu-1) + \frac{1}{2}\delta_y F_y \mu$$

FROM ELASTIC IMPACT CASE, WE HAVE SHOWN THAT

$$v^2 = \left(\frac{m}{m+M}\right)^2 v_0^2 \quad (II.9)$$

THEN

$$\frac{1}{2}(m+M)\left(\frac{m}{m+M}\right)^2 v_0^2 = \frac{1}{2}\delta_y^2(k_1-k_2)(\mu-1) + \frac{1}{2}\delta_y F_y \mu$$

$$\frac{m^2}{(m+M)} v_0^2 = \delta_y^2(k_1-k_2)(\mu-1) + \delta_y F_y \mu$$

OR

$$F_d \delta_y \mu = \frac{m^2}{(m+M)} v_0^2 - (k_1-k_2)(\mu-1)\delta_y^2$$

$$F_d = \frac{(m^2 v_0^2)}{(m+M)\mu\delta_y} + (k_1-k_2)\left(1-\frac{1}{\mu}\right)\delta_y$$

$$F_d = \frac{(m^2 v_0^2)}{(m+M)\mu\delta_y} + \left(1-\frac{k_2}{k_1}\right)\left(1-\frac{1}{\mu}\right)k_1\delta_y \quad \cdots (II.10)$$

USING BILINEAR SLOP RATIO $= \xi = \frac{k_2}{k_1}$ ---- (II.11)

$$\boxed{F_d = \frac{(m^2 v_0^2)}{(m+M)\mu\delta_y} + (1-\xi)\left(1-\frac{1}{\mu}\right)k_1\delta_y} \quad \text{---- (II.12)}$$

IF $k_1 = k_2$ = ELASTIC $F_d = F_y = k_1\delta_y$, EQ. (II.12) BECOMES

$$F = \frac{m^2 v_0^2}{\mu\frac{F}{k_1}(m+M)} \Rightarrow F^2 = \frac{m^2 v_0^2}{\mu\frac{(m+M)}{k_1}} = \frac{m^2 v_0^2 \omega^2}{\mu}$$

$$\Rightarrow \quad \boxed{F = \frac{m v_0 \omega}{\sqrt{\mu}}}$$

IT'S AGREE WITH ELASTIC RESULT

EQUATION (II.12) CAN BE REWRITTEN TO INCLUDE $K.E. = \frac{1}{2}mv_0^2$

$$F_d = \frac{\frac{1}{2}(mv_0^2)m}{\frac{1}{2}(m+M)\mu\delta_y} + (1-\xi)\left(1-\frac{1}{\mu}\right)F_y$$

$$\Rightarrow \quad \boxed{F_d = \frac{2(K.E)}{\mu\delta_y\left(1+\frac{M}{m}\right)} + (1-\xi)\left(1-\frac{1}{\mu}\right)F_y} \quad \text{---- (II.12a)}$$

II.3. DERIVATION OF IMPACT LOAD BY APPLYING CONSERVATION OF ENERGY (K.E.) + (P.E.) = CONSTANT

THE TOTAL WORK DONE IN COMPRESSING THE SPRING IS EQ. TO THE TOTAL K.E. AVAILABLE AT THE TIME LOCAL INELASTIC DEFORMATION IS COMPLETE PLUS THE POTENTIAL ENERGY AVAILABLE RESULTING FROM THE DISPLACEMENT OF SPRING. THIS ADDITIONAL P.E. TO THE INPUT ENERGY IS NOT CONSIDERED IN THE RAYLEIGH'S PRINCIPLE.

THE TOTAL AVAILABLE INPUT ENERGY IS

$$E_i = K.E. + P.E. \quad \text{-------------} \quad II.3.1$$

$$E_i = \frac{1}{2}(m+M)v^2 + (m+M)g\,\delta_d \quad \text{------} \quad II.3.2$$

$$E_i = \frac{1}{2}\frac{m^2}{(m+M)}v_0^2 + (m+M)g\,\delta_d \quad \text{-------} \quad II.3.3$$

THEN, BY ENERGY BALANCE

$$E_i = E_o$$

$$\frac{1}{2}\frac{m^2}{(m+M)}v_0^2 + (m+M)g\,\delta_d = \frac{1}{2}(k_1-k_2)(\mu-1)\delta_y^2 + \frac{1}{2}\delta_y F_d\,\mu$$

$$F_d\,\mu\,\delta_y = \frac{m^2v_0^2}{(m+M)} + 2(m+M)g\,\delta_d - (k_1-k_2)(\mu-1)\delta_y^2$$

$$F_d = \frac{m^2v_0^2}{(m+M)\mu\delta_y} + 2(m+M)g\frac{1}{\mu}\cdot\frac{\delta_d}{\delta_y} - (k_1-k_2)(\frac{1}{\mu}-1)\delta_y$$

$$F_d = \frac{m^2v_0^2}{(m+M)\mu\delta_y} + 2(m+M)g - (k_1-k_2)(\frac{1}{\mu}-1)\delta_y$$

$$= \frac{m^2v_0^2}{(m+M)\mu\delta_y} + 2(m+M)g - (1-\frac{k_2}{k_1})(\frac{1}{\mu}-1)k_1\delta_y$$

$$\boxed{F_d = \frac{m^2v_0^2}{(m+M)\mu\delta_y} + 2(m+M)g - (1-\xi)(\frac{1}{\mu}-1)k_1\delta_y} \quad II.3.4$$

IF THIS IS PERFECT PLASTIC, THEN $F_d = F_y = k_1\delta_y$ $\quad \xi = 0$

$$F_d = \frac{m^2v_0^2}{(m+M)\mu\delta_y} + 2(m+M)g + (\frac{1}{\mu}-1)F_d$$

$$F_d = \frac{2mghc}{\mu\delta_y} + 2(m+M)g + (\frac{\delta_y}{\delta_d}-1)F_d$$

$$= \frac{2mghc}{\delta_d} + 2(m+M)g + \frac{(\delta_y-\delta_d)}{\delta_d}F_d$$

$$F_d\delta_d = 2mghc + 2(m+M)g\delta_d + (\delta_y-\delta_d)F_d$$

$$F_d\delta_d = mghc + (m+M)g\delta_d + F_d\frac{\delta_y}{2}$$

$$F_d\delta_d - F_d\frac{\delta_y}{2} = mghc + (m+M)g\delta_d \quad \text{------} \quad II.3.5$$

IS THE SAME AS EQ. (10) WHICH IS FOR PERFECT PLASTIC CASE, AND THE IMPACT IS PROVED TO BE :

$$F_u = \frac{2\pi m V_0}{T}\sqrt{\frac{1}{3A-1}}$$

III. CORRELATION BETWEEN EQUIVALENT ELASTIC IMPACT LOAD AND PLASTIC LOAD

RELATIONSHIP BETWEEN EQUIVALENT ELASTIC IMPACT LOAD F_e OR DEMAND D, AND PERFECT PLASTIC IMPACT LOAD F_p OR CAPACITY C IN TERMS OF BILINEAR SLOP RATIO, ξ, AND DUCTILITY RATIO, μ. IS BASED ON EQUATING THE ENERGY ABSORBED BY THE INELASTIC CAPACITY MODEL WITH AN ASSUMED EQUIVALENT PERFECT ELASTIC DEMAND MODEL

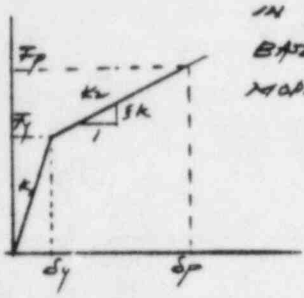

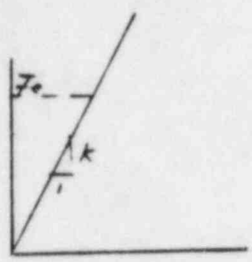

FOR ELASTIC DEMAND MODEL

$$E_e = \frac{1}{2}\frac{F_e^2}{k_1} \quad \text{------------- (III.1)}$$

FOR THE INELASTIC CAPACITY MODEL

$$E_p = \frac{1}{2}\frac{F_y^2}{k_1} + \left(\frac{F_p + F_y}{2}\right)(\delta_p - \delta_y) \quad \text{----- (III.2)}$$

BUT

$$\begin{aligned} F_p &= k_1\delta_y + k_2(\delta_p - \delta_y) \\ &= k_1\delta_y + \xi k_1(\delta_p - \delta_y) = k_1\delta_y + \xi k_1\delta_y(\mu - 1) \\ &= k_1\delta_y\{1 + \xi(\mu-1)\} \end{aligned}$$

$$\boxed{F_p = k_1\delta_y\{1 + \xi(\mu-1)\}} \quad \text{--------- (III.3)}$$

$$\begin{aligned} E_p &= \tfrac{1}{2}k_1\delta_y + \tfrac{1}{2}(F_p + F_y)(\delta_p - \delta_y) \\ &= \tfrac{1}{2}k_1\delta_y + \tfrac{1}{2}(F_p + F_y)(\mu - 1)\delta_y \\ &= \tfrac{1}{2}k_1\delta_y + \tfrac{1}{2}\{k_1\delta_y + k_1\delta_y + k_1\delta_y\xi(\mu-1)\}(\mu-1)\delta_y \\ &= \tfrac{1}{2}k_1\delta_y + \tfrac{1}{2}\{k_1\delta_y[2 + \xi(\mu-1)]\}(\mu-1)\delta_y \\ &= \tfrac{1}{2}k_1\delta_y + \tfrac{1}{2}\{k_1\delta_y[2(\mu-1)] + \xi(\mu-1)^2 k_1\delta_y\}\delta_y \end{aligned}$$

$$E_p = \tfrac{1}{2}k_1\delta_y\{1 + 2(\mu-1) + \xi(\mu-1)^2\}$$

$$E_p = \frac{1}{2}\frac{F_y^2}{k_1}\{1 + 2(\mu-1) + \xi(\mu-1)^2\} \quad \text{------ (III.4)}$$

EQUATE (III.1) TO (III.4), YIELDS

$$\frac{1}{2}\frac{F_e^2}{k_1} = \frac{1}{2}\frac{F_y^2}{k_1}[1 + 2(\mu-1) + \xi(\mu-1)^2] \quad \text{----- (III.5)}$$

$$\left(\frac{F_e}{F_y}\right)^2 = 1 + 2(\mu-1) + \xi(\mu-1)^2$$

$$\left(\frac{F_o}{F_y}\right)^2 = 1 + 2(\mu - 1) + \xi(\mu^2 - 2\mu + 1)$$

$$= 1 + 2\mu - 2 + \mu^2\xi - 2\mu\xi + \xi = \xi\mu^2 + 2(1-\xi)\mu + (\xi - 1)$$

$$\Rightarrow \quad \xi\mu^2 + 2(1-\xi)\mu + (\xi-1) - \left(\frac{F_o}{F_y}\right)^2 = 0$$

$$\mu^2 + 2\left(\frac{1}{\xi} - 1\right)\mu + \left(1 - \frac{1}{\xi}\right) - \left(\frac{F_o}{F_y}\right)^2 \frac{1}{\xi} = 0$$

$$\Rightarrow \quad \mu = \left(1 - \frac{1}{\xi}\right) + \sqrt{\left(\frac{1}{\xi} - 1\right)^2 - \left[\left(1 - \frac{1}{\xi}\right) - \left(\frac{F_o}{F_y}\right)^2 \frac{1}{\xi}\right]}$$

$$= \left(1 - \frac{1}{\xi}\right) + \sqrt{\left[\left(1 - \frac{1}{\xi}\right) - 1\right]\left(1 - \frac{1}{\xi}\right) + \left(\frac{F_o}{F_y}\right)^2 \frac{1}{\xi}}$$

$$= \left(1 - \frac{1}{\xi}\right) + \sqrt{\left(\frac{1}{\xi} - 1\right)\frac{1}{\xi} + \left(\frac{F_o}{F_y}\right)^2 \frac{1}{\xi}}$$

$$\boxed{\mu = \left(1 - \frac{1}{\xi}\right) + \left[\frac{1}{\xi}\left(\frac{1}{\xi} - 1 + \left(\frac{F_o}{F_y}\right)^2\right)\right]^{\frac{1}{2}}} \quad ----- \quad (\text{III}.6)$$

SINCE $\quad \frac{F_o}{F_y} = \frac{D}{C}$

$$\boxed{\mu = \left(1 - \frac{1}{\xi}\right) + \left[\frac{1}{\xi}\left(\frac{1}{\xi} - 1 + \left(\frac{D}{C}\right)^2\right)\right]^{\frac{1}{2}}} \quad ----- \quad (\text{III}.7)$$

FOR ELASTIC-PLASTIC CASE $\xi = 0$

$$\boxed{\mu = \frac{1}{2}\left[\left(\frac{D}{C}\right)^2 + 1\right]} \quad ------- \quad (\text{III}.8)$$

OR $\quad \left(\frac{D}{C}\right) = \sqrt{2\mu - 1}$

$$\boxed{C = \frac{D}{\sqrt{2\mu - 1}}} \quad ------- \quad (\text{III}.9)$$

ENGINEERING MECHANICS DIVISION
COMPUTER LOG
****

CALCULATION NUMBER: SQE - 2043 - 2 **S&M COMP. AUTH#** 7557 **CHARGE NUMBER:** *** **OTHER:**

PROGRAM NAME	LIBRARY REF. NUMBER	VERSION / LEVEL	RUN NO.	JOB SUBMITTAL NUMBER	FICHE LOC SECT	FICHE LOC PAGE	PREPARED BY: NAME	PREPARED BY: DATE	COMPUTER USED **	COMMENTS / OTHER PERTINENT INFORMATION
ANSYS	ST-348	04/1C	1	6270		737	J. GWINN	6/22/85	3xW	PRE-IMPACT
:	:	:	2	910		737	:	6/26/85	:	AFTER IMPACT
:	:	:	3	2009		:	:	6/26/85	:	SEAT-32 FORCE DEFLECTION CURVES
:	:	:	4	3297		:	:	6/26/85	:	SEAT-10
:	:	:	5	1839		:	:	6/30/85	:	DISK 3&G
:	:	:	6	1486		:	:	7/3/85	:	DISK 10

* = COMPUTER GENERATED JOB SUBMITTAL NUMBER
** = COMPUTER USED (SMEC OR OTHER)
*** = IF OTHER THAN SMEC COMPUTER IS USED

STONE & WEBSTER ENGINEERING CORPORATION

CALCULATION SHEET 757

5010.65

CALCULATION IDENTIFICATION NUMBER				PAGE ____
J.O. OR W.O. NO.	DIVISION & GROUP	CALCULATION NO.	OPTIONAL TASK CODE	

Microfiches of

Appen. F

FOR DETAILS PLEASE SEE
THE ATTACHED HARD COPIES OF
COMPUTER OUTPUTS.

STONE & WEBSTER ENGINEERING CORPORATION

738

CALCULATION SHEET

▲5010.65

CALCULATION IDENTIFICATION NUMBER				
J.O. OR W.O. NO.	DIVISION & GROUP	CALCULATION NO.	OPTIONAL TASK CODE	PAGE 6
14764.07	NM(C)	2043	SQE	REV. 1

REVISION STATUS TABLE

VOID

REV. NO.	PAGES REVISED CHANGED	PAGES REVISED ADDED	DESCRIPTION & REASON	ORIGINATOR & DATE	REVIEWER & DATE
0	—	—	Original Issue	J. Gwinn 10/26/84	[illegible] 10/27/84
1	7, 18, 19, 21, 22, 23, 24, 25, 26, 27, 28, 29, 5, 9, 13, 17, 30, D-8, D-9, SECTION 9 & 10, TITLE PAGE, 2, 4, 15.	31, A-6, A-7	Revisions to clarify the results of analysis and data input sources.	J. Gwinn 12/7/84	CAM T. LY 12/7/84

12210 EMD/EQS SQE 2043 Appendix F F39

Stone and Webster Engineering Corporation
CALCULATION SHEET

Calculation Identification Number				
J.O./W.O. NO. 12210	DIVISION & GROUP NM(C)	CALCULATION NO. 2043	OPTIONAL CODE SQE	PAGE 4 REV 1

APPENDIX

	Page
A-Plastic Strain Energy for Beams of Various Cross-section	
B-Plastic Strain Energy for a Circular Plate in Bending	
C-Miscellaneous Reference Material	
D-Computer Log and Microfiche	
E- VOID PAGES (38 PAGES)	

| REV. 1

List of Tables

VOID

4.1	Mass Properties	15
4.2	Materials	15
4.3	Dimensions	16
4.4	Material Properties at 500F	17
4.5	Section Properties	17
4.6	Impact Speed and Hammer Pressure	17
5.1	Summary of Results	19
8.1	Pre-impact Loads	22
8.2	Point Impact - Kickback Loads on AOVF32	25
8.3	Point Impact - Kickback Loads on F010	26
8.4	Uniform Impact - Kickback Loads on AOVF32	27
8.5	Uniform Impact - Kickback Loads on F010	27
8.6	Disk Rim Nodal Loads for AOVF32	28

List of Figures

1.1	Piping Model Showing the Location of the Postulated Pipe Rupture	9
1.2	Cross-section of the AOVF32 Check Valve	10
1.3	Cross-section of the F010 Check Valve	11
1.4	Sketch of the Tail Link/Disk Assembly	12

12210 EMD/EQS SQE 2043 Appendix F F 40

Stone and Webster Engineering Corporation
CALCULATION SHEET

Calculation Identification Number				
J.O./W.O. NO. 12210	DIVISION & GROUP NM(C)	CALCULATION NO. 2043	OPTIONAL CODE SQE	PAGE 7 REV 1

SUMMARY

VOID

The reactor vessel water is protected from blowdown following a postulated rupture of the feedwater piping outside the containment, by the Velan check valve 1B21*F010A,B inside the containment and by the Atwood/Morrill testable check valve 1B21*AOVF32A,B outside the containment. Breaks are not postulated in the piping between the valves because that region is classified as break exclusion.

The reverse flow caused by the sudden pressure reduction at the break rapidly closes both valves. This calculation examines the ability of these valves to withstand the impact of the disk on the seat without excessive leakage thereafter.

Loads on the critical elements,i.e., the disk, tail link, rockshaft and seat, were computed by simulation of the impact dynamics using the STARDYNE and GTSTRUDL computer programs. Both uniform and point impact were considered in search of the worst case kickback loads generated by the point of impact not being at the center of percussion. Seismic, hydrodynamic and dead loads were not considered because of their insignificant magnitude compared to impact loads.

In those cases where linear stresses were not below their allowables, a strain energy analysis or a non-linear time history strain analysis was conducted to demonstrate integrity. REV. 1

It is concluded that both valves will remain intact and that the leakage will be within the make-up capability of the High Pressure Core Spray(HPCS) or the Reactor Core Injection Cooling(RCIC) system, following rupture of the feedwater piping outside the containment.